

9-2008

## Modeling and Parameter Estimation of Spacecraft Lateral Fuel Slosh

Yadira Rodriguez Chatman  
*Embry-Riddle Aeronautical University - Daytona Beach*

Follow this and additional works at: <https://commons.erau.edu/db-theses>



Part of the [Aerospace Engineering Commons](#)

---

### Scholarly Commons Citation

Chatman, Yadira Rodriguez, "Modeling and Parameter Estimation of Spacecraft Lateral Fuel Slosh" (2008).  
*Theses - Daytona Beach*. 28.  
<https://commons.erau.edu/db-theses/28>

This thesis is brought to you for free and open access by Embry-Riddle Aeronautical University – Daytona Beach at ERAU Scholarly Commons. It has been accepted for inclusion in the Theses - Daytona Beach collection by an authorized administrator of ERAU Scholarly Commons. For more information, please contact [commons@erau.edu](mailto:commons@erau.edu).

**MODELING AND PARAMETER ESTIMATION OF SPACECRAFT  
LATERAL FUEL SLOSH**

**By**

**Yadira Rodriguez Chatman**

**A Thesis Submitted to the  
Graduate Studies Office  
In Partial Fulfillment of the Requirements for the Degree of  
Master of Science in Aerospace Engineering**

**Embry-Riddle Aeronautical University  
Daytona Beach, Florida  
September 2008**

UMI Number: EP32012

### INFORMATION TO USERS

The quality of this reproduction is dependent upon the quality of the copy submitted. Broken or indistinct print, colored or poor quality illustrations\* and photographs, print bleed-through, substandard margins, and improper alignment can adversely affect reproduction.

In the unlikely event that the author did not send a complete manuscript and there are missing pages, these will be noted. Also, if unauthorized copyright material had to be removed, a note will indicate the deletion.

**UMI<sup>®</sup>**

---

UMI Microform EP32012  
Copyright 2011 by ProQuest LLC  
All rights reserved. This microform edition is protected against  
unauthorized copying under Title 17, United States Code.

---

ProQuest LLC  
789 East Eisenhower Parkway  
P.O. Box 1346  
Ann Arbor, MI 48106-1346

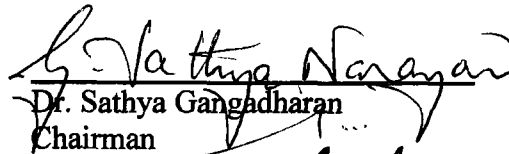
# MODELING AND PARAMETER ESTIMATION OF SPACECRAFT LATERAL FUEL SLOSH

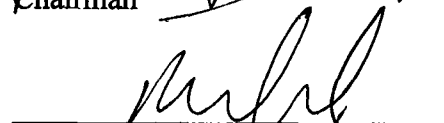
By


Yadira Rodriguez Chatman


This thesis was prepared under the direction of the candidate's thesis committee chairman, Dr. Sathya Gangadharan, Department of Mechanical, Civil, Electrical Engineering and Engineering Science, and has been approved by the members of her thesis committee. It was submitted to the Aerospace Engineering Department and was accepted in partial fulfillment of the requirements for the degree of Master of Science of Aerospace Engineering.


## THESIS COMMITTEE:

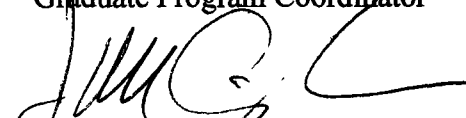
  
Dr. Sathya Gangadharan  
Chairman

  
Dr. Reda Mankbadi  
Co-Chairman

  
Mr. James Sudermann  
Member

  
Dr. Habib Eslami  
Department Chair, Aerospace Engineering

  
Dr. Yi Zhao  
Graduate Program Coordinator

  
Dr. James Cunningham  
Associate Provost

## **ACKNOWLEDGEMENTS**

The author wishes to express thanks to James Sudermann, Keith Schlee, James Ristow and John Bauschlicher, from the Launch Services Program at NASA Kennedy Space Center, whose constant encouragement, helpful counsel and practical suggestions were essential to the successful outcome of this thesis. The author would like to thank the Thesis Chairman, Dr. Sathya Gangadharan, Dr. Reda Mankbadi and Dr. Carl Hubert at Hubert Astronautics for their support. Appreciation is also due to Brandon Marsell, Craig Czapinski for his lab time, and David Majko for his help fabricating some of the experimental set-up components.

The author appreciates the patience and encouragement of her family and friends provided during the needed time to complete this project. Specially, the author would like to dedicate this work effort to two most important people in her life; to Tatiana and Denzel.

## ABSTRACT

Author: Yadira Rodriguez Chatman  
Title: Modeling and Parameter Estimation of Spacecraft Lateral Fuel Slosh  
Institution: Embry-Riddle Aeronautical University  
Degree: Master of Science in Aerospace Engineering  
Year: 2008

Predicting the effect of fuel slosh on spacecraft and launch vehicle attitude control systems has been a very important and challenging task and has been the subject of considerable research over the past years. Analytic determination of the slosh analog parameters has been met with mixed success and is made more difficult by the introduction of propellant management devices such as elastomeric diaphragms. The experimental set-up in this research incorporates a diaphragm in a simulated spacecraft fuel tank subjected to lateral slosh behavior. This research focuses on the parameter estimation of a SimMechanics model of the simulated spacecraft propellant tank with diaphragms using lateral fuel slosh experiment data. An experimental investigation was conducted to determine and measure the slosh forces response of free surface slosh and diaphragms in an eight inch diameter spherical tank. The lateral slosh testing consisted of the tank assembly partially filled with different liquids, for other tests, diaphragms were incorporated into the tank. The experiment results from different testing conditions were compared for estimation of unknown parameter characteristics that include the pendulum model stiffness constants and damping coefficients.

## TABLE OF CONTENTS

ACKNOWLEDGEMENTS .....	iii
ABSTRACT .....	iv
LIST OF FIGURES.....	vii
LIST OF TABLES .....	x
1 INTRODUCTION.....	11
2 STATEMENT OF THE PROBLEM .....	14
3 METHOD OF APPROACH .....	18
3.1 Fuel Slosh Pendulum Modeling .....	18
3.2 SLOSH Code Estimation .....	21
4 EXPERIMENTAL SETUP .....	25
4.1 Lateral Slosh Test Setup.....	25
4.2 Test Tanks .....	29
4.3 Test Fluids .....	30
4.4 Test Diaphragms .....	31
4.5 Test Setup Calibration.....	34
4.6 Test Matrix .....	35
5 EXPERIMENT PROCEDURE.....	37
5.1 Data Acquisition.....	37
5.2 MATLAB SimMechanics .....	40
5.3 MATLAB Parameter Estimation .....	44
5.4 Preliminary Testing.....	46
5.4.1 Sweep Test .....	46
5.4.2 Damping Test .....	48
5.4.3 Force vs. Position Test .....	55
6 EXPERIMENT RESULTS AND DATA ANALYSIS.....	59
6.1 Locomotive Assembly Testing.....	59
6.1.1 Water .....	60
6.1.2 Glycerine .....	61
6.1.3 Corn Syrup .....	62
6.2 Frozen Mass .....	64

6.3	Free Surface .....	66
6.3.1	Water.....	67
6.3.2	Glycerine.....	69
6.3.3	Corn Syrup.....	71
6.4	Diaphragm Testing.....	72
6.4.1	Spike Diaphragm .....	73
6.4.2	Sky Diaphragm .....	78
6.4.3	Yellow Diaphragm.....	82
7	DIAPHRAGM DATA VERSUS SLOSH CODE .....	86
8	DISCUSSION AND RECOMMENDATIONS.....	90
9	CONCLUSIONS .....	91
10	FUTURE WORK.....	92
	REFERENCES .....	93
	APPENDIX.....	95
	A. Experiment Matrix .....	95
	B. Damping Characteristics .....	96
	C. Force Comparison among Diaphragms.....	98
	CD. Experimental Database (attached Compact Disk).....	98



## LIST OF FIGURES

Figure 2-1. Photograph of the test rig for lateral slosh mode at SwRI.....	14
Figure 2-2. Diaphragm in (A) and (B) shape .....	15
Figure 2-3. Parameter estimation process flowchart.....	17
Figure 3-1. Mechanical analog model of fuel slosh.....	19
Figure 3-2. Free body diagram for slosh pendulum.....	19
Figure 3-3. SLOSH code program input.....	21
Figure 3-4. SLOSH code program outputs.....	22
Figure 3-5. SLOSH code first and second slosh frequencies.....	23
Figure 4-1. Aerotech linear actuator .....	25
Figure 4-2. Mounted linear actuator.....	26
Figure 4-3. Aluminum stock in the Haas Vertical Milling Center.....	27
Figure 4-4. Machined part profile during fabrication .....	27
Figure 4-5. Attachment part on “shaker” .....	28
Figure 4-6. Linear actuator assembly attached to tank.....	28
Figure 4-7. CATIA model of the experimental set up .....	29
Figure 4-8. Schematic diagram of experimental tank with the diaphragm.....	30
Figure 4-9. Photograph of an elastomeric diaphragm (Courtesy: PSI).....	31
Figure 4-10. Diaphragm tanks.....	33
Figure 4-11. Force transducer calibration .....	34
Figure 4-12. Free surface test flow diagram .....	35
Figure 4-13. Diaphragm test flow diagram .....	36
Figure 5-1. Soloist hardware .....	38
Figure 5-2. Soloist HMI interface screen display .....	38
Figure 5-3. LabVIEW interface screen display.....	39
Figure 5-4. Experimental set-up SimMechanics model.....	40
Figure 5-5. SimMechanics model sine wave input.....	41
Figure 5-6. Linear actuator assembly subgroup.....	42
Figure 5-7. Test tank and force transducer arrangement.....	42
Figure 5-8. Pendulum mechanical analog model.....	43
Figure 5-9. SimMechanics model animation of the linear actuator assembly .....	44

Figure 5-10. Parameter Estimation Toolbox project simulation .....	45
Figure 5-11. Measured vs. simulated plot of reaction forces .....	45
Figure 5-12. Sweep test graph.....	46
Figure 5-13. Spike diaphragm sweep test .....	47
Figure 5-14. Yellow diaphragm sweep test.....	48
Figure 5-15. Damping graph water at 60% fill level excited at 2.15Hz .....	49
Figure 5-16. Damping slope water at 60% fill level excited at 2.15Hz .....	50
Figure 5-17. Damping graph glycerine at 60% fill level excited at 2.25Hz .....	51
Figure 5-18. Damping slope glycerine at 60% fill level excited at 2.25Hz .....	51
Figure 5-19. Damping graph corn syrup at 60% fill level excited at 2.375Hz .....	52
Figure 5-20. Damping slope corn syrup at 60% fill level excited at 2.375Hz .....	53
Figure 5-21. Damping graph Spike diaphragm at 60% fill level .....	53
Figure 5-22. Damping graph Yellow diaphragm at 60% fill level excited at 4.75Hz .....	54
Figure 5-23. Force-displacement plot for free surface slosh approaching resonance .....	56
Figure 5-24. Force-displacement plot for free surface slosh at resonance.....	56
Figure 5-25. Force-displacement plot for Spike diaphragm tank.....	57
Figure 5-26. Force-displacement plot for Yellow diaphragm tank.....	58
Figure 6-1. Locomotive arm experimental set-up.....	60
Figure 6-2. Locomotive arm assembly glycerine 60% fill level excited at 1.75Hz.....	61
Figure 6-3. Locomotive arm assembly testing for corn syrup .....	62
Figure 6-4. Locomotive arm assembly corn syrup 60% fill level excited at 1.75Hz.....	62
Figure 6-5. Frozen water tank testing.....	64
Figure 6-6. Fixed mass model of the frozen tank testing .....	65
Figure 6-7. Fixed mass test comparison between the empirical data and estimation .....	66
Figure 6-8. Free surface water vs. model simulation .....	67
Figure 6-9. Free surface water data vs. model simulation .....	68
Figure 6-10. Parameter values simulation for free surface water .....	68
Figure 6-11. Parameter estimation plot for free surface glycerine.....	69
Figure 6-12. Free surface glycerine data vs. model simulation .....	70
Figure 6-13. Parameter values simulation for free surface glycerine .....	70
Figure 6-14. Parameter Estimation plot for free surface corn syrup.....	71

Figure 6-15. Free surface corn syrup data vs. model simulation .....	71
Figure 6-16. Parameter values simulation for free surface corn syrup .....	72
Figure 6-17. Spike diaphragm testing .....	74
Figure 6-18. Plot for Spike diaphragm filled with water .....	75
Figure 6-19. Parameters trajectory for Spike filled with water.....	75
Figure 6-20. Plot for Spike diaphragm filled with glycerine .....	76
Figure 6-21. Parameters trajectory for Spike filled with glycerine.....	76
Figure 6-22. Plot for Spike diaphragm filled with corn syrup .....	77
Figure 6-23. Parameters trajectory for Spike filled with corn syrup.....	77
Figure 6-24. Sky diaphragm testing .....	78
Figure 6-25. Plot for Sky diaphragm filled with water .....	79
Figure 6-26. Parameters trajectory for Sky filled with water.....	79
Figure 6-27. Plot for Sky diaphragm filled with glycerine .....	80
Figure 6-28. Parameters trajectory for Sky filled with glycerine.....	80
Figure 6-29. Plot for Sky diaphragm filled with corn syrup .....	81
Figure 6-30. Parameters trajectory for Sky filled with corn syrup.....	81
Figure 6-31. Yellow diaphragm testing.....	82
Figure 6-32. Plot for Yellow diaphragm filled with water.....	83
Figure 6-33. Parameters trajectory for Yellow filled with water .....	83
Figure 6-34. Plot for Yellow diaphragm filled with glycerine.....	84
Figure 6-35. Parameters trajectory for Yellow filled with glycerine .....	84
Figure 6-36. Plot for Yellow diaphragm filled with corn syrup.....	85
Figure 6-37. Parameters trajectory for Yellow filled with corn syrup .....	85
Figure 7-1. Gravity value inputs based on tank fill level.....	87
Figure 7-2. Viscosity inputs based on tank fill level.....	87
Figure 7-3. General equation for viscosity input.....	88
Figure 7-4. General equation for gravity input .....	89
Figure 7-5. SLOSH code screen illustrating frequency output .....	89

## LIST OF TABLES

Table 3-1. SLOSH code prediction for all tested liquids .....	24
Table 4-1. Comparison of viscosities of different liquids .....	31
Table 4-2. Diaphragm tanks characteristics comparison .....	33
Table 4-3. Comparison on force transducer readings .....	34
Table 6-1. Comparison of results among different liquids.....	63
Table 6-2. Free surface testing parameter values results .....	67
Table 6-3. Parameter Estimation parameter values.....	73
Table 7-1. SLOSH codes parameters inputs and outputs.....	86
Table 7-2. SwRI results vs. modified SLOSH code results .....	89

## 1 INTRODUCTION

Propellant sloshing is a potential source of disturbance which may be critical to the stability or structural integrity of space vehicles, as large forces and moments may be produced by the propellant oscillating at one of its fundamental frequencies in a partially filled tank. This could cause a failure of structural components within the vehicle or excessive deviation from its planned flight path.<sup>1</sup> There are different kinds of liquid motions of varying complexity that could be induced in space vehicles. Lateral sloshing is a type of liquid motion that occurs primarily in response to translational or pitching motions of the tank.<sup>1</sup> During portions of the launch profile, the spacecraft could be subjected to nearly purely translational oscillatory lateral motions as the launch vehicle control system guides the rocket along its flight path. This research project describes the on-going research effort to improve the accuracy and efficiency of modeling techniques used to predict these types of motions. In particular, a comparison of some of the preliminary results with and without diaphragms is made to illustrate the effect of diaphragms on the slosh dynamics.

The outcome of space vehicles missions could be seriously affected by fuel slosh effects. Even a minute amount of liquid, such as 1.2 kg, can lead to catastrophic failure, as exemplified by the loss of the 452 kg ATS-V spacecraft in 1969. Other missions that were affected by fuel slosh include the unexpected behavior of the Intelsat IV series spacecraft, various problems with ESA spacecraft and the NEAR Shoemaker mission to Eros during the spacecraft's reorientation maneuver.<sup>2</sup>

A more recent example of the effects due to this behavior is last years' Space X Falcon 1 mission. After the failure of the mission, an investigation took place and the post flight review of telemetry has verified that oscillation of the second stage late in the mission is the only factor that stopped Falcon 1 from reaching its full orbital velocity. Telemetry data shows that engine shutdown occurred about ninety seconds before schedule. This was due to oscillations causing the propellant to slosh away from the sump. The data shows that the increasing oscillation of the second stage was likely due to the slosh frequency in the liquid oxygen tank coupling with the thrust vector control system. This started out as a pitch-yaw movement and then transitioned into a "corkscrewing" motion. The simulations prior to flight indicated that the control system would be able to dampen the slosh effects. The slosh effects could be controlled by adding baffles to the second stage of the liquid oxygen tank and adjusting the control logic. The third Falcon 1 mission was scheduled for late July 2008.

There are three categories of slosh that can be caused by launch vehicles and/or spacecraft maneuvers when the fuel is in the presence of an acceleration field. These include bulk fluid motion, subsurface wave motion, and free surface slosh.<sup>3</sup> Each of these slosh types have a periodic component that is defined by either a spinning or lateral motion. Bulk fluid motion and free surface slosh can affect the lateral slosh characteristics. Moreover, slosh effects can be induced by interaction with a spinning or rotating spacecraft. This type of slosh can be bulk fluid motion and/or subsurface wave motion and almost always is periodic because of the spin. For either case, fluid behavior induced with lateral or spin motions, an unpredicted coupled resonance between the vehicle or spacecraft and the on-board fuel can have mission threatening effects. For

example, missions have been lost because of uncontrolled growth in nutation driven by resonant fuel slosh.<sup>4</sup>

Many research efforts have been dedicated to explore these types of slosh dynamics. Former slosh behavior research varies from characterizing the fluid motion, the effects of the propellant tank geometry on the slosh behavior, and the effects of propellant management devices (PMD) among other related topics. Reviews on various sloshing problems and investigations associated with liquid propellant vehicles were addressed as well as a comprehensive exposition on virtually all aspects of liquid dynamic behavior in moving container on Abramson's research work.<sup>5,6</sup> The presence of a diaphragm inside the propellant tank adds uncertainty to the vehicle dynamics of spinning spacecrafts. Tests performed on these vehicles have showed that adding diaphragms to the propellant tanks decreased the divergent nutation time constant by a factor of about 7 relative to a tank without a diaphragm.<sup>7</sup>

The current research project is focused on the modeling and simulation of a lateral slosh experimental setup. The goal of this research work is to improve the accuracy and efficiency of modeling techniques used to predict these types of lateral fluid motions. In particular, efforts will focus on analyzing the effects of viscoelastic diaphragms on slosh dynamics. The experimental setup was designed, fabricated and installed at Embry-Riddle Aeronautical University which includes the state-of-the-art linear actuator that induces the lateral motion to the tank assembly. The experimental data collected was analyzed and compared with model simulation data in order to determine the parameter values.

## 2 STATEMENT OF THE PROBLEM

Previous research used mechanical analogs such as pendulums and rotors to simulate sloshing mass as a common alternative to fluid modeling. Testing has been done to understand and measure the forces and torques generated by the liquid in lateral excitation modes at Southwest Research Institute (SwRI). Experimental set-ups for lateral slosh studies have been developed at SwRI to test and determine the characteristics of a model spacecraft fuel tank under these dynamic conditions. Activities to date at SwRI have primarily been concerned with testing of full scale tanks with diaphragms and bladders. They have performed fluid dynamics measurements on tanks used on the *Genesis*, *Contour*, *Stereo* and *Dawn* missions. The testing has been done to determine the parameters that are affected by the fuel slosh in both spinning and lateral excitation modes. Test rigs have been developed for both modes.<sup>8</sup> The Spinning Slosh Test Rig (SSTR) can subject a test tank to nutation motion conditions, while the lateral slosh test setup is conducted by imposing an axial forced sinusoidal displacement to the test tank. Figure 2-1 illustrates the lateral slosh testing setup at SwRI in San Antonio, Texas.

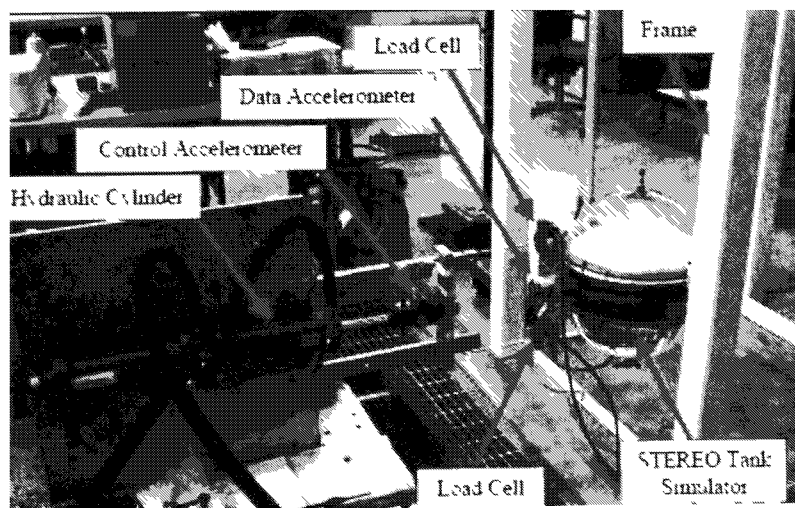
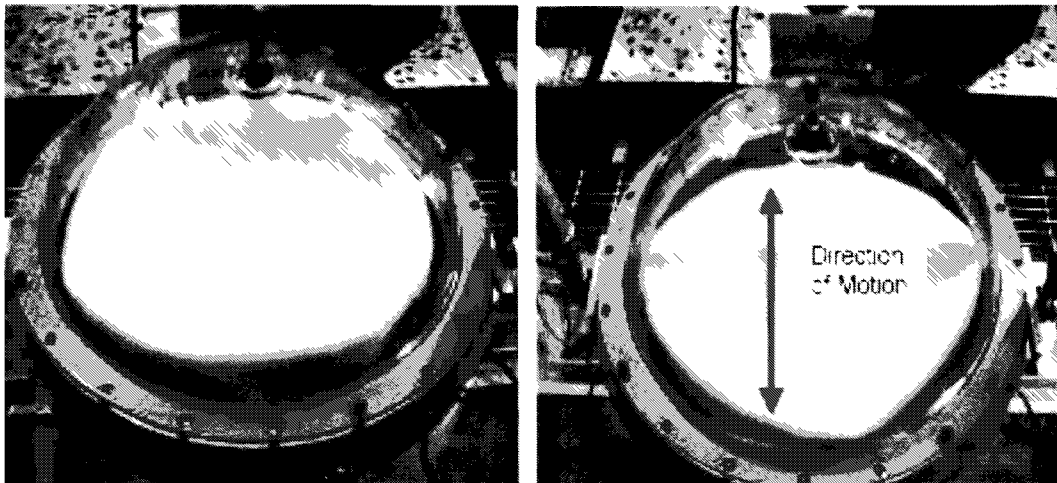


Figure 2-1. Photograph of the test rig for lateral slosh mode at SwRI



The testing included a tank suspended from a steel frame by pendulum tubes which was attached to a hydraulic cylinder, as well as accelerometers, loadcells, and strain gages to record the forces and moments present on the specified testing conditions. The clear acrylic testing tank included a flight-like diaphragm inside. Figure 2-2 illustrates the diaphragm tanks and the diaphragm placement to simulate features of actual spacecraft vehicle flight hardware.<sup>8</sup>



**A: “Crater shape”**

**B: “Ridge shape”**

**Figure 2-2. Diaphragm in (A) and (B) shape**

SwRI has completed a lateral slosh test series which included the use of a diaphragm as the PMD. As in previously conducted research, conceptual pendulum models were applied as an analog to the fluid dynamic behavior in the analysis of measured slosh forces and moments.<sup>9</sup> Although these models and analysis methods were previously tested at ERAU without a diaphragm constraining the liquid, it can now be validated when applied to the test data for the tank including a diaphragm.<sup>10</sup> In addition, SwRI studied the diaphragm shape and the vibration effects on the initial shape of the diaphragm.

Historically, it has been possible to predict free-surface lateral slosh of bulk fluid motion with a great deal of confidence and accuracy using codes such as the Dodge SLOSH program.<sup>11</sup> The SLOSH code assumes a pendulum as a mechanical analog for the slosh motion. Additional types of mechanical analogs (such as rotors and suspended masses) are being considered to develop a more generalized method of modeling fuel motion. The difficulty increases and the confidence of the model will diminish when a diaphragm or a bladder is introduced into a fuel tank.

Extensive analysis has been done on the different tank shapes and locations, as well as the use of PMDs. A summary of this analysis, like that reported by Hubert<sup>12</sup> shows the vast differences in possible behaviors of different designs. For example, a number of relatively simple mechanical models have been developed for cylindrical tanks with hemispherical end-caps mounted outboard of the spin axis. This type of tank has been popular in a number of spacecraft programs. Hubert also notes that one of the most difficult aspects of employing such mechanical models is in the selection of appropriate parameters in the model.

One of the most practical types of spacecraft propulsion fluid control devices has proven to be the diaphragm, which uses an elastomeric material to create an effective barrier between the inert gas under pressure and the liquid propellant. These devices are used to separate the fuel from the gas ullage (usually pressurized) so as to ensure a pure liquid flow to the spacecraft engines. They have become very popular with spacecraft designers since they can guarantee smooth engine performance in any orientation and gravity field (or lack thereof). They also do a very good job of ensuring that a very high percentage of the available fuel is utilized. The main advantages of currently available

diaphragms over other PMDs are that they are easier to manufacture and that they are light weight.<sup>13</sup> It has been found that the diaphragm shape can profoundly affect slosh behavior and, surprisingly, many of these diaphragms will hold their initial shape throughout launch vibration and maneuvers.<sup>14</sup>

The parameter estimation process taken during this research project is illustrated in Figure 2-3.

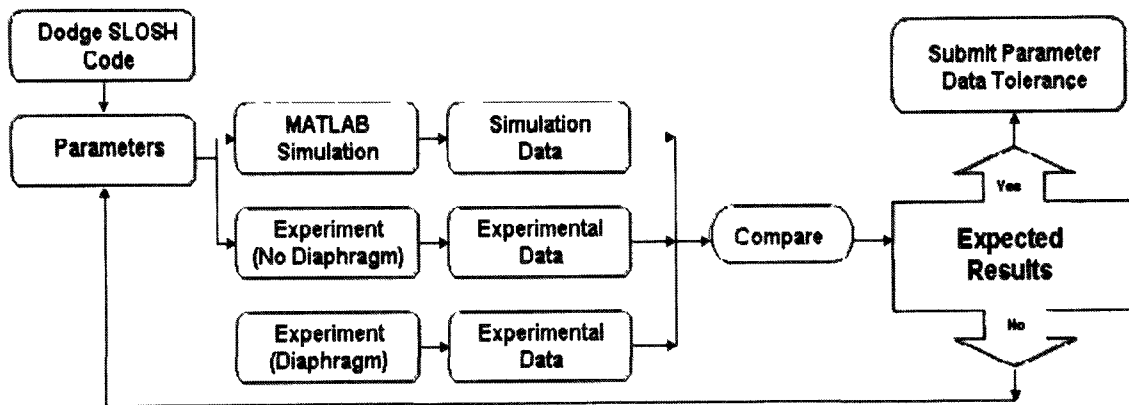


Figure 2-3. Parameter estimation process flowchart

The objective of this current research is to deliver a MATLAB/SimMechanics model which can simulate the lateral slosh testing setup and be used in conjunction with the MATLAB/Parameter Estimator to derive parameters for spacecraft dynamics simulations.

### **3 METHOD OF APPROACH**

The fluid imposes forces and moments on the tank walls when a partially filled tank is excited and an oscillatory lateral motion is applied. If the liquid sloshing amplitude is minimal and there are no breaking waves in the surface of the liquid, then the mechanical dynamic effects of liquid sloshing can be represented by a fixed mass and a slosh mass.<sup>14</sup> The theory of this mechanical pendulum analog is demonstrated and established on Abramson et al.<sup>1</sup> This mechanical pendulum concept is the basic approach applied in the data analysis and model simulations. The sloshing activity assumed in this mechanical model of the surface wave is simulated by the pendulum mass. The rest of the liquid is basically stationary and can be treated like a fixed mass.<sup>4</sup> Initial pendulum properties for free surface slosh are found by the use of the SLOSH code, developed at SwRI where it predicts the modes of the fuel tank with that of a pendulum.<sup>9</sup> In the case of testing tanks with diaphragm, the SLOSH code results were used as initial estimates for the needed parameters values.

#### **3.1 Fuel Slosh Pendulum Modeling**

Dynamic models of fuel slosh inside a tank undergoing oscillatory lateral motion can be created using a pendulum analog. When a spacecraft fuel tank is excited, the sloshing of the fuel creates forces and moments that need to be taken into account when designing any type of spacecraft. Figure 3-1 illustrates the mechanical model analog of the pendulum slosh model. The liquid inside the tank can be thought of as having two parts. The first part is the fraction of the fluid that is stationary with respect to the tank. This part is modeled as a fixed mass. The second part of the fluid is where the sloshing

activity occurs. This part can be modeled as a pendulum with a spring/damper combination that takes into account effects caused by viscous forces. In addition, the effects due to a diaphragm can also be considered as part of the spring/damper combination.<sup>14</sup>

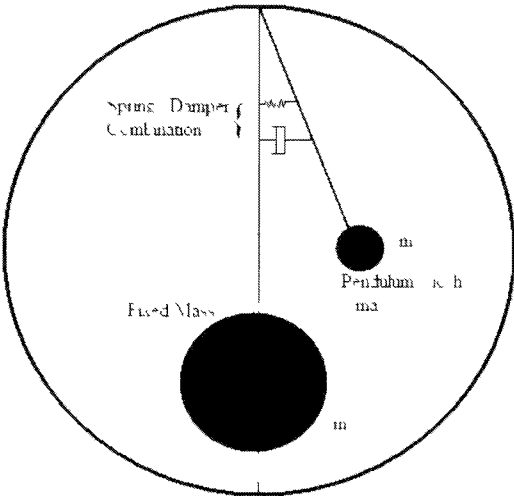


Figure 3-1. Mechanical analog model of fuel slosh

The pendulum mechanical analog equations derived from model can aid in the determination of the model parameters and can be then compared with the experimental measured data. Figure 3-2 illustrates the free body diagram for the slosh mass pendulum.

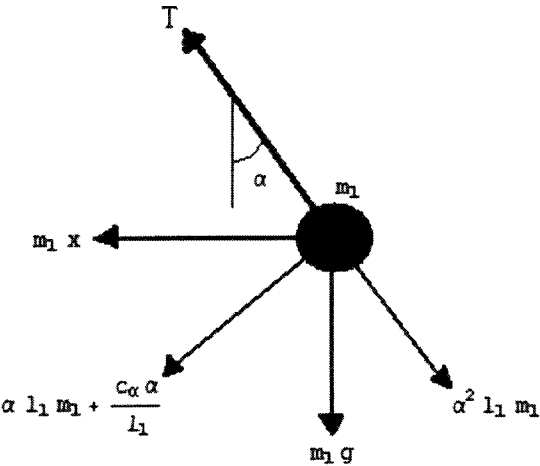


Figure 3-2. Free body diagram for slosh pendulum

As sketched there are five main forces acting on the pendulum. The first force is the force due to the tension (T) in the pendulum arm (massless). Also shown is the force due to acceleration of the mass, the centripetal force, the force due to gravity, and the damping force.<sup>15</sup> Note the damping force contains a term that models a rotational viscous damper with coefficient  $c_\alpha$ . Summing all of the forces in the horizontal direction we arrive at the following Equation 3-1.

$$\sum F_{\text{Horizontal}} = m_1 \ddot{x} + \left( \ddot{\alpha} l_1 m_1 + \frac{c_\alpha \dot{\alpha}}{l_1} \right) \text{Cos}(\alpha) - \dot{\alpha}^2 l_1 m_1 \text{Sin}(\alpha) + T \text{Sin}(\alpha) \quad [3-1]$$

Using the same free body diagram, we can solve for T.

$$T = \dot{\alpha}^2 l_1 m_1 + m_1 g \text{Cos}(\alpha) - m_1 \ddot{x} \text{Sin}(\alpha) \quad [3-2]$$

Substituting for T and taking into account the small angle approximation, we can solve for the force applied to the tank, where  $F_r$  is the reaction force of the slosh pendulum, and F is the applied force to the tank.<sup>15</sup>

$$F = \ddot{x}(m_T + m_0) + F_r \quad [3-3]$$

After dividing by  $\ddot{x}$  we get an equation representing the apparent mass of the tank. Equation 3-4 is now written in terms of the frequencies where  $m_T$  is the dry mass of the tank,  $m_0$  is the fixed mass of the liquid, and  $\omega$  is the pendulum frequency.<sup>15</sup>

$$W(\omega) = m_T + m_0 + \sum_{j=1}^N m_j \left\{ 1 + \frac{\omega^2}{\omega_j^2 - \omega^2 + 2i\beta_j \omega_j \omega} \right\} \quad [3-4]$$

Equation 3-5 can be used to extract the parameters for the slosh mass and slosh mass pendulum frequency. This data can then be used in conjunction with equation two in order to calculate the diaphragm torsional stiffness. Data must be taken for two liquids

of different densities in order to calculate the slosh pendulum length and diaphragm torsional stiffness.<sup>15</sup>

$$\omega_n = \sqrt{\frac{g}{l_p} + \frac{K_\theta}{m_p l_p^2}} \quad [3-5]$$

Using MATLAB, a M-File program can be created that theoretically calculates all of these values, which can later be used for comparison with the experimental results.

### 3.2 SLOSH Code Estimation

The pendulum model parameters can be initially determined by utilizing a code program developed by Frank Dodge in SwRI, San Antonio. The Dodge SLOSH code, or SLOSH code, is a tool to predict the parameters that describes the pendulum characteristics and behavior.<sup>11</sup> Both the tank and liquid parameters such as tank's shape, liquid's kinematic viscosity, and liquid fill level are provided as input to the program. Figure 3-3 illustrates the program input for an eight inch spherical tank filled with water at a 50% fill level.

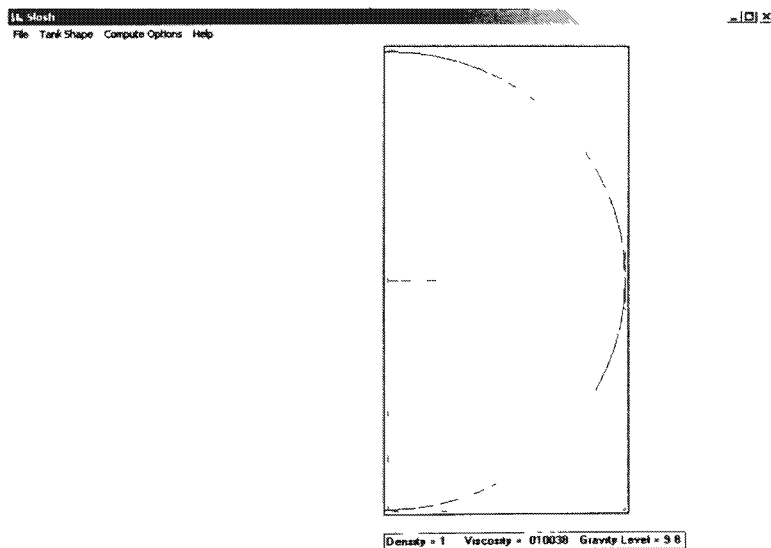


Figure 3-3. SLOSH code program input

Using these parameters, the code can then determine the proper pendulum equivalent that explains the slosh behavior in that specified filled tank. The parameters calculated by the code include the tank's fixed and liquid mass as well as the fixed mass parameters. Other parameters included as code output are both the first and second mode parameters for the pendulum mechanical model, among these the pendulum mass and length as well as critical damping characteristics. Figure 3-4 illustrates the mechanical model parameters program outputs obtained for the testing tank sample.

MECHANICAL MODEL PARAMETERS	
LIQUID MASS [mass units]	= 2.184E-03
LIQUID SURFACE HEIGHT above z=0 [length units]	= 1.012E-01
FIRST MODE PARAMETERS	
Pendulum mass [mass units]	= 1.270E-03
Pendulum length [length units]	= 6.530E-02
Pendulum hinge z-location [length units]	= 1.018E-01
Pendulum % critical damping	= 1.711E+01
Ratio of slosh amplitude to pendulum amplitude	= 1.337E+00
SECOND MODE PARAMETERS	
Pendulum mass [mass units]	= 3.160E-05
Pendulum length [length units]	= 1.926E-02
Pendulum hinge z-location [length units]	= 9.881E-02
Pendulum % critical damping	= 1.711E+01
Ratio of slosh amplitude to pendulum amplitude	= 3.267E-01
FIXED MASS PARAMETERS	
Mass [mass units]	= 8.819E-04
Z-location [length units]	= 1.013E-01
Mom. Inertia [mass*length <sup>2</sup> units]	= 3.633E-06

Figure 3-4. SLOSH code program outputs

The first and second slosh frequencies are also additional program parameter output as shown in Figure 3-5.



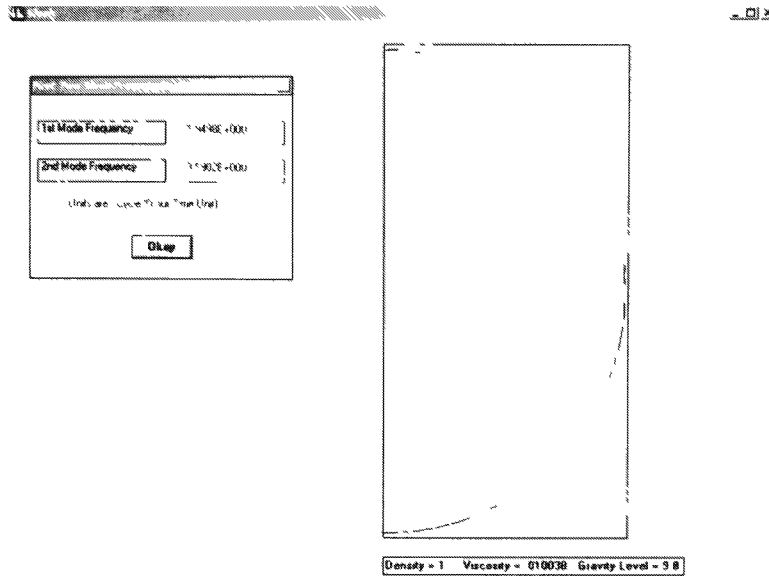


**Figure 3-5. SLOSH code first and second slosh frequencies**

The SLOSH code was also utilized to obtain the model characteristic and properties for the new liquids. Using the same tank geometry and different fill levels, the SLOSH code provided mechanical system properties and they were compared with the previous results obtained with water. Table 3-1 illustrates the SLOSH code output for the liquids in the experiment.

Several conditions were tested using the SLOSH code with several liquids filled a different fill levels. The code results consider the free surface slosh conditions for all liquids and different fill level tests. These values obtained were then used as the initial values and parameter estimation values for the tests that include a diaphragm in the tank.

Table 3-1. SLOSH code prediction for all tested liquids

Fill Level %	Glycerine			Corn Syrup			Water		
	60	70	80	60	70	80	60	70	80
Liquid Mass (kg)	3 587	4 340	4 960	3 900	4 719	5 393	2 842	3 438	3 929
Liquid Surface Height (M)	0 122	0 142	0 163	0 122	0 142	0 163	0 122	0 142	0 163
First Mode Parameters									
Pend. Mass (kg)	1 689	1 532	1 133	1 836	1 666	1 232	1 338	1 214	0 898
Pend. Length (M)	0 057	0 047	0 037	0 057	0 047	0 037	0 057	0 047	0 037
Pend. Hinge z-location (M)	0 102	0 104	0 109	0 102	0 104	0 109	0 102	0 104	0 109
Pend. % crit. Damping	8 839	10 990	15 300	10 360	12 880	17 930	0 703	0 874	1 217
Ratio of Slosh Amplitude to pend. Amplitude	1 448	1 541	1 635	1 448	1 541	1 635	1 448	1 541	1 635
Second Mode Parameters									
Pend. Mass (kg)	0 060	0 079	0 083	0 066	0 086	0 091	0 048	0 063	0 066
Pend. Length (M)	0 018	0 017	0 014	0 018	0 017	0 014	0 018	0 017	0 014
Pend. Hinge z-location (M)	0 100	0 100	0 095	0 100	0 100	0 095	0 100	0 100	0 095
Pend. % crit. Damping	8 839	10 990	15 300	10 360	12 880	17 930	0 703	0 874	1 217
Ratio of Slosh Amplitude to pend. Amplitude	0 405	0 506	0 627	0 405	0 506	0 627	0 405	0 506	0 627
Fixed Mass Parameters									
Mass (kg)	1 838	2 728	3 743	1 998	2 966	4 070	1 456	2 161	2 965
Z-location (M)	0 101	0 100	0 099	0 101	0 100	0 099	0 101	0 100	0 099
Mom. Inertia (kg*M <sup>2</sup> )	0 008	0 013	0 018	0 009	0 014	0 019	0 007	0 010	0 014
1st Mode Slosh Frequency	2 092	2 288	2 600	2 092	2 288	2 600	2 093	2 289	2 601
2nd Mode Slosh Frequency	3 664	3 828	4 147	3 664	3 828	4 147	3 666	3 830	4 149
*Frequencies are cycles/sec.									

As predicted with the SLOSH code output, damping is a critical parameter when comparing the liquids with different viscosities. Parameters such as the slosh frequency and pendulum length remain the same for all liquids regardless of their viscosities.

## 4 EXPERIMENTAL SETUP

The experimental set-up was incorporated and assembled to include a linear actuator that excites the filled tanks in a lateral motion. This equipment allows for better lateral control movements and more accurate data reading and collection. The whole assembly consists of a linear actuator assembly that includes a force transducer attachment and the test tank assembly. The tank is a spherical transparent container which is filled with the liquid's fill level defined for testing. The tank is excited by the linear actuator as it oscillates at a predetermined frequency and displacement amplitude. The forces due to fuel slosh will be measured using a force transducer mounted on the fixture.

### 4.1 Lateral Slosh Test Setup

The experimental setup was updated and modified to include a state-of-the-art linear actuator. The linear actuator is an Aerotech model LMA-ES 16062 (Figure 4-1). The “shaker”, commonly referred to as the linear actuator, needed to be securely anchored on a table stand.

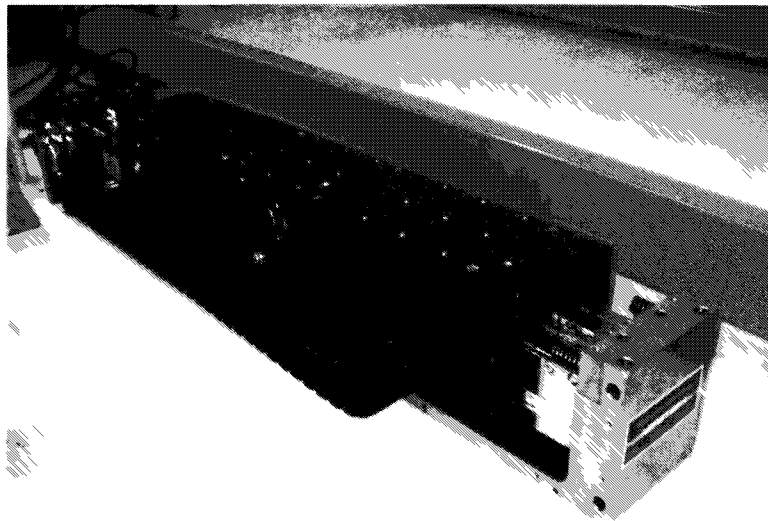
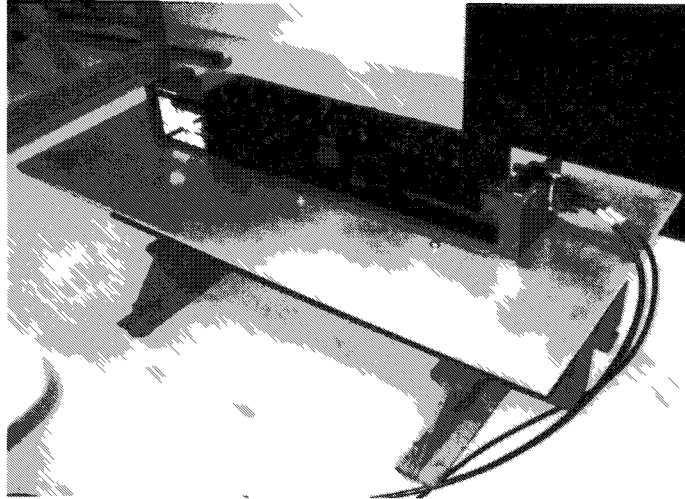


Figure 4-1. Aerotech linear actuator

The “shaker” table stand consisted of two steel beams and an aluminum plate. After securely bolting the “shaker” onto the stand (Figure 4-2), the linear actuator was ready for the installation of the software.



**Figure 4-2. Mounted linear actuator**

The motion of the tank is induced by this linear actuator and the attachment assembly. An attachment part was designed and fabricated which served as the connection between the linear actuator and the test tank. The design for the attachment part allowed the part to be bolted on the top surface of the linear actuator, subsequently the placement of the attachment could be modified depending on the testing conditions and the needed displacement.

First, a CATIA solid model was created for the attachment part. Utilizing the Haas Vertical Milling Center, located in the manufacturing lab at ERAU, a block of 6061 Aluminum was utilized to fabricate the attachment part. Figure 4-3, illustrates the block of aluminum stock being prepared by the Milling machine. The Milling machine proceeded to cut the stock to the dimensions prescribed by the CAD file thus producing the final product.

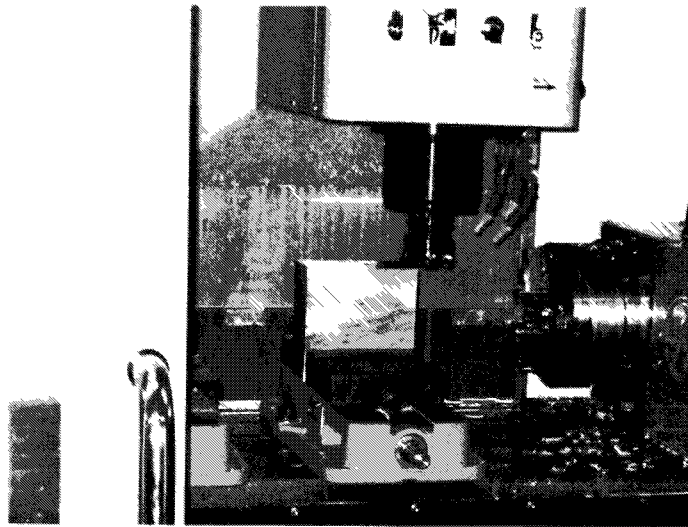


**Figure 4-3. Aluminum stock in the Haas Vertical Milling Center**

After several stages, the aluminum stock was prepared, and bolted on a fixture that will restrain the stock while the part profile is being cut by the machine. The part profile is almost completed and the part's shape is more defined as illustrated in Figure 4-4

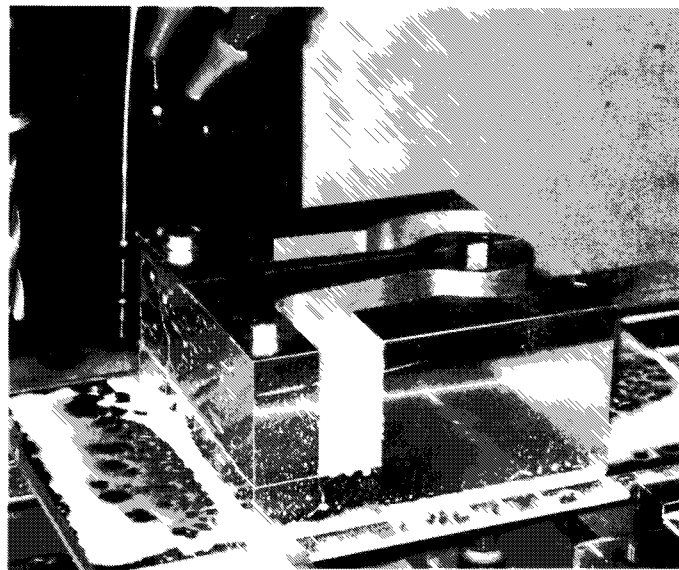


**Figure 4-4. Machined part profile during fabrication**

The attachment part was completed and bolted on the top of the linear actuator surface, as shown in Figure 4-5. The attachment part can be adapted to other applications such as exciting much larger tanks and to apply larger displacements to the testing tanks.



**Figure 4-5. Attachment part on “shaker”**

The attachment part is fixed to a push rod where the force transducer is fastened and joins the tank to the whole system. The attachment part and the push rod (stinger) complete the linear actuator assembly for the lateral slosh experimental set-up.

The force transducer used to obtain the experimental data is the same force transducer used by previous research<sup>16</sup>, a Honeywell Sensotec model  $31 \pm 5$  lb load cell. For the data acquisition recording a Measurement Computing PMD-1680FS, external USB data acquisition card is used. Figure 4-6, illustrates the linear actuator assembly including the force transducer and the testing tank.

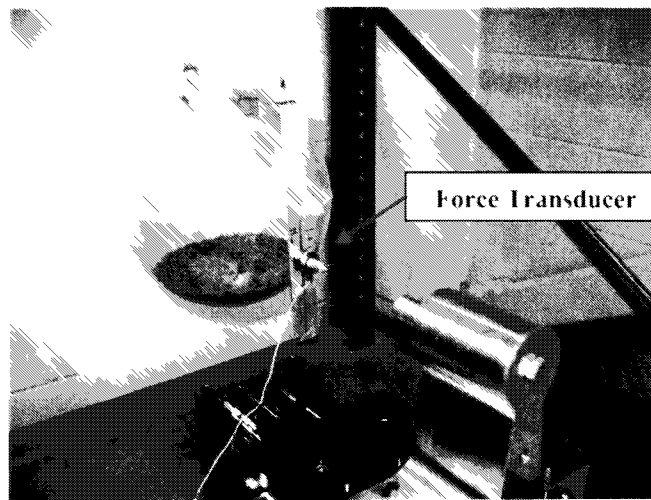


**Figure 4-6. Linear actuator assembly attached to tank**

Figure 4-7 illustrates the CATIA model of the experimental set up and the components included in the assembly. The 3-D solid model includes the components in the linear actuator assembly: linear actuator, attachment part, push rod, and transducer. In addition the model incorporates the tank assembly including the hanging cables as well as the overall frame structure.

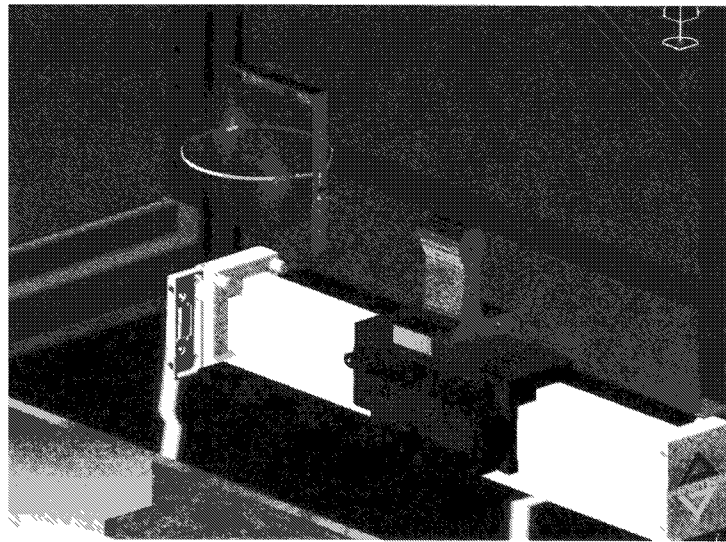


**Figure 4-7. CATIA model of the experimental set up**

## **4.2 Test Tanks**

Spherical tanks have been investigated both analytically and experimentally to determine the sloshing frequencies and forces for unrestricted liquid oscillations.<sup>17</sup> The tanks used in the experiment set-up are eight inch spherical clear acrylic globes. The tanks have an opening which allow for the placement of eye bolts where the cables are attached and the tank is suspended. The force transducer is attached to the tank's bracket which has the marked locations of the tank's center of gravity for each of the tested fill levels. Figure 4-8 illustrates the experimental tank set-up including the force transducer attachment location to the linear assembly.

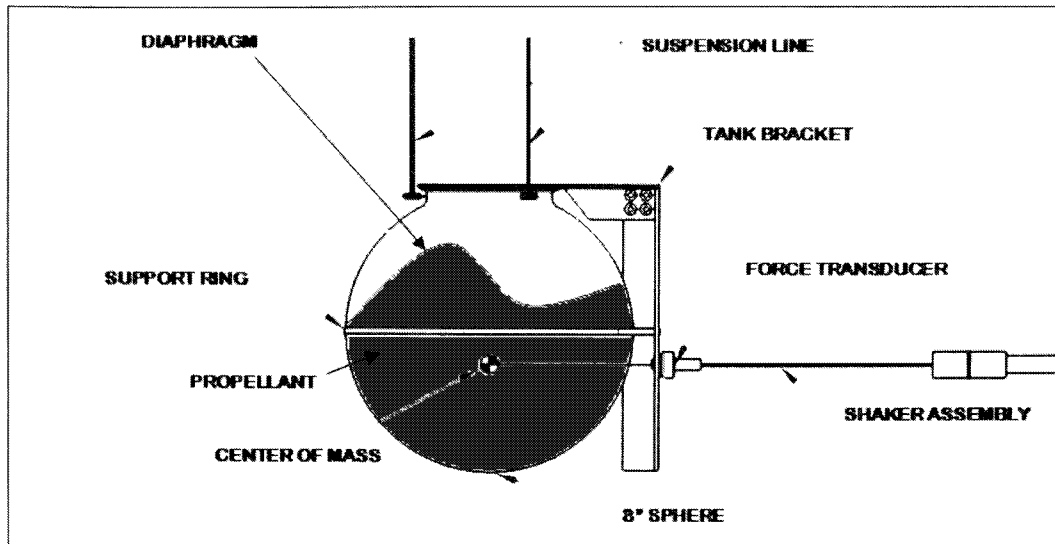


Figure 4-8. Schematic diagram of experimental tank with the diaphragm

For the diaphragm tanks, the tanks were split in half in order to attach the diaphragm in the middle of the tank. In addition, the tanks have a valve in the bottom part of the tank for addition or removal of liquid from the tank.

### 4.3 Test Fluids

The liquid chosen for testing was water which is an excellent and frequently used substitute for hazardous propellants. Water's fluid properties (density, viscosity, etc.) are nearly identical to those of hydrazine, the most commonly used propellant. The first step is to experiment with several liquids with different viscosities in order to better understand the lateral fuel slosh effects. The resistance to flow of a fluid and the resistance to the movement of an object through a fluid are usually stated in terms of the viscosity of the fluid. By utilizing variation of viscosity, other fluids can be tested and the results can be compared with the previously obtained results. Liquids of varying viscosities and physical characteristics different from water are used in the test propellant tank (Table 4-1). It is assumed that for higher viscosities the resonance frequency is slightly higher than the predicted value for an ideal liquid, as reported in prior research.<sup>18</sup>



**Table 4-1. Comparison of viscosities of different liquids**

<b>Liquid</b>	<b>Viscosity (Poise)</b>
Hydrazine	0.01
Water	0.01
Glycerine	13
Corn Syrup	22

This assumption about the liquids frequency is one of the few parameters that can be determined with the execution of the free surface slosh experimental set-up. In addition, the results of the data obtained from the different liquids will evaluate the effectiveness of the fuel slosh modeling previously used. Consequently, this prepares the experiment for the inclusion of the diaphragms.

#### **4.4 Test Diaphragms**

Extensive analysis has been done on the different tank shapes and locations, as well as the use of PMDs. Companies like Pressure Systems Inc. (PSI) have been manufacturing diaphragm tanks for many years and have tested and demonstrated that the diaphragm provides an inherently superior slosh control compared to other PMDs. Figure 4-9 shows one of the PSI elastomeric diaphragms undergoing slosh testing.

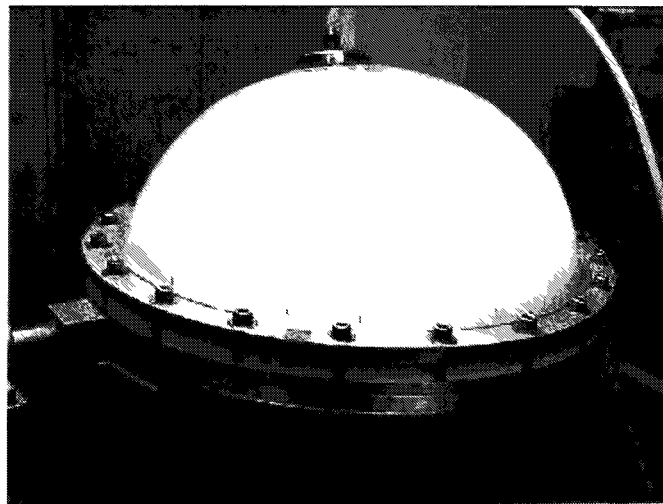


**Figure 4-9. Photograph of an elastomeric diaphragm (Courtesy: PSI)**

The diaphragm tanks are eight inch acrylic spheres that include the mounting bracket, to securely and accurately fasten the force transducer, also a location where the tank will attach to the hanging cables. Each of the diaphragms is made of different materials with differing stiffness characteristics. The difference in stiffness of the diaphragms is a parameter that will be taken in consideration during simulation as well as allowing for association in behavior among the diaphragm tanks under testing conditions.

The first material is from a “toy ball” with the same diameter as the test tank. The thickness of this ball’s material is 0.609mm (.024in). Also, the material have “spikes” over the surface, which are 6.35mm (.25in) tall and about in a 19.05mm (.75in)-spaced pattern over the entire surface. Another material used for the other diaphragm test tank was from a small yellow marine buoy. The thickness of this diaphragm is the about 2.263mm (.081in). The material thickness for this tank is over three times of the Spike diaphragm tank. The thickness difference among the diaphragm materials will allow for a comparison and contrast of the effects the diaphragm has on the slosh behavior. The thickness characteristics and values can aid for the determination of other parameters such as the stiffness of the system. Other parameters that can be determined with the diaphragm tank tests are the level of slosh damping and also the effective mass of liquid participating in the sloshing of the fluid. Figure 4-10 illustrates the finished diaphragm tanks and the free surface test tank which is attached to the linear actuator assembly.



Figure 4-10. Diaphragm tanks

Although there were four diaphragm tanks, two of these tanks were replaced by other tanks and a different diaphragm material due to the prior diaphragms being very rigid. Table 4-2 illustrates the differences among the diaphragm material used for the tanks.

**Table 4-2. Diaphragm tanks characteristics comparison**

<b>Diaphragm</b>	<b>Spike</b>	<b>Yellow</b>	<b>Sky</b>
Color	Purple	Yellow	Blue
Weight (g)	50	152	44
Thickness (mm)	0.609	2.263	.660

Using various diaphragm materials allowed for the visualization of the damping effects present in these test tanks. Diaphragms provide a substantial level of slosh damping as a result of the combination of viscoelastic flexing of the diaphragm and the increased viscous effects at the liquid-diaphragm interface.<sup>19</sup> A diaphragm also increases the slosh natural frequency because of the constraints imposed on the free surface shape. In addition, the effective mass of liquid participating in the sloshing is slightly smaller than for a tank of the same shape and fill level without a diaphragm.

#### 4.5 Test Setup Calibration

In order to obtain accurate results, an initial calibration of the force transducer was necessary. Several readings were collected and compared with the actual values to determine the accuracy of the force transducer. Figure 4-11 illustrates that with the aid of the “stinger”, very small readings were used in the calibration process.

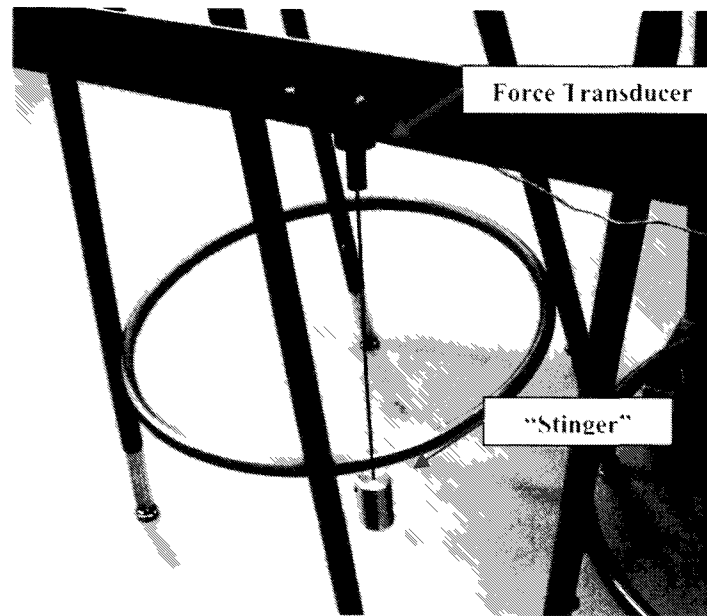


Figure 4-11. Force transducer calibration

The following Table 4-3 illustrates the comparison of the transducer readings when a force or weight was applied to induce tension. The force transducer reads for each one volt the equivalent to a pound reading.

Table 4-3. Comparison on force transducer readings

Transducer Calibration	
True Mass (lb)	Transducer Reading (Volts)
0.05	0.058
0.075	0.078
0.125	0.128

For each of the test runs, besides the initial force transducer calibration, the force reading was calibrated at the beginning of each test to assure that at no applied force the transducer reading was zero.

#### 4.6 Test Matrix

The research test matrix was specified to determine the necessary number and types of tests to be performed. First, a test matrix was designed for free surface testing which included the various liquids. The free surface testing matrix was summarized with the following flow diagram, Figure 4-12.

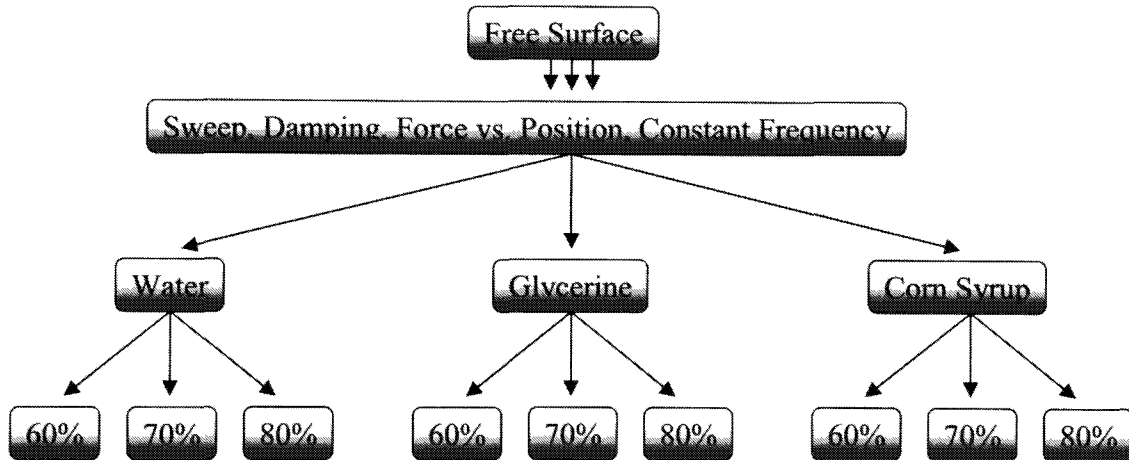


Figure 4-12. Free surface test flow diagram

The free surface condition testing was performed on tanks that were filled with water, glycerine, and corn syrup. Several tests were run for each of the liquids, but preliminary tests were necessary in order to obtain some initial values needed for future tests. The sweep, damping, and force vs. position tests were executed to aid with the estimation, or in the case of free surface testing, to verify the SLOSH code outputs values such as

frequency among other parameters. The next set of tests consisted of several constant frequency tests for all liquids at several fill levels.

The same approach was taken for the diaphragm tanks tests. First, the preliminary tests were executed to assist with verification since the SLOSH code does not offer estimated parameter values that can aid with the modeling of the experimental set-up. The sweep, damping, and force vs. position tests allowed for an estimation and approximation of natural frequency values as well as visualizing when the resonance occurs for these specific diaphragm cases. Subsequently, the various constant frequency tests were performed with the three diaphragm tanks filled at the different fill levels.

Figure 4-13 illustrates the flow diagram for diaphragm tank tests.

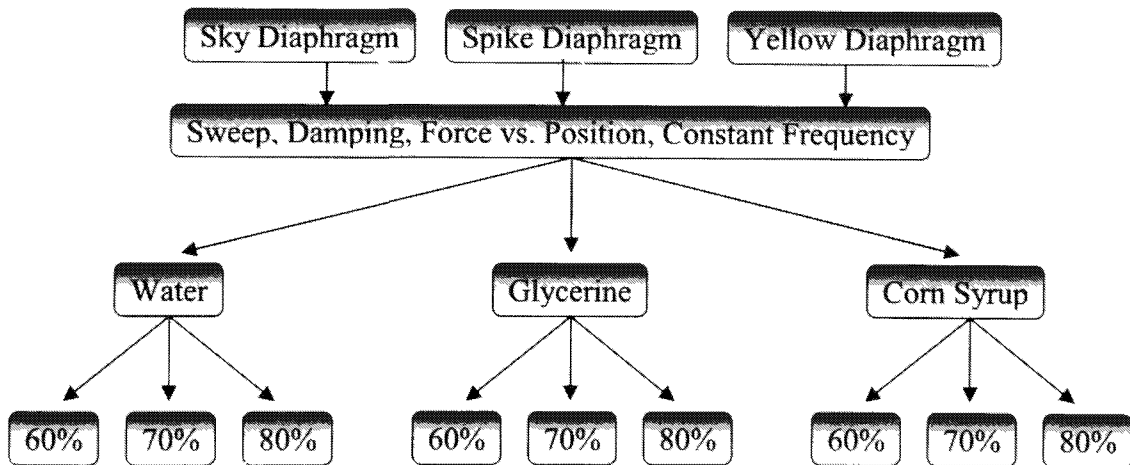


Figure 4-13. Diaphragm test flow diagram

A more detailed test matrix for constant frequency runs for all test conditions that lists the frequencies tested for all tank conditions is included in Appendix A.

## **5 EXPERIMENT PROCEDURE**

Prior to the initiation of testing and data collection, the data acquisition system has to be arranged accordingly and organized for data collection and documentation. The data measured using the force transducer is recorded via the data acquisition card and the data acquisition software assists with the analysis and interpretation of the collected data.

After the data collection is completed, the next step was to construct a model of the experimental set-up and execute simulations to compare and contrast results with the obtained data. MATLAB's Simulink software package enables the creation of the model and its simulation. SimMechanics toolbox and Parameter Estimation toolbox were used to complete the modeling procedures. SimMechanics aided with the modeling of the system where as Parameter Estimation enables the simulation of the created model and the comparison of the simulated and the empirical data.

In addition, preliminary testing was needed in order to obtain and determine some of the parameters needed for the creation and simulation of the experimental set-up model. Among these tests were the sweep test, damping test, and force vs. position test.

### **5.1 Data Acquisition**

The linear actuator included a single axis servo controller that combines the power supply, the amplifier, and the position controller in a single package. The Soloist (Figure 5-1) has a high position latch inputs and advanced data logging capabilities that made it ideal for this research and testing application.



Figure 5-1. Soloist hardware

The advanced software architecture integrated with the linear actuator facilitates the manipulation of the testing force and displacement specified for each of the test conditions. The Soloist interface application assists with every control component and with the complete description of the systems status. Figure 5-2 shows the Soloist HMI interface displaying a test script

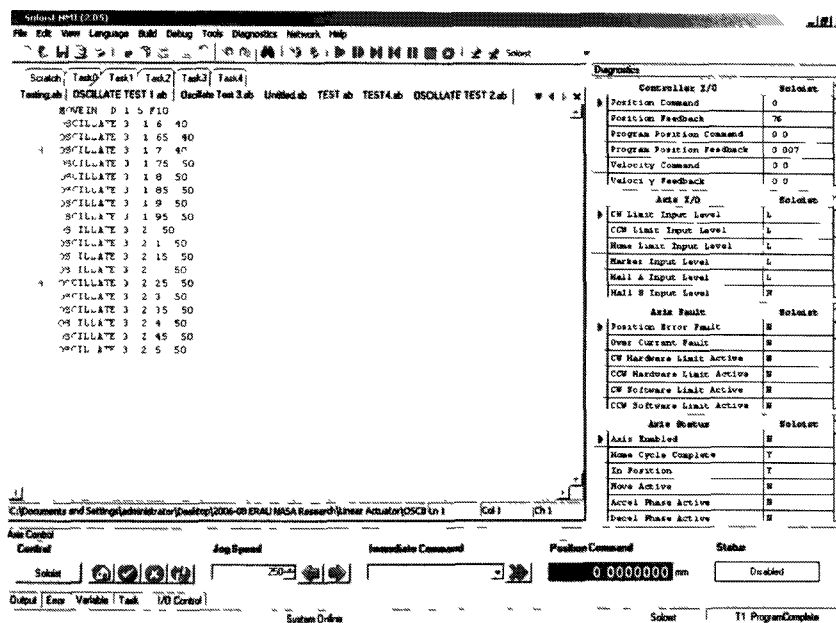


Figure 5-2. Soloist HMI interface screen display



The test script describes the force, the displacement, the type of movement, and the duration of the test. Also the interface allows for modifications on where the linear actuator home is located and can be adjusted accommodating the test requirements. The Soloist software also includes support for the software program LabVIEW. A library of block diagrams is integrated to assist in the creation of custom Graphical User Interface (GUI) applications. Figure 5-3 illustrates the GUI provided by the Soloist software that can be run through the LabVIEW program. In this case, a script is not necessary because the GUI controls the linear actuator behavior.

The measured data was collected and using the LabVIEW program. The force transducer readings were displayed in real time during each of the tests. The force transducer is rated at one Volt per pound measured. Therefore, the LabVIEW block diagram was adjusted and the interface displaying the measured readings included this relation.

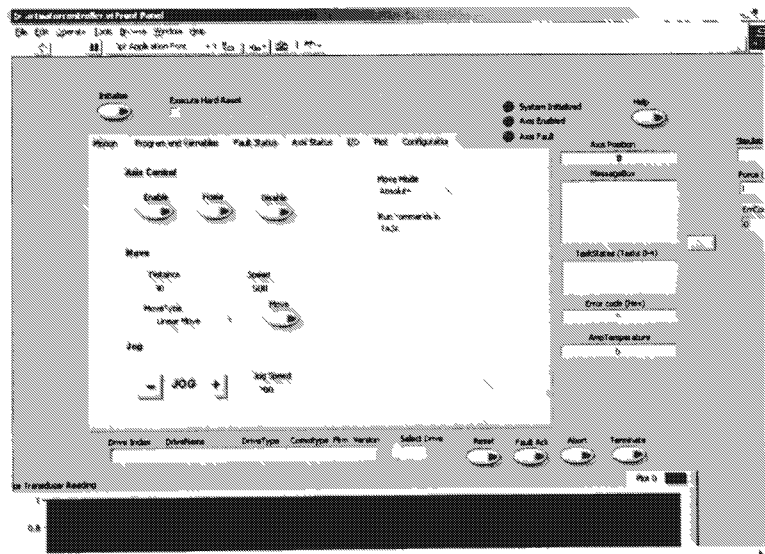


Figure 5-3. LabVIEW interface screen display

Once the test is finished, the information was then saved as an Excel file. Subsequently, the data can be analyzed using both Excel and MATLAB.



The model consists of body, joint, sensor, and actuator blocks which are organized and arranged in a way that describes the actual behavior of the experimental set-up. The body blocks include the mass and inertia characteristics of the components in the system, then the joints blocks describe the way the bodies are connected and directly affect the other connected bodies. The actuator blocks specify the actual movement or force that either the bodies or joints have in order to follow the actual behavior of the system components.

The SimMechanics model can be divided in several main groups with specific functions and components. The first group is the one that includes the blocks that describes the motion behavior of the linear actuator. In the case of this model, a sine wave input arrangement was integrated to control the linear actuator assembly movement as shown in Figure 5-5 .

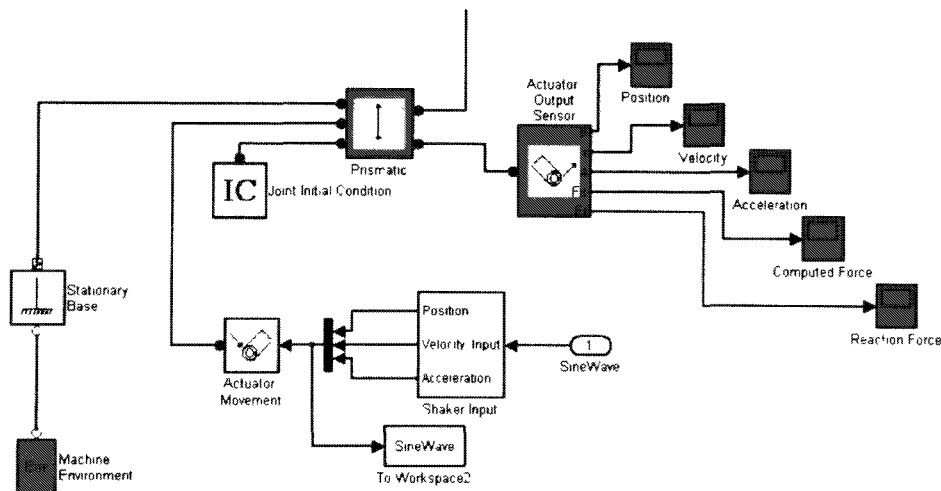


**Figure 5-5. SimMechanics model sine wave input**

The sine wave parameters describe the same frequency and displacement prescribed during testing procedures. With the aid of Simulink blocks, the necessary equations were introduced and applied to simulate the linear actuator behavior.

The linear actuator assembly was constructed in a subgroup (Figure 5-6) that included several components such as the moving base of the actuator, attachment part, and stinger.

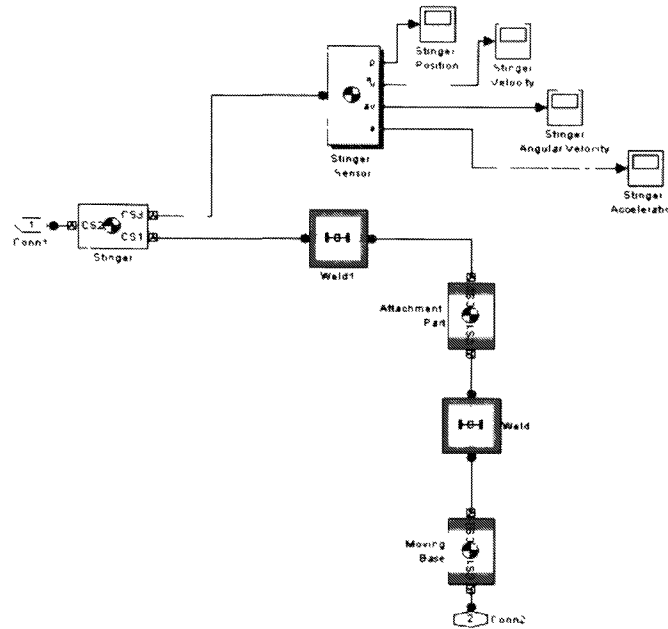


Figure 5-6. Linear actuator assembly subgroup

The singer is the component of this group that is also attached to the test tank. In the same connection, a force transducer is located and fixed with proper sensors for data reading. Figure 5-7 illustrates both the test tank and the force transducer arrangements.

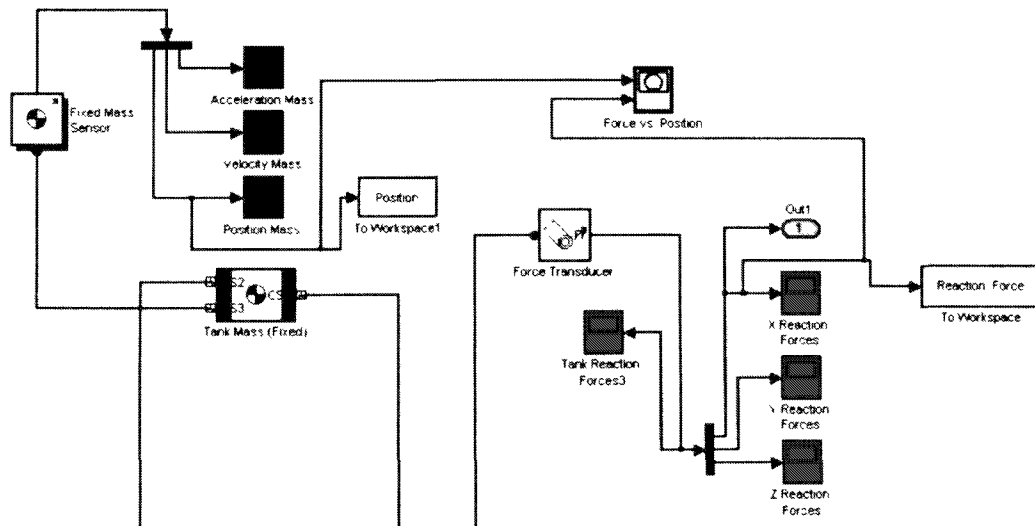
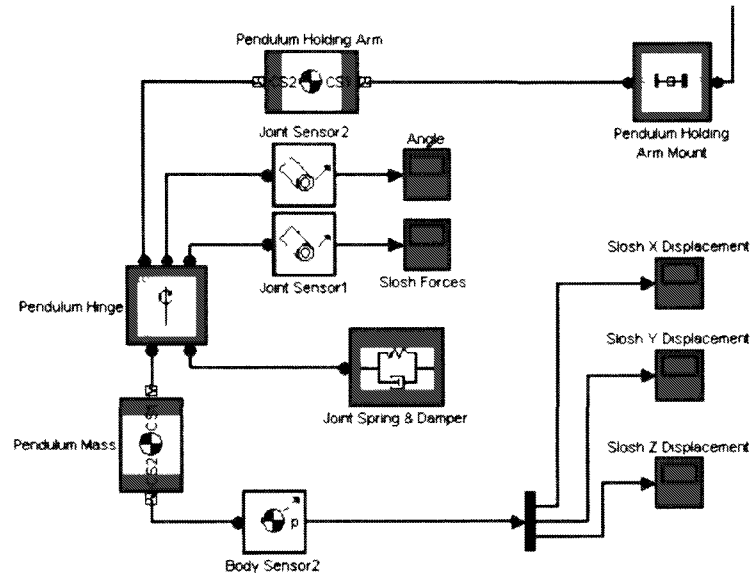


Figure 5-7. Test tank and force transducer arrangement

The test tank includes the fixed mass parameter value previously explained as part of the pendulum mechanical model application. There are two masses inside the tank that describes the model theory, fixed mass and sloshing mass. Then the test tank was linked to the pendulum mechanical analog model which simulates the sloshing behavior of the liquid in the tank (Figure 5-8).



**Figure 5-8. Pendulum mechanical analog model**

The pendulum model included a pendulum holding arm with a specific length and an attached hinge where the pendulum mass was directly linked. The pendulum mass or sloshing mass is another parameter previously determined from the SLOSH code for free surface conditions. However, the sloshing mass is a critical parameter during model simulation as well as the pendulum length, stiffness, and damping during diaphragm testing.

The introduction of diaphragms to this experimental set-up will aid for a better and more complete estimation of fuel slosh characteristics for future applications. Modeling the diaphragm and the bulk motion and subsurface inertial waves generated in

lateral slosh in the presence of a diaphragm using SimMechanics will require the addition of a spring-damper combination to the existing model.

With the aid of the tools and interfaces of the SimMechanics software, the complete modeling of the experimental set-up was arranged. The SimMechanics model animation of the linear actuator attachment assembly and the test tank are illustrated in Figure 5-9.

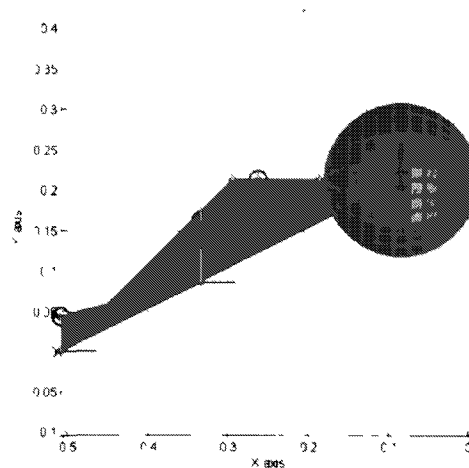


**Figure 5-9. SimMechanics model animation of the linear actuator assembly**

Once the body and joints blocks are defined and configured, the model animation can be used as a tool to verify the behavior of the system. This allows the user to minimized model errors early in the model build up process.

### **5.3 MATLAB Parameter Estimation**

Parameter Estimation is a MATLAB based product used for estimating a Simulink model's parameters based on experimental results. In order to use the software, the user needs to open Parameter Estimation from the "Tools" pull down menu in SimMechanics. Next, the input and output data must be imported into the model. The software allows the user to select the parameters to be estimated and enter an initial guess

for the parameter. For both the free surface and diaphragm models the following parameters were estimated: dampening ( $b$ ), stiffness ( $k$ ), slosh mass ( $smass$ ), and pendulum length ( $h$ ). Configuring the estimation allows the user to set the available data views, display plots, and edit the cost function settings. Figure 5-10 illustrates the model project under the simulation procedure and how the Control and Estimation tools manager aids with the simulation progress for better evaluation and monitoring.

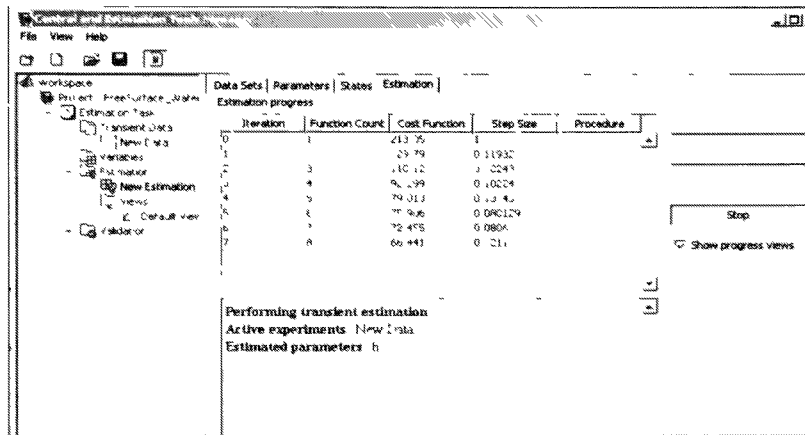


Figure 5-10. Parameter Estimation Toolbox project simulation

While the simulation is executing, the measured vs. simulated force responses are plotted for better visualization of the accuracy of the model (Figure 5-11).

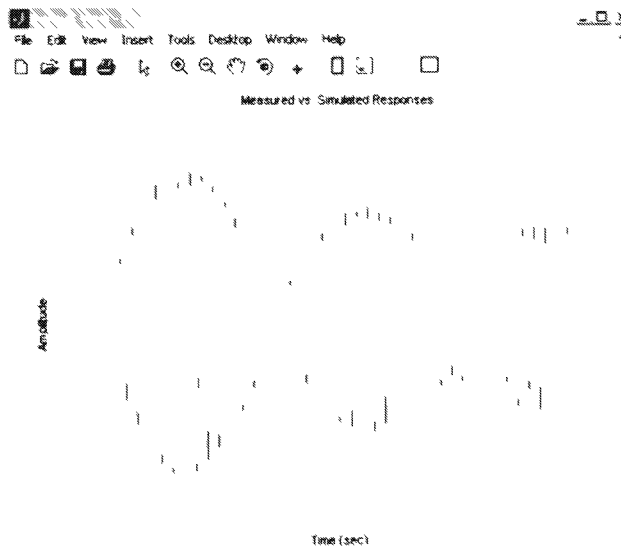


Figure 5-11. Measured vs. simulated plot of reaction forces

## 5.4 Preliminary Testing

The preliminary testing for this research project consisted of three different tests that were performed to aid with some of the assumptions and initial estimations that needed to be taken into consideration. This was especially true for the diaphragm tests. These tests were the sweep test, damping test, and force vs. position test.

### 5.4.1 Sweep Test

The sweep test consisted of allowing the test tanks to experience a range of frequency inputs which gradually increased in magnitude for a number of cycles. This test allows for the visualization of response force reaching maximum amplitude at resonance.

One of the completed tests included a tank filled with water to the 60% fill level and it was linearly excited for over a frequency range of 1.6Hz to 2.3Hz. Figure 5-12 illustrates the graph of the data showing a resonance at about 2.1Hz.

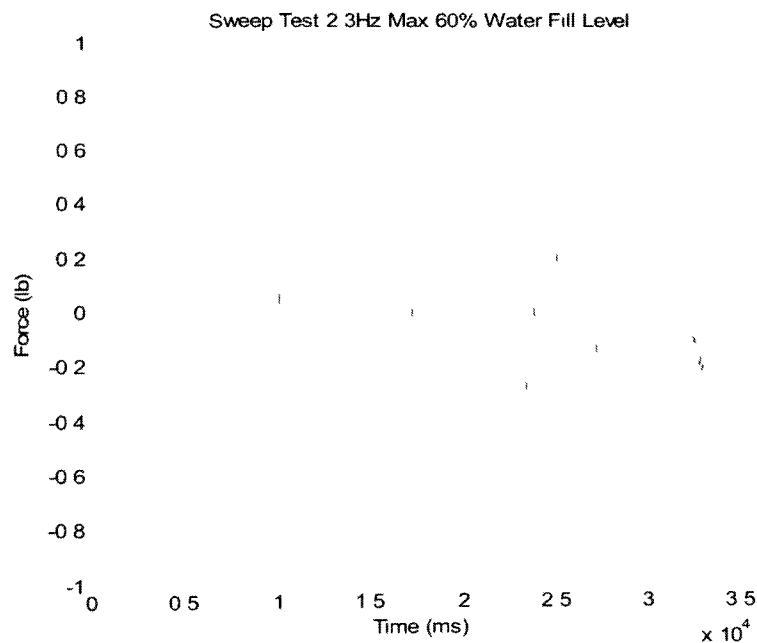


Figure 5-12. Sweep test graph



After evaluating the data, the estimated natural frequency can be verified from the graph. The sweep test was performed for all three fill levels (60%, 70%, and 80%) for water, as well with glycerine, and corn syrup under free surface conditions. The same test was considered for the diaphragm tanks as a way to determine the natural frequency. For free surface tanks, the SLOSH code was used as an initial estimate for parameters and pendulum model characteristics. However, this is not the case for the diaphragm tanks. For the previous test example, the resonance frequency was experimentally determined to be about 2.1Hz. These results verified with the SLOSH code prediction of a resonance frequency of 2.09Hz for water free surface testing at 60% fill level.

On the other hand, the sweep test results for the diaphragm tanks were quite different from the free surface results. As can be seen in Figure 5-13, it became difficult to graphically determine resonance for the diaphragm test.

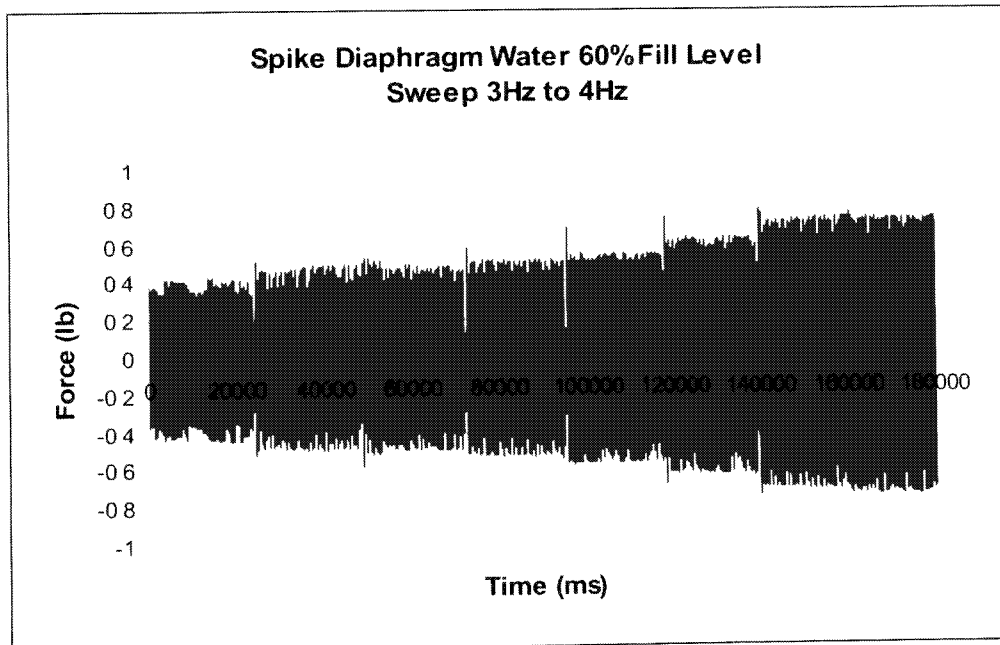


Figure 5-13. Spike diaphragm sweep test

In this case, the force amplitude kept increasing as the linear actuator increased the frequency input and the force amplitude did not decrease during the test. The same behavior was experienced with the Yellow diaphragm. As illustrated in Figure 5-14, the force amplitude kept increasing with frequency, even after the frequency input doubled from the previous free surface tests.

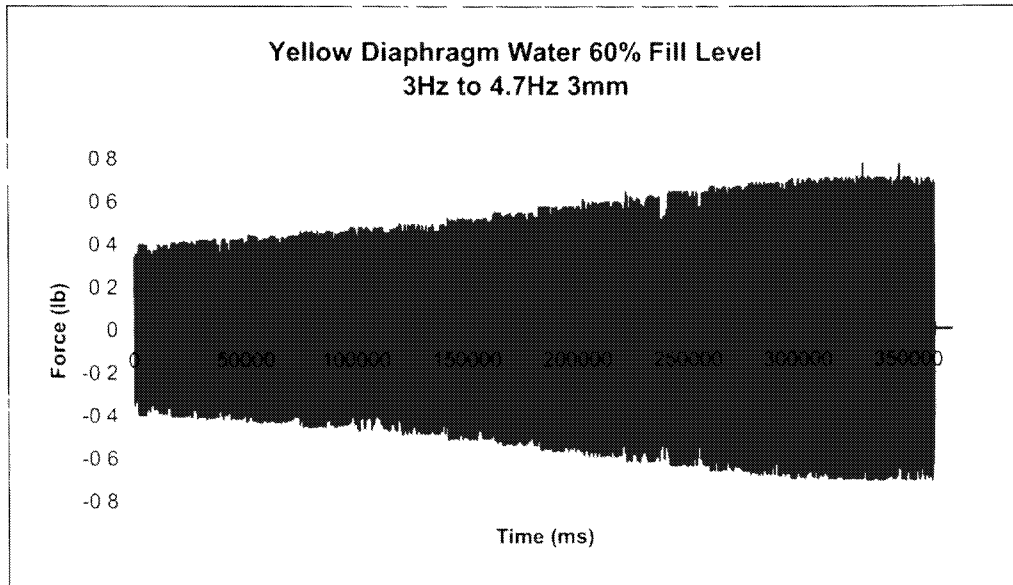


Figure 5-14. Yellow diaphragm sweep test

It was concluded, that even though the sweep test was another way to verify the values already given by the SLOSH code, for the case of the diaphragm tests, these sweep tests were not sufficient to determine the resonance on these tanks.

#### 5.4.2 Damping Test

Damping testing was performed on all test conditions to determine and calculate the logarithmic decrement and damping ratios. The tanks were laterally excited at different frequencies, from 1.757Hz up to 4.5Hz, for as much as 250 cycles. The tanks were linearly excited to the defined cycles, and then the linear actuator was stopped while the data was still recording the response forces of the tank. The tests were performed for

both free surface slosh and diaphragm testing conditions. The following data results include some of the experimental data of tanks filled to a 60% fill level with water, glycerine, and corn syrup for free surface and the “Spike” and “Yellow” diaphragm tanks.

The experimental data points were graphed and a trendline was also determined to obtain the function of the line. The logarithmic decrement  $\delta$  was calculated using its definition in Equation 5-1, is the natural logarithm of the ratio of the amplitudes of vibration on successive cycles, where  $T_d$  is the period of free underdamped vibrations or damped period.

$$\delta = \frac{1}{n} \ln \left( \frac{x(t)}{x(t+nT_d)} \right) \quad [5-1]$$

The following graph, Figure 5-15, illustrates the damping behavior of the water tank test filled at 60% fill level excited at a frequency of 2.15Hz and displacement amplitude of 3mm. Once the linear actuator stopped its lateral movement at a prescribed frequency and position input, the tank’s response force measurement was recorded and plotted. The vibration cycles were analyzed and their peak values were obtained.

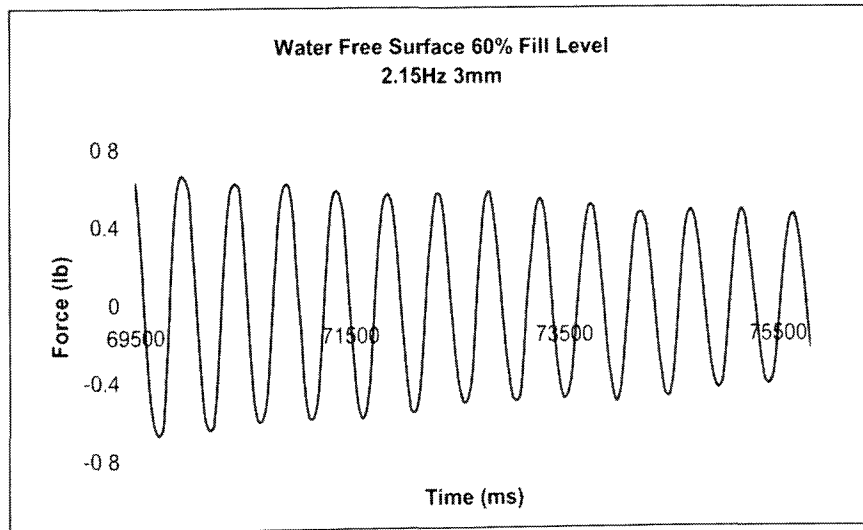


Figure 5-15. Damping graph water at 60% fill level excited at 2.15Hz

From the vibration cycle peak values, the slope was determined and plotted as illustrated in the following graph. Also the trendline of the data set was calculated, and the function was established as shown in Figure 5-16.

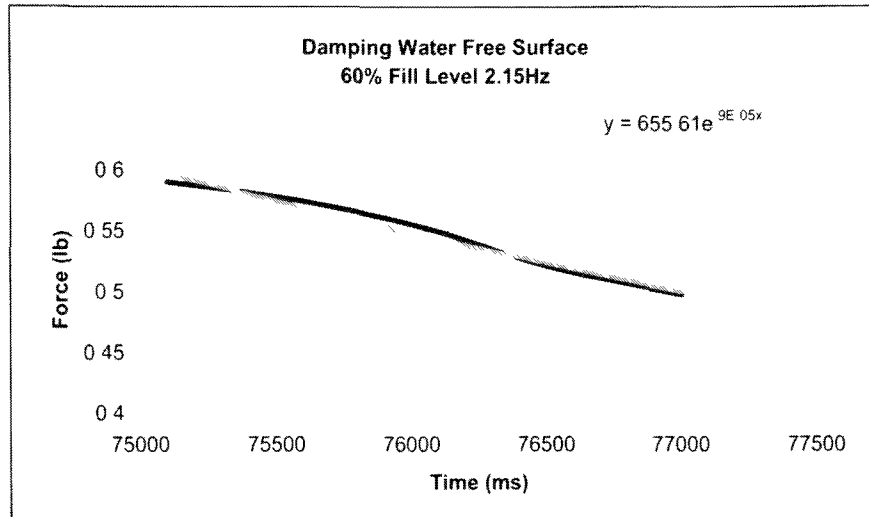


Figure 5-16. Damping slope water at 60% fill level excited at 2.15Hz

In addition, the damping ratios were calculated using Equation 5-2. For small damping ratio, the logarithmic decrement can be defined as function of the damping ratio. The damping ratio was approximately 0.002054 for this case of free surface condition for water filed at 60% fill level excited at a frequency of 2.15Hz.

$$\delta = 2\pi\zeta \quad [5-2]$$

The same procedure and analysis was repeated with the tank filled at 60% fill level with glycerine at free surface conditions. Figure 5-17 illustrates the damping data collected for the glycerine tank. It is easy to see the difference when comparing against the water test. The damping characteristics of the glycerine tank increase much more than the water tank, yielding a larger damping ratio. In addition, after obtaining the damping

slope for this glycerine test, the slope was found to be much steeper than the water test damping slope.

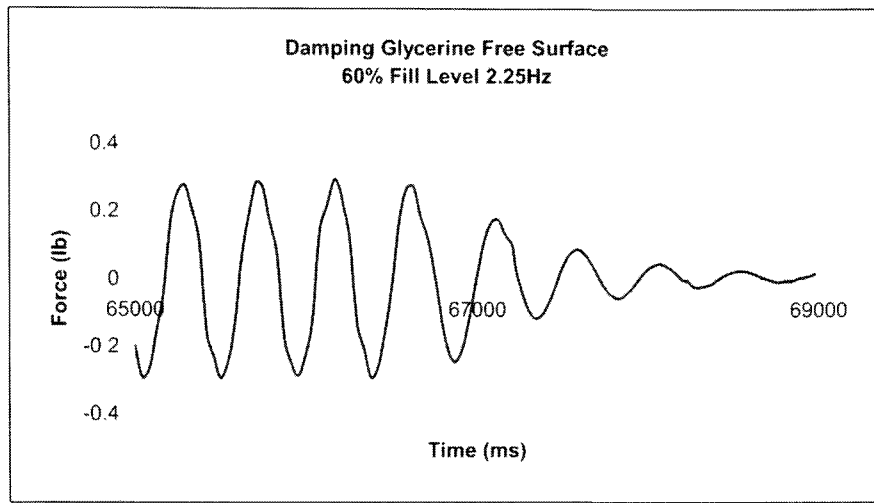


Figure 5-17. Damping graph glycerine at 60% fill level excited at 2.25Hz

Figure 5-18 illustrates the damping slope obtained with the peak vibration values acquired from the test data. The trendline was also determined from the data.

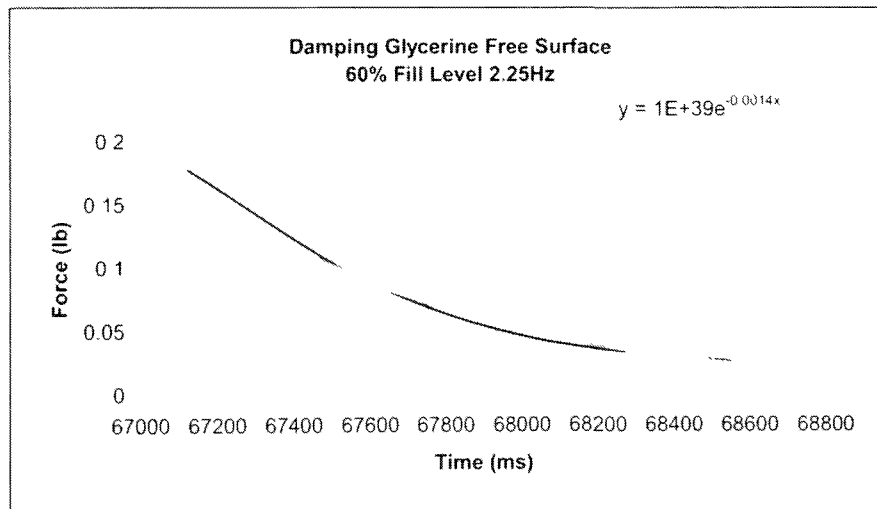
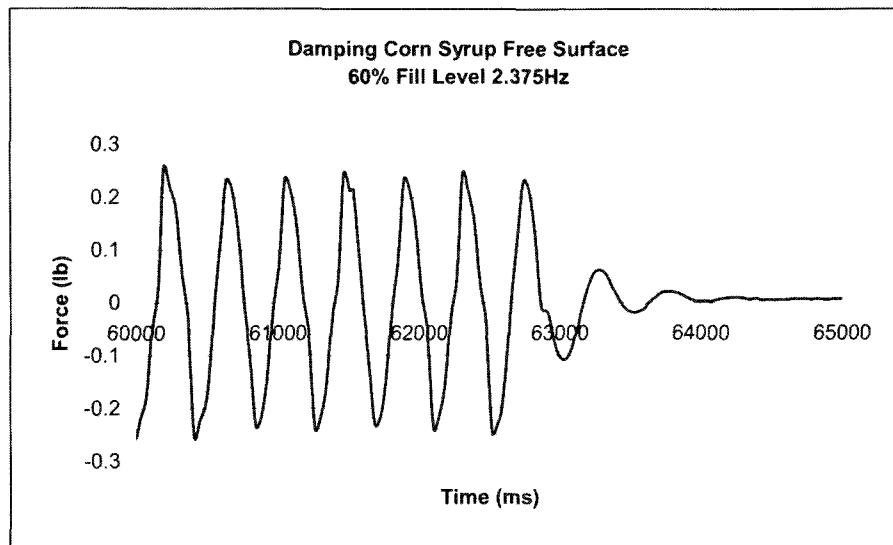


Figure 5-18. Damping slope glycerine at 60% fill level excited at 2.25Hz

The logarithmic decrement value was calculated using Equation 5-1. As can be seen by observing both water and glycerine free surface testing damping slope plots, the decrement values are quite different. For the glycerine, the decrement values are almost

24 times greater than the values for water. Subsequently, the damping ratios for glycerine are greater than that obtained for water of about 0.1085.

Next, the corn syrup tank filled to a 60% fill level was excited at a frequency of 2.375Hz. The observation and analysis was repeated for corn syrup free surface testing as previously described for both the water and glycerine free surface tests. Figure 5-19 illustrates the damping plot obtained with the test data for the tank free surface corn syrup tank at 60% fill level excited at a frequency of 2.375Hz.



**Figure 5-19. Damping graph corn syrup at 60% fill level excited at 2.375Hz**

Both Equation 5-1 and Equation 5-2 were used as previously described to calculate the values for the logarithmic decrement and damping ratio. It can be estimated that both the logarithmic decrement and damping ratio will be greater with the corn syrup test results than with all the other liquids in free surface testing conditions involved in this research (Figure 5-20).

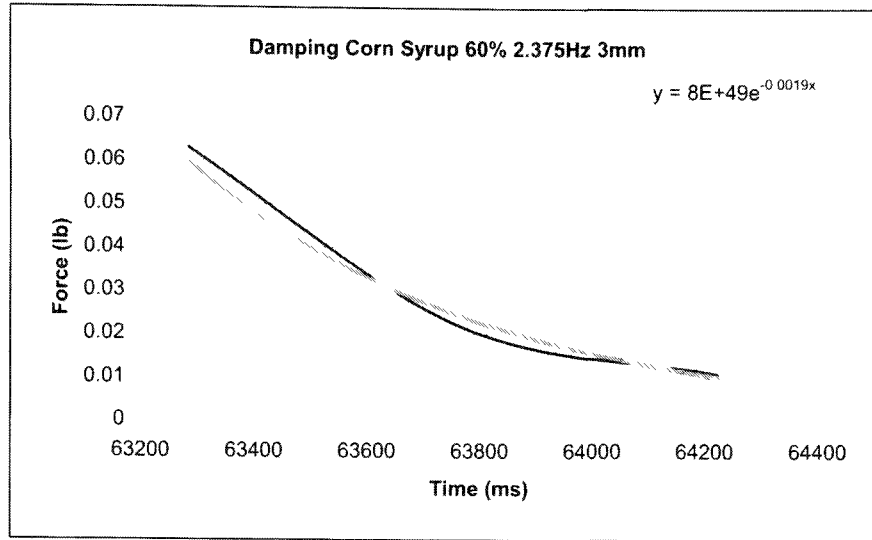


Figure 5-20. Damping slope corn syrup at 60% fill level excited at 2.375Hz

After reviewing the plots, both values the logarithmic decrement and the damping ratio are the greatest among the liquids tested for the free surface conditions. The damping ratio in this case is also the greatest for free surface with a value of 0.1675.

The following results include damping plots for both Spike and Yellow diaphragm tanks and calculations for logarithmic decrement and damping ratio. Several test runs were performed for the Spike diaphragm tank analysis (Figure 5-21).

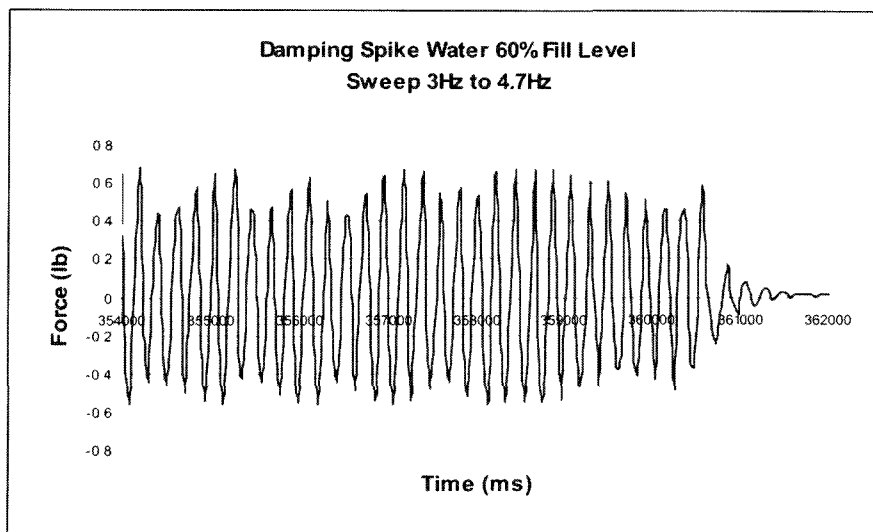
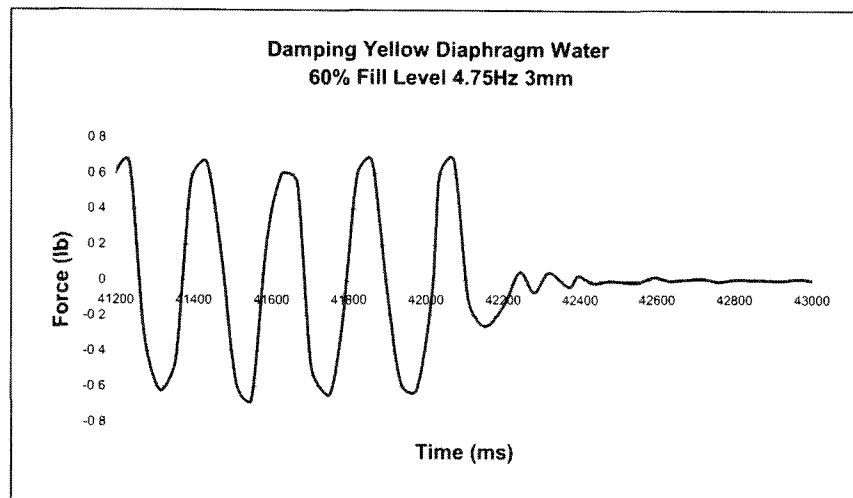


Figure 5-21. Damping graph Spike diaphragm at 60% fill level

The results for the Spike diaphragm were considerably higher when compared with water in free surface slosh conditions. On the other hand, for glycerine and corn syrup the results are similar, the logarithmic decrement value calculated is 1.0750 and the damping ratio value is 0.1711.

Several test runs were performed on the Yellow diaphragm tank for data collection and analysis (Figure 5-22).



**Figure 5-22. Damping graph Yellow diaphragm at 60% fill level excited at 4.75Hz**

When comparing both diaphragms, the only difference between them is the diaphragm material characteristics. Same liquid filled at same fill level and excited at the same frequency and displacement. Yet, the Yellow diaphragm is thicker than the Spike diaphragm. When the Yellow diaphragm is under testing conditions, it seems that the diaphragm dramatically restricts fluid motion. Even after increasing the frequency of the testing condition, the Yellow diaphragm contained the liquid much better than the Spike diaphragm. The values for logarithmic decrement and damping ratio were determined from the Yellow diaphragm data. The values are considerably higher than the Spike diaphragm values as the logarithmic decrement is 1.7047 and the damping ratio is 0.2713.



### 5.4.3 Force vs. Position Test

During testing, the response force values were collected for each of the tanks, both free surface slosh and diaphragm conditions. These values were plotted against the tank's position. The force vs. position plot illustrates the relation between the amplitude of the response force and the position for given excitation frequency. The response force is found to be largest when the frequency of excitation is closer to the resonance state. Resonance can be identified by linear grouping between force and position which was illustrated during the different frequency tests.

Throughout the free surface testing, force vs. position plots were obtained for all liquids. The results of the plots were compared with the natural frequency estimations and calculated values. After comparing the estimation values with the behavior of the plots, there was a noticeable correlation and agreement between the estimations and the plots results. For water testing, the values estimated and the plots obtained correlated successfully. Figure 5-23 illustrates the force vs. position plot obtained for the tank filled with glycerine at a 60% fill level, excited at a frequency of 2.15Hz, with displacement amplitude of 3mm. For the glycerine tests, the estimation for the natural frequency was slightly higher than with water tanks under free surface slosh conditions. In Figure 5-23, glycerine was excited at the frequency which water reached resonance, it can be seen that the system is not resonating at this frequency due to the non-linear grouping of the force vs. position plot.

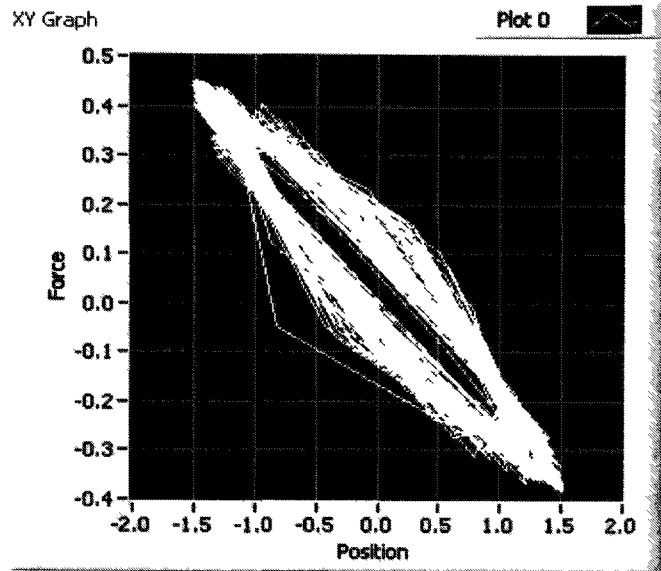


Figure 5-23. Force-displacement plot for free surface slosh approaching resonance (glycerine, 60% fill level, 2.15Hz, 3mm amplitude)

Figure 5-24 illustrate the force vs. position plot obtained for the tank filled with corn syrup at a 60% fill level, excited at a frequency of 2.375Hz, with displacement amplitude of 3mm. The resonance frequency for the corn syrup tank is illustrated in Figure 5-24, which is slightly higher when compared to the glycerine test case.

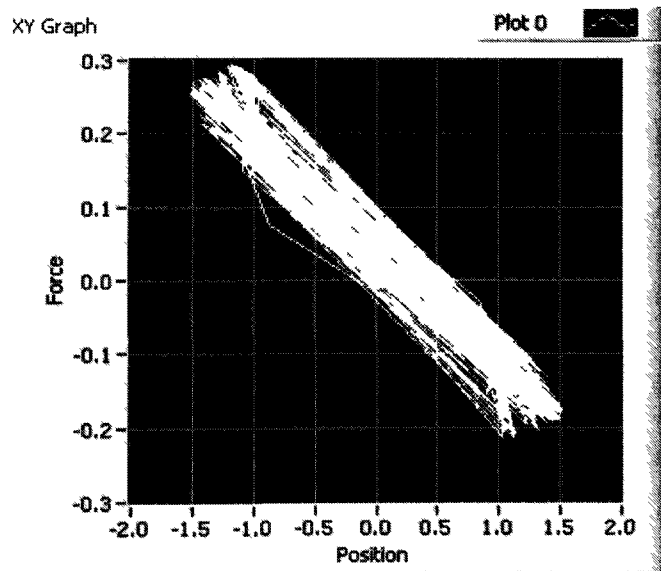


Figure 5-24. Force-displacement plot for free surface slosh at resonance (corn syrup, 60% fill level, 2.375Hz, 3mm amplitude)

The force vs. position plots serve as a method to verify the estimated resonant frequency for the filled tanks. As the resonance is reached, the forces vs. position plots illustrate the phase shift that occurs. The free surface slosh conditions with the different liquids can be compared with the plots obtained with the diaphragm tanks. The diaphragm tanks included the three different diaphragm materials for comparison.

The force vs. position test results and resonance estimations are compared with the estimation based on the SLOSH code although this is only accurate for the free surface tests. For the diaphragm tests, the force vs. position test result comparison is made between the sweep tests and the damping tests.

Figure 5-25 illustrates the plot obtained for the Spike diaphragm excited at the same frequency as glycerine in Figure 5-23.

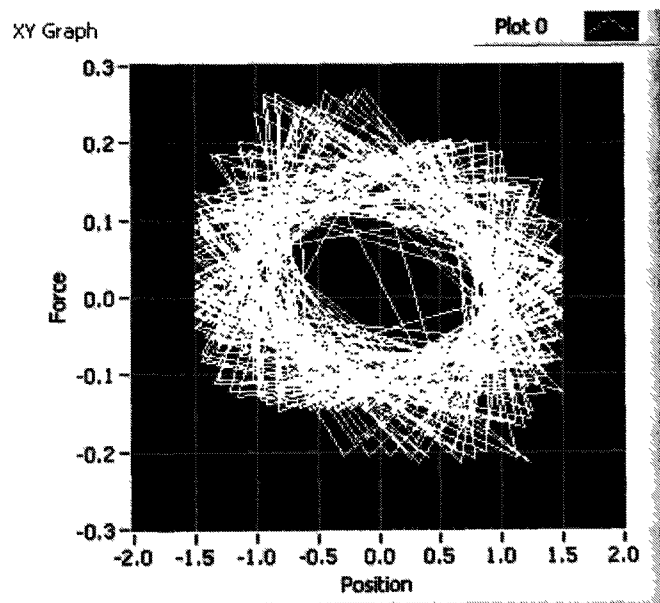


Figure 5-25. Force-displacement plot for Spike diaphragm tank (water, 60% fill level, 2.15Hz, 3mm amplitude)

While the glycerine tank was close to resonance under these testing conditions, the Spike diaphragm tank was not near resonance at this point, as illustrated in Figure 5-25.

The same can be concluded in the case of the other diaphragm tested, the Yellow diaphragm as shown on Figure 5-26. Both of the diaphragm tanks were filled with water for these tests at a 60% fill level.

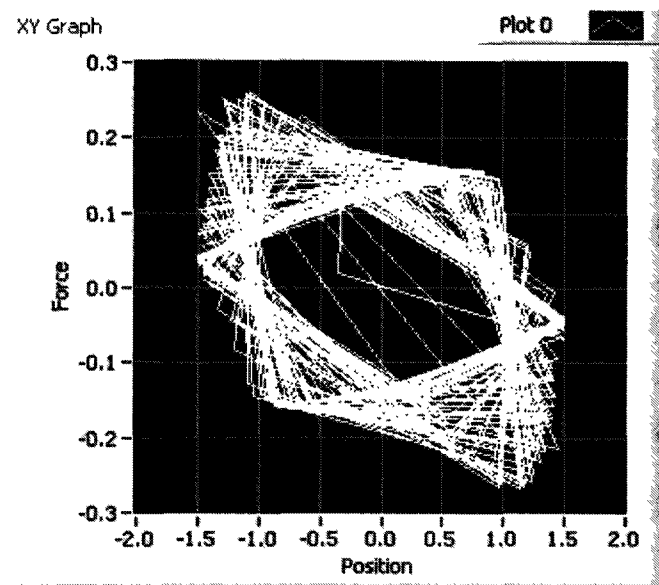


Figure 5-26. Force-displacement plot for Yellow diaphragm tank (water, 60% fill level, 2.25Hz, 3mm amplitude)

## **6 EXPERIMENT RESULTS AND DATA ANALYSIS**

Several tests were carried out to ensure that all the data needed was collected. Preliminary tests such as sweep test, damping test, and force vs. position assisted with the determination of parameters values that the SLOSH code was unable to estimate. Also, the constant frequency testing was executed for all test conditions which included several runs with a frequency range of 1.757Hz to 4.5Hz. The data collected from these tests are included in the Appendix CD as well as every test performed for all conditions and tank configurations.

In order to illustrate the last step of the research, a single excitation frequency was used for the comparison between the empirical data and the simulated data. This was done by using the SimMechanics model and the Parameter Estimation toolbox. In addition, a fixed mass tank test was performed to aid in the validation of the SimMechanics model. Lastly, to verify the previous research, testing with different liquids was performed using the prior experimental set-up which included the locomotive arm assembly. The results of the parameters estimated by the model previously created are included for comparison.

### **6.1 Locomotive Assembly Testing**

The previous research effort conducted at ERAU was directed toward modeling fuel slosh on spinning spacecraft using simple 1-DOF pendulum analogs. An electric motor induced the motion of the pendulum via a locomotive arm assembly to simulate free surface slosh (Figure 6-1). The pendulum analog modeled a spherical tank with no PMD. Parameters describing the simple pendulum models include pendulum length,

pendulum hinge spring/damping constants, fixed mass, and several other parameters related to the DC motor/locomotive arm assembly.

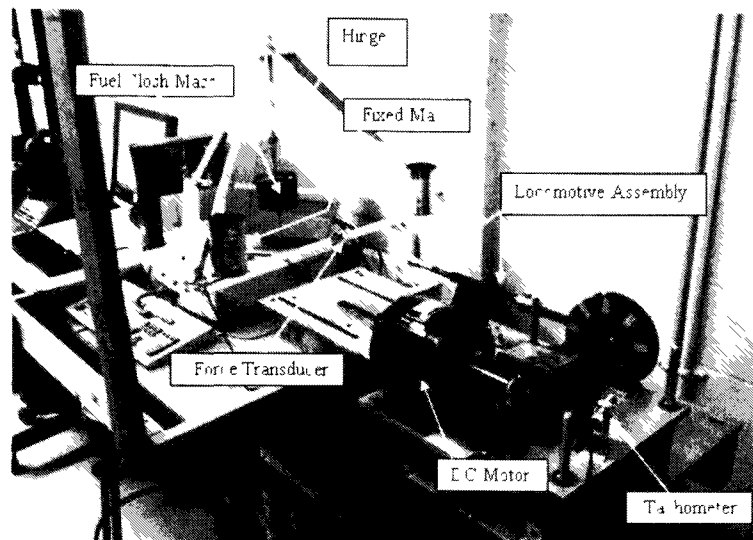


**Figure 6-1. Locomotive arm experimental set-up**

The first step for this research project was to experiment with liquids of different viscosities in order to better understand the lateral fuel slosh effects. The previous experimental set-up was used to perform free surface slosh testing for various liquids such as water, glycerine, and corn syrup.

### **6.1.1 Water**

Tests for water tanks filled at different fill levels and excited at several frequencies were performed previously using the locomotive arm assembly. The empirical data was compared with the SLOSH code predictions and the results proved to be satisfactory.

Subsequently, the results of these tests were compared with the tests performed for other liquids such glycerine and corn syrup.

### 6.1.2 Glycerine

After obtaining the experimental data for the different fill levels (60%, 70% and 80%) for both glycerine and corn syrup, the experimental data was then imported to the Parameter Estimation Toolbox. With the use of MATLAB's Parameter Estimation Toolbox, the simulation for glycerine and corn syrup under free surface slosh conditions were simulated. The SimMechanics model was updated and adjusted for simulation using liquids other than water. As mentioned before, the SLOSH code was used to aid in the estimation of pendulum properties for each of the liquids. For free surface slosh conditions the mass differences were accounted in the model. The parameters to be estimated were the initial flywheel angle, the angular velocity correction, the pendulum hinge spring constant, and the pendulum damping constant. Figure 6-2 illustrates the comparison between the experimental data and the simulated data for glycerine at 60% fill level.

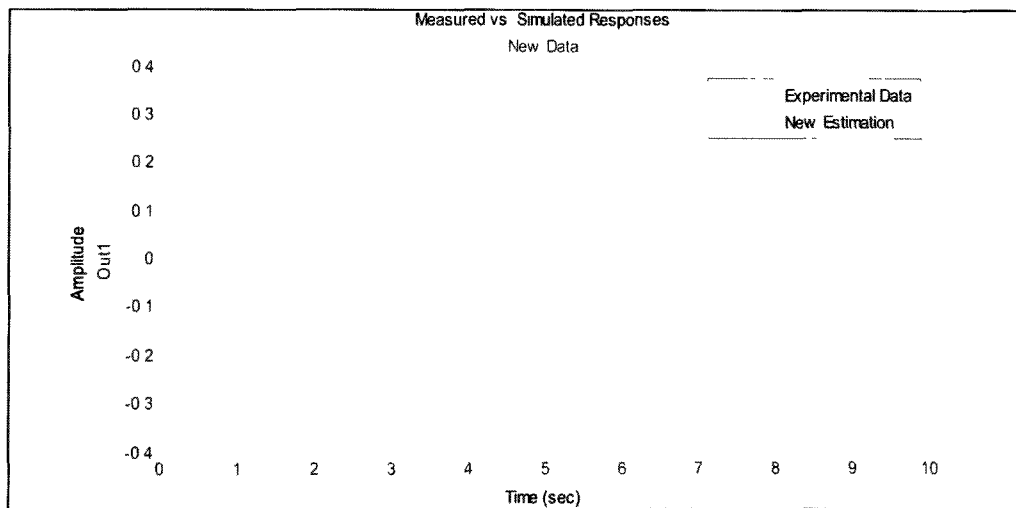


**Figure 6-2. Locomotive arm assembly glycerine 60% fill level excited at 1.75Hz**

### 6.1.3 Corn Syrup

The testing procedure was repeated with corn syrup (Figure 6-3) Several tests were performed under different excitation frequency conditions

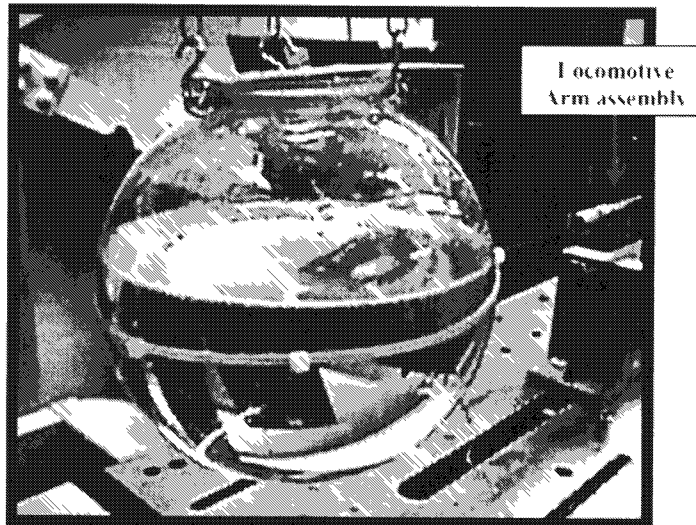


Figure 6-3. Locomotive arm assembly testing for corn syrup

The experimental data collected for locomotive arm assembly for free surface corn syrup tank testing was also imported to the Parameter Estimation Toolbox. The same procedure was followed to test and simulate the corn syrup at 60% fill level conditions, illustrated in Figure 6-4.

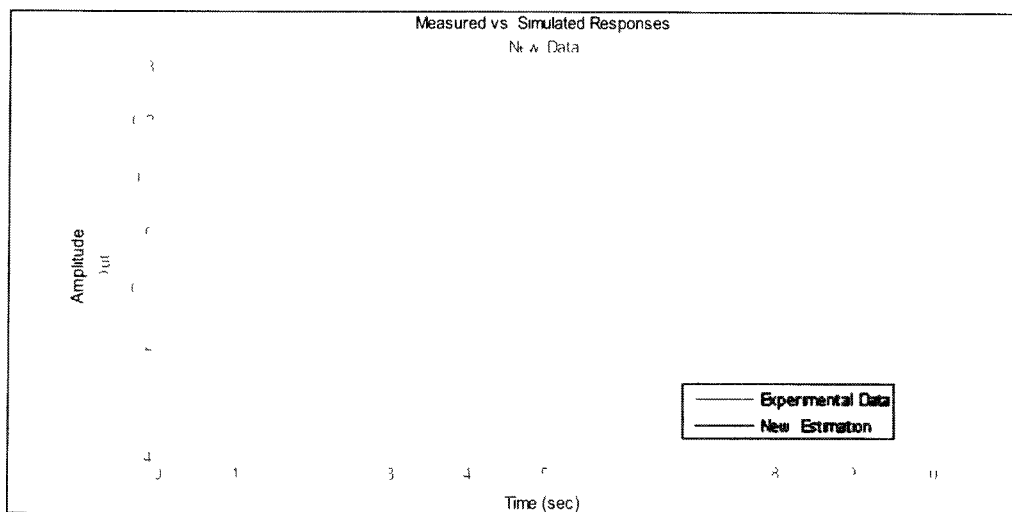


Figure 6-4. Locomotive arm assembly corn syrup 60% fill level excited at 1.75Hz



The following table illustrates all three liquids results obtained with the MATLAB Parameter Estimation Toolbox. The results (Table 6-1) were compared and some of the values were as expected yet the damping value for glycerine was surprisingly lower than expected.

**Table 6-1. Comparison of results among different liquids**

Tank Simulation (Parameter Estimation)		
Water		
60% Fill Level	Fixed Mass (lb)	Pendulum Mass (lb)
	3.210	3.055
Parameter Estimation: 4 Parameters		
Measured Test Frequency (Hz)	1.757	
Angular Velocity Correction (rad/s)	-0.151930	
Flywheel Initial Angle (rad)	0.212970	
Pendulum Spring Constant (ft-lb/rad)	0.167660	
Pendulum Damping Constant (ft-lb/rad/sec)	0.010487	
Glycerine		
60% Fill Level	Fixed Mass (lb)	Pendulum Mass (lb)
	4.052	3.856
Parameter Estimation: 4 Parameters		
Measured Test Frequency (Hz)	1.757	
Angular Velocity Correction (rad/s)	-0.113750	
Flywheel Initial Angle (rad)	-4.849900	
Pendulum Spring Constant (ft-lb/rad)	0.261830	
Pendulum Damping Constant (ft-lb/rad/sec)	0.004307	
Corn Syrup		
60% Fill Level	Fixed Mass (lb)	Pendulum Mass (lb)
	4.405	4.192
Parameter Estimation: 4 Parameters		
Measured Test Frequency (Hz)	1.757	
Angular Velocity Correction (rad/s)	-0.042086	
Flywheel Initial Angle (rad)	-4.944100	
Pendulum Spring Constant (ft-lb/rad)	0.404120	
Pendulum Damping Constant (ft-lb/rad/sec)	0.020734	

## 6.2 Frozen Mass

In order to simulate the response force of a solid mass tank, a frozen water tank was prepared and tested. The results obtained from this test would allow for more accurate modeling of the experimental set-up and interpretation of the forces involved. The free surface tank was filled with water at a 60% fill level and the water in the tank was frozen overnight. Figure 6-5 illustrates the frozen water tank under testing conditions.

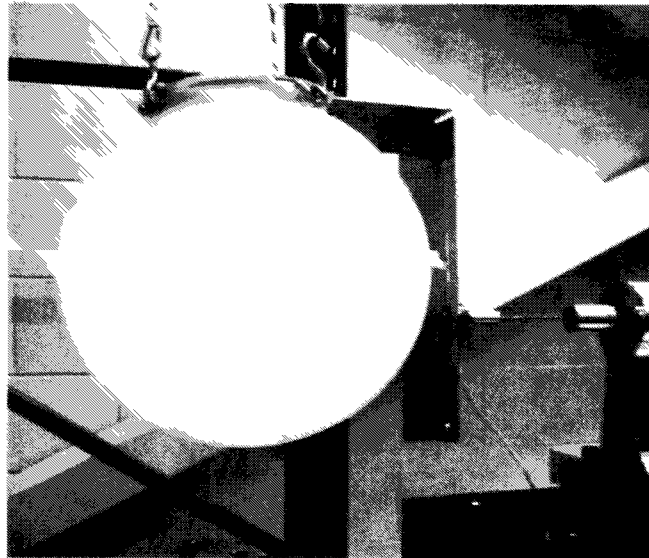


Figure 6-5. Frozen water tank testing

After collecting the data of several runs, the next step is to test the SimMechanics model under fixed mass conditions similar to the empirical data. Basically, the SimMechanics model would have all the components needed for the simulation except the components that describe the sloshing behavior. The pendulum mechanical analog model would not be included in this fixed mass test allowing for the evaluation of the accuracy of the model. Figure 6-6 illustrates the completed SimMechanics fixed mass model for the frozen tank testing. It is expected that when the model simulation is executed, the behavior of the model should closely match the collected frozen tank force readings.

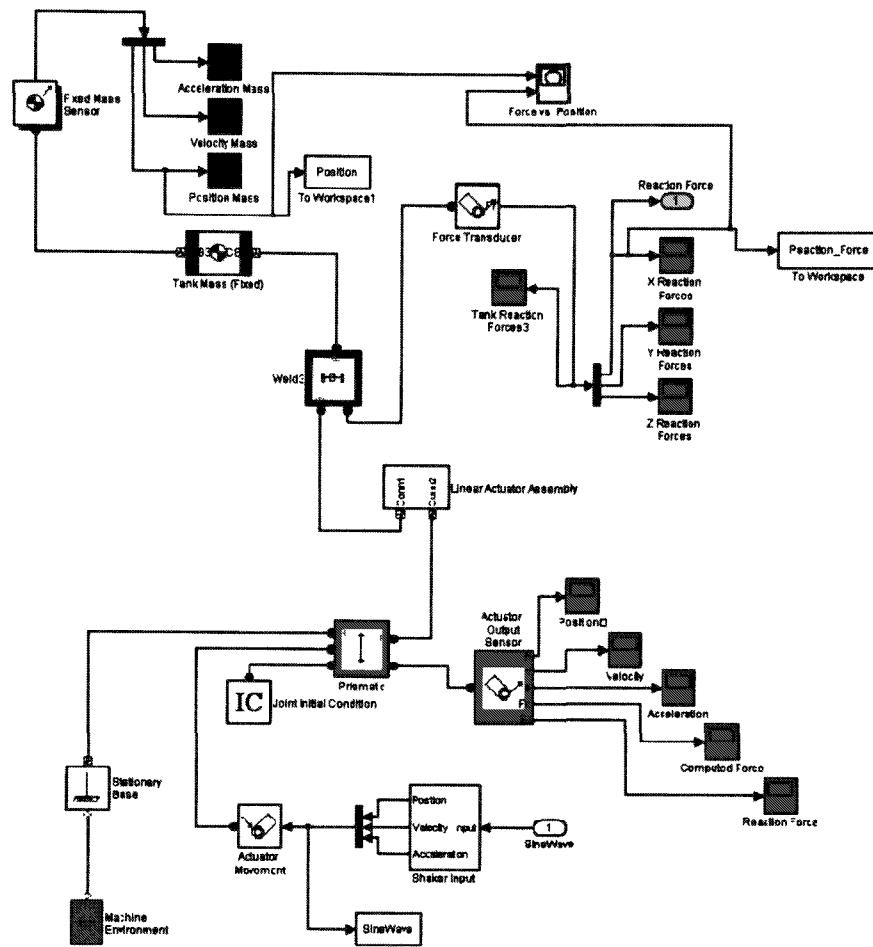
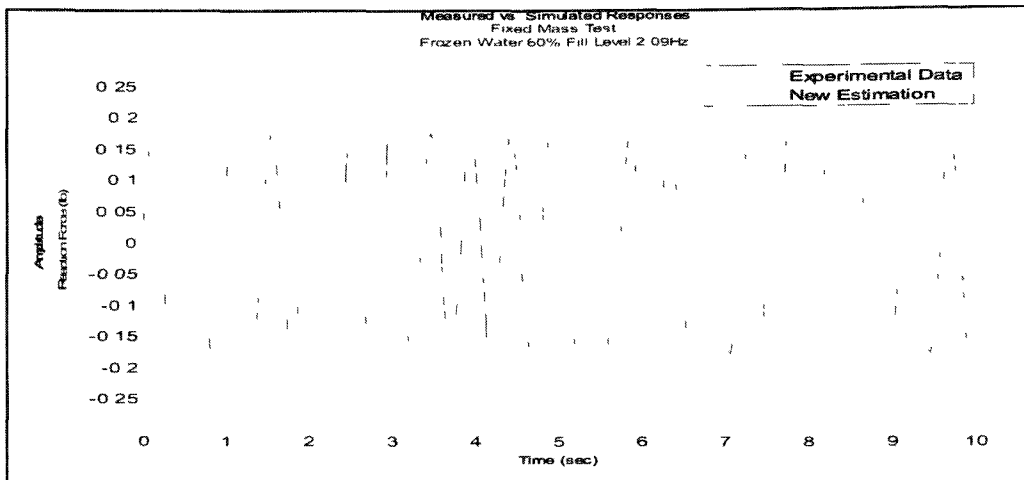


Figure 6-6. Fixed mass model of the frozen tank testing

Utilizing the MATLAB Parameter Estimation toolbox, the empirical data and the simulated model data can be compared and analyzed. Following the necessary procedure steps for the Parameter Estimation, parameters can be defined and values can be determined after the comparison of the response force against the model simulation and the empirical data. Figure 6-7 illustrates the comparison plot for the frozen tank testing data and the simulation based on the fixed mass model. It can be noted, that the error for the overall amplitude is of approximately five percent. Some of the error could be due to the fact that the actual testing data encountered the problem of the ice melting faster than expected.



**Figure 6-7. Fixed mass test comparison between the empirical data and estimation**

The result of this fixed mass test was also compared with the results obtained with the previous research data. It can be noted that the reaction force magnitude of the estimation data is considerably similar.<sup>16</sup> After finishing the fixed mass tests the liquid testing can begin.

### **6.3 Free Surface**

The first set of tests scheduled was the free surface tests. As previously mentioned, the liquids used for testing were water, glycerine, and corn syrup. For each of the liquids, a number of tests were performed and data was collected. This empirical data will allow for a comparison between free surface conditions and a diaphragm's affect on the slosh behavior. Aside from the preliminary tests conducted on the free surface tanks constant frequency tests were also executed. From the constant frequency test data, the Parameter Estimation software is used to evaluate and determine parameters needed to simulate the data. The results obtained for all three liquids after running the model simulation are listed in Table 6-2.

**Table 6-2. Free surface testing parameter values results**

<b>Free Surface Testing</b>			
	<b>Water</b>	<b>Glycerine</b>	<b>Corn Syrup</b>
<b>b (lbf-s/in)</b>	0.0239	0.1974	0.1986
<b>k (lbf/in)</b>	2.2911	23.1586	1.3703
<b>h (in)</b>	1.0559	1.0979	1.3818
<b>smass (kg)</b>	1.2953	3.2237	1.0001

The results were close to what was expected. However, the glycerine values were rather high for both the stiffness and sloshing mass. Conversely, the results for water and corn syrup were found to be in good agreement.

### 6.3.1 Water

The first liquid to be tested was water. Preliminary tests were performed including the verification of the mechanical model parameters through the results from the SLOSH code. After collecting and recording all the data for the water tests, the next step was to run the model simulation and estimate the pendulum mechanical analog parameters with Parameter Estimation Toolbox (Figure 6-8).

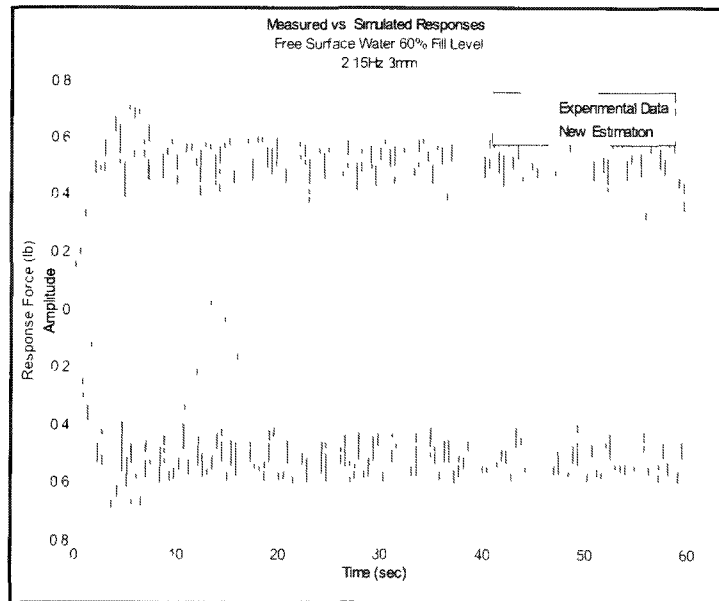


**Figure 6-8. Free surface water vs. model simulation**

After the parameter estimation process is executed various plots are created which describe the parameter values and the simulation behavior compared with the empirical data, as shown in Figure 6-9. The simulation results were very close to the empirical data.

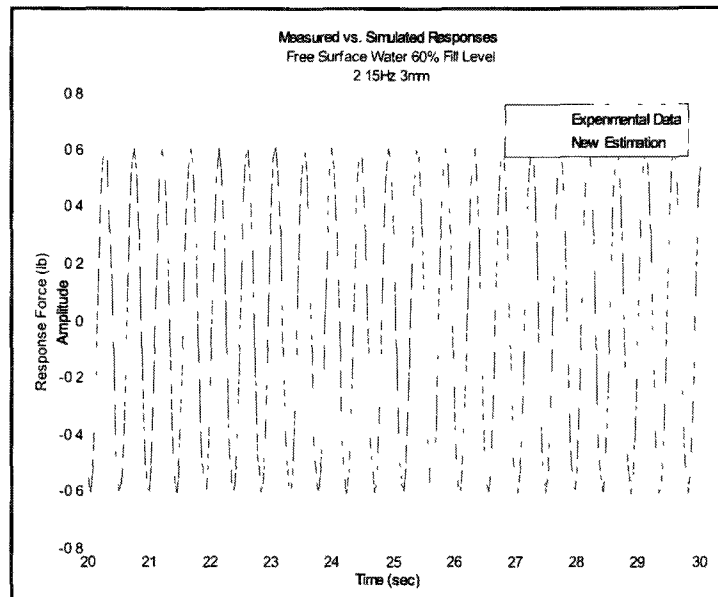


Figure 6-9. Free surface water data vs. model simulation

In addition to the plot that includes both measured and simulated data, the parameter value progress can be observed after each iteration (Figure 6-10).

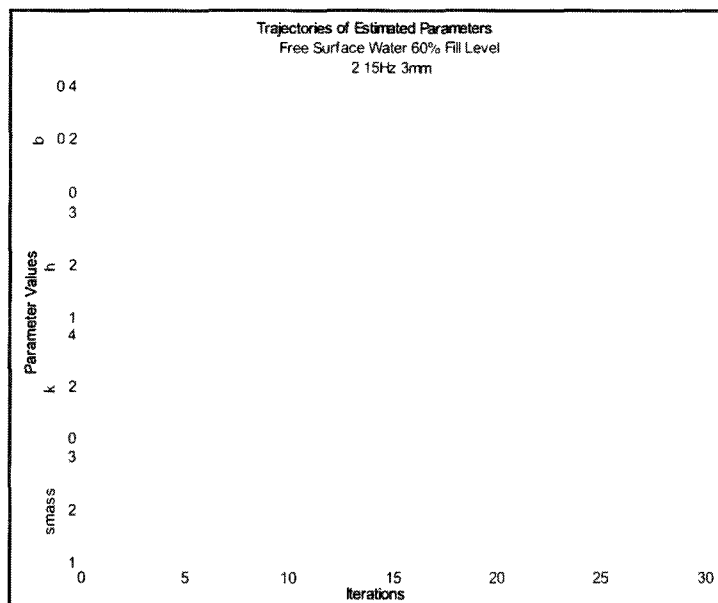


Figure 6-10. Parameter values simulation for free surface water

### 6.3.2 Glycerine

The SimMechanics model was modified to simulate glycerine in the tank for this case, which means the total mass for the tank is higher than for the water. The other parameters were able to be modified by the program as needed based on the parameter identification process. The results obtained for glycerine after evaluating the measured vs. simulated data are very similar, as with the case of free surface water testing for this fill level (Figure 6-11).

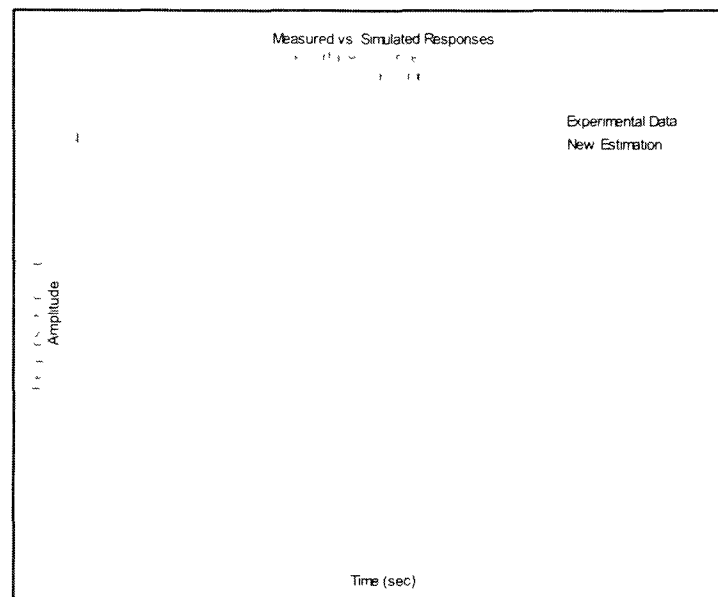
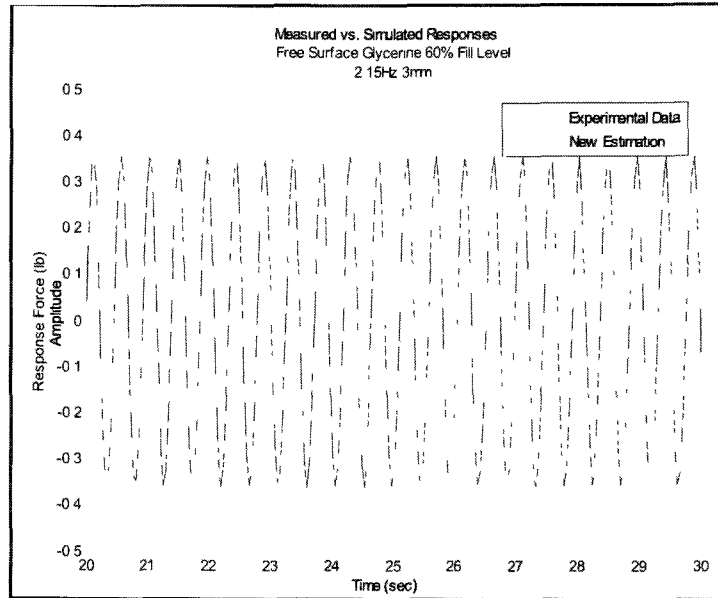


Figure 6-11. Parameter estimation plot for free surface glycerine

The parameter identification process was repeated several times varying the parameters to be estimated as well as the initial conditions and parameters limits. First, some of the parameters were kept constant and others were adjusted as required. The pendulum length is one of the parameter that was kept constant at the beginning of the simulation runs. However, this parameter was also allowed to change as the parameter identification process advanced. Four parameters were estimated based on the empirical data and the model simulation: pendulum length, stiffness, damping, and sloshing mass.



**Figure 6-12. Free surface glycerine data vs. model simulation**

Ultimately, the four parameters were estimated and their estimation trajectory is illustrated in Figure 6-13. The parameters values were acceptable except that the stiffness value seemed higher than expected.

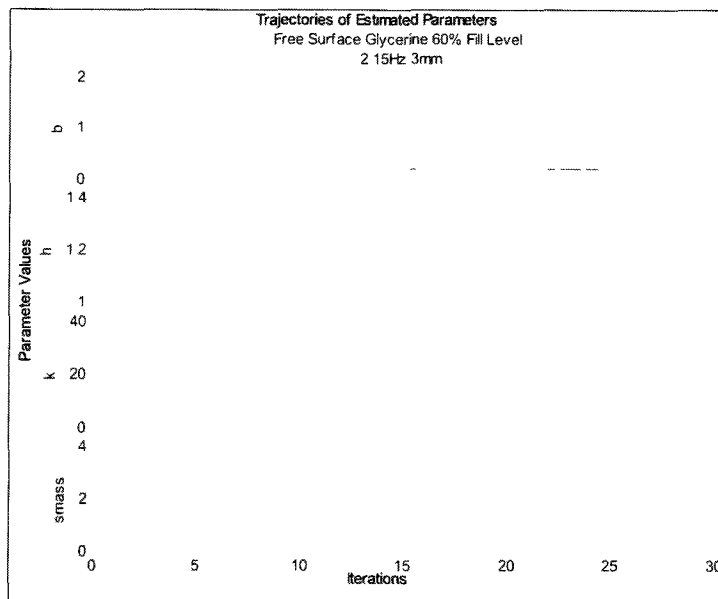


**Figure 6-13. Parameter values simulation for free surface glycerine**



### 6.3.3 Corn Syrup

The last of the free surface tank tests is the corn syrup tank. In this case, the response force is lower when compared with the water and glycerine results. Figure 6-14 illustrates the comparison between the empirical data and the model simulation.

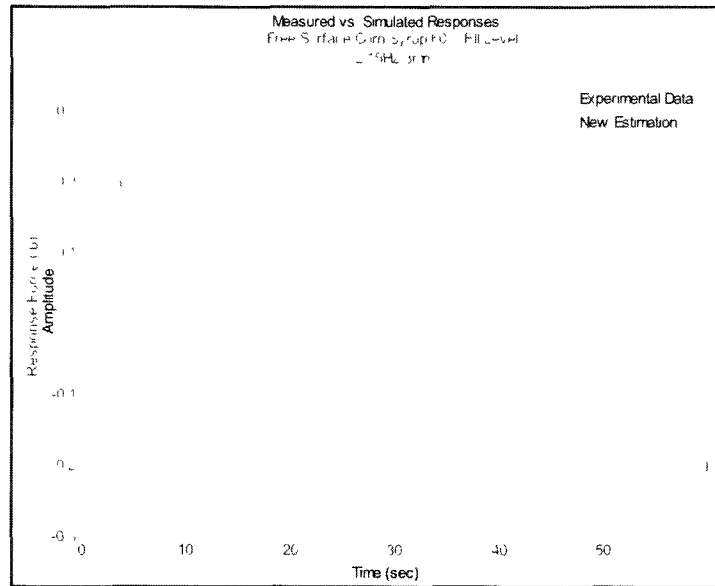


Figure 6-14. Parameter Estimation plot for free surface corn syrup

Although it seems that the data may need to be filtered, in Figure 6-15 shows a closer look of the plot and allows one to visualize the small difference between data.

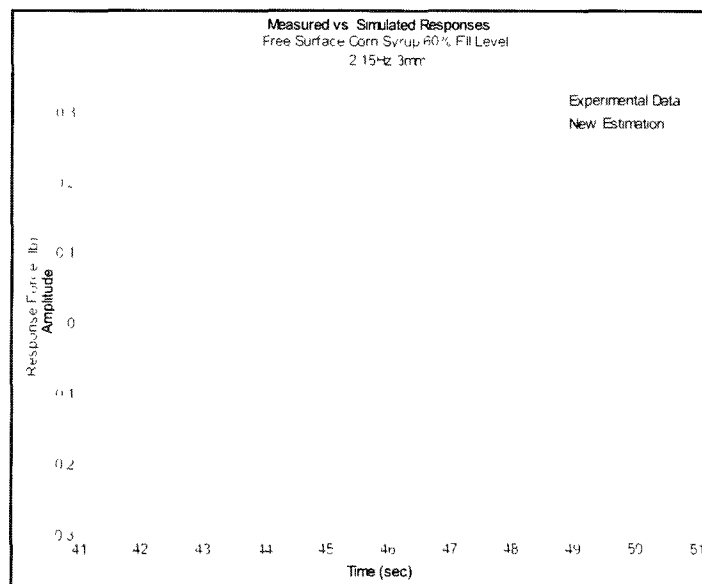


Figure 6-15. Free surface corn syrup data vs. model simulation

The parameters estimated behave as expected, as the slosh mass decreases the damping increases (Figure 6-16).

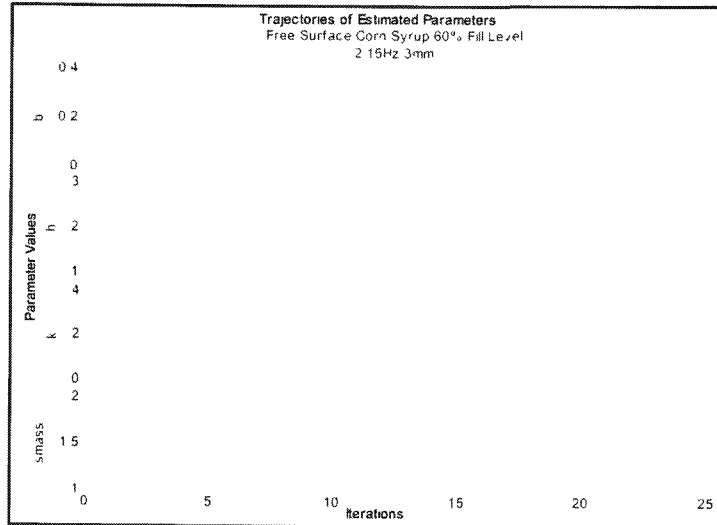


Figure 6-16. Parameter values simulation for free surface corn syrup

#### 6.4 Diaphragm Testing

The introduction of a diaphragm in the tank could induce a more complex behavior than free surface slosh. A step-by-step approach similar to the one used for the free surface slosh is utilized to estimate parameters in the presence of a diaphragm. Three diaphragms were tested and compared with the free surface data. Aside from the preliminary testing (sweep, damping test and force vs. position test), constant frequency testing was also performed for each diaphragm with each of the liquids at different fill levels.

During testing, some changes in the fill levels tested were necessary due to problems encountered when the corresponding fill level volume exceeded the unstretched volume of the diaphragm tank. For the Yellow and the Spike diaphragms, the 80% fill level testing was not performed. However, the Sky diaphragm was tested under 80% fill level for all liquids.

The SimMechanics model was modified to incorporate the diaphragms into the system (Figure 5-4). Parameter Estimation assisted to obtain the parameters that characterized the model under the diaphragm conditions. These parameters are the pendulum length, the stiffness, the damping, and the slosh mass of the pendulum modeled in the SimMechanics model (Table 6-3).

**Table 6-3. Parameter Estimation parameter values**

<b>Diaphragm Testing</b>			
<b>Sky Diaphragm</b>			
	Water	Glycerine	Com Syrup
<i>b</i> (lbf-s/in)	6.803-7	0.7457	0.001332
<i>k</i> (lbf/in)	1.441	9.9011	1.183
<i>h</i> (in)	1.203	1.5901	1.458
<i>smass</i> (kg)	6.368-6	2.3425	0.4464

<b>Yellow Diaphragm</b>			
	Water	Glycerine	Com Syrup
<i>b</i> (lbf-s/in)	0.03286	0.01016	2.562
<i>k</i> (lbf/in)	0.4781	1.314	0.1332
<i>h</i> (in)	0.7914	1.14	0.4461
<i>smass</i> (kg)	0.7605	0.7875	1.301

<b>Spike Diaphragm</b>			
	Water	Glycerine	Com Syrup
<i>b</i> (lbf-s/in)	0.0001188	8.25E-09	0.005403
<i>k</i> (lbf/in)	3.954	1.168	1.574
<i>h</i> (in)	0.5053	1.356	1.16
<i>smass</i> (kg)	0.3488	0.0009454	0.4946

During the estimation phase, the simulations were modified several times to prevent the estimated values from being adversely restricted by the parameter limits. In addition, the success of the parameter estimation process can be evaluated by the trajectory of the estimation as it is in progress.

#### **6.4.1 Spike Diaphragm**

The first diaphragm to be tested was the Spike diaphragm (Figure 6-17). The preliminary tests mentioned before were performed for all three liquids at each respective

fill level. Consequently, the constant frequency runs were executed and the data was recorded and prepared for the analysis and simulation process.

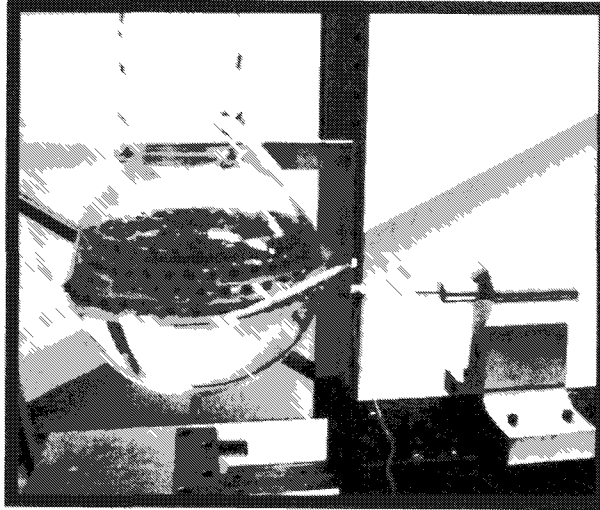


**Figure 6-17. Spike diaphragm testing**

#### **6.4.1.1 Water**

The Parameter Estimation toolbox was utilized in order to begin with the parameter identification process. The following Parameter Estimation analyses are the results obtained after comparing the empirical data with the model simulation. In this case, the Spike diaphragm was evaluated against the model simulated data. Figure 6-18 illustrates both the experimental and simulation data plotted for comparison. Once the diaphragm is part of the tank assembly, the dissimilarities of the tank behavior when compared with the free surface tank testing are noticeable. The interaction between the diaphragm and the liquid sloshing allows for a decrease in response force when compared with the same test requirements but under free surface conditions.

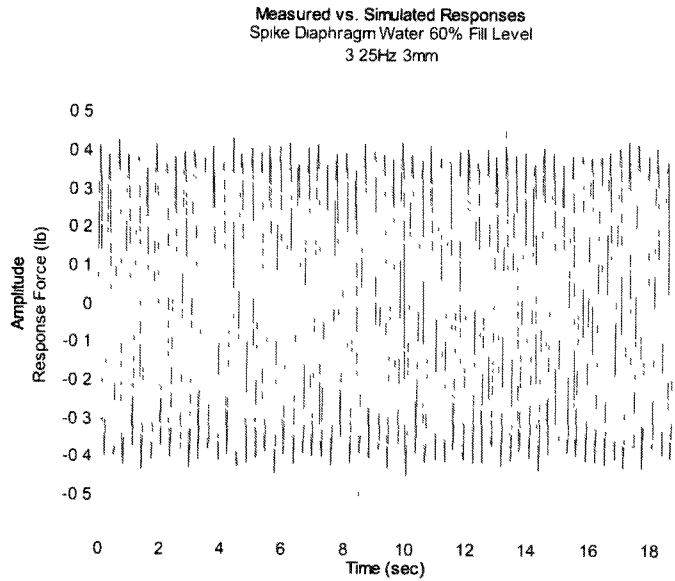


**Figure 6-18. Plot for Spike diaphragm filled with water**

During the simulation, the estimated parameters are displayed as the simulation progresses. Figure 6-19 illustrates the parameters and their progression as the iterations are executed.

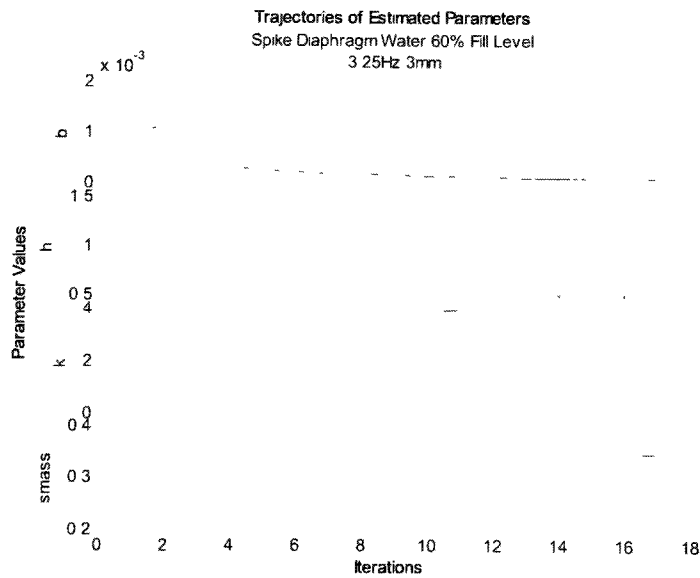


**Figure 6-19. Parameters trajectory for Spike filled with water**

### 6.4.1.2 Glycerine

For the glycerine testing, the behavior of the model simulation is quite different than the water testing for the Spike diaphragm. Both Figure 6-20 and Figure 6-21 illustrate the results of the process for glycerine in the Spike diaphragm tank.

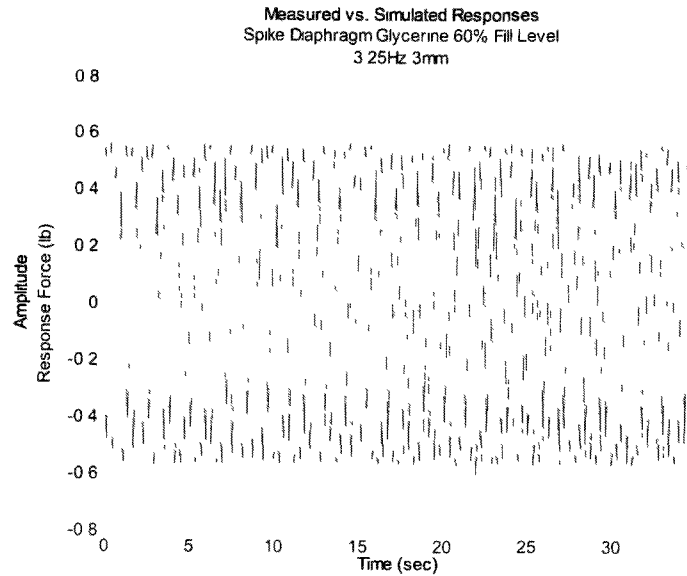


Figure 6-20. Plot for Spike diaphragm filled with glycerine

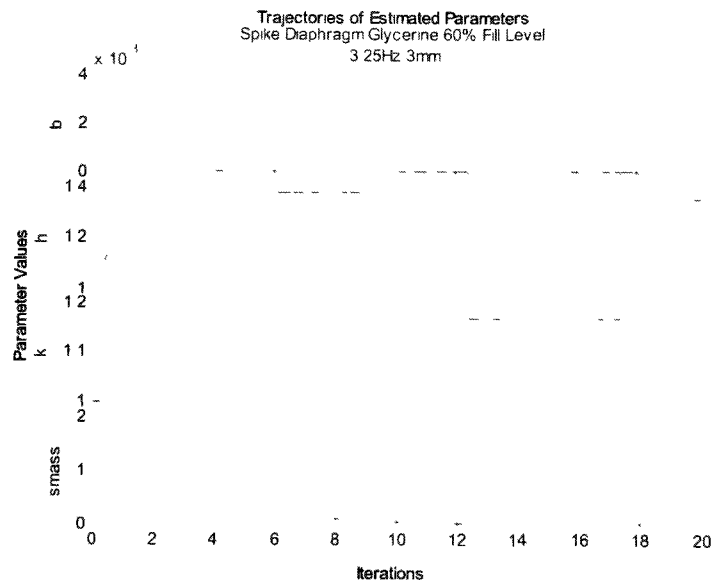


Figure 6-21. Parameters trajectory for Spike filled with glycerine

### 6.4.1.3 Corn Syrup

For the corn syrup testing, the behavior of the model simulation is quite different than the water testing for the Spike diaphragm. Both Figure 6-22 and Figure 6-23 illustrate the results of the process for corn syrup in the Spike diaphragm tank.

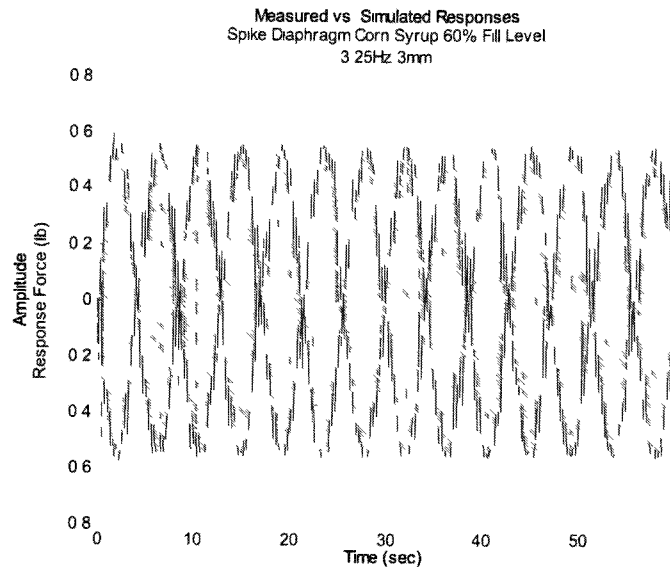


Figure 6-22. Plot for Spike diaphragm filled with corn syrup

As far as the parameter results, the values were improved when compared with the values obtained with the glycerine results.

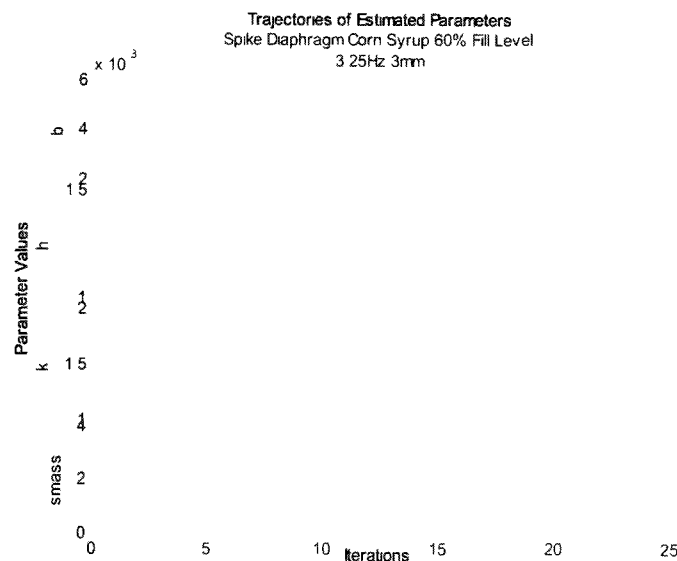


Figure 6-23. Parameters trajectory for Spike filled with corn syrup

## 6.4.2 Sky Diaphragm

The next diaphragm to be tested was the Sky diaphragm (Figure 6-24). The preliminary tests mentioned before were performed for all three liquids at each respective fill level. Consequently, the constant frequency runs were executed and the data was recorded and prepared for analysis and simulation process.

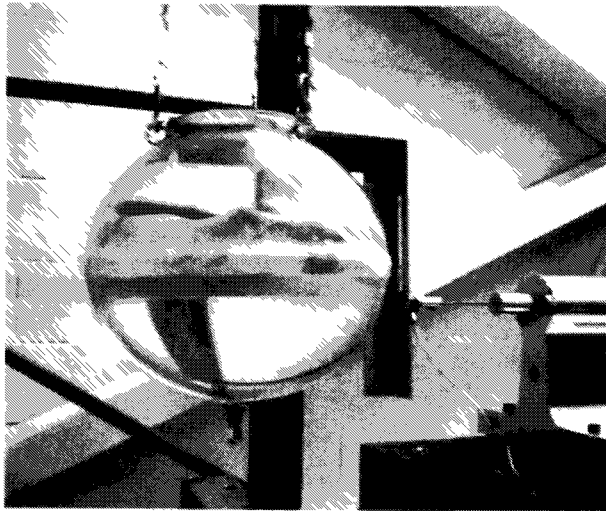
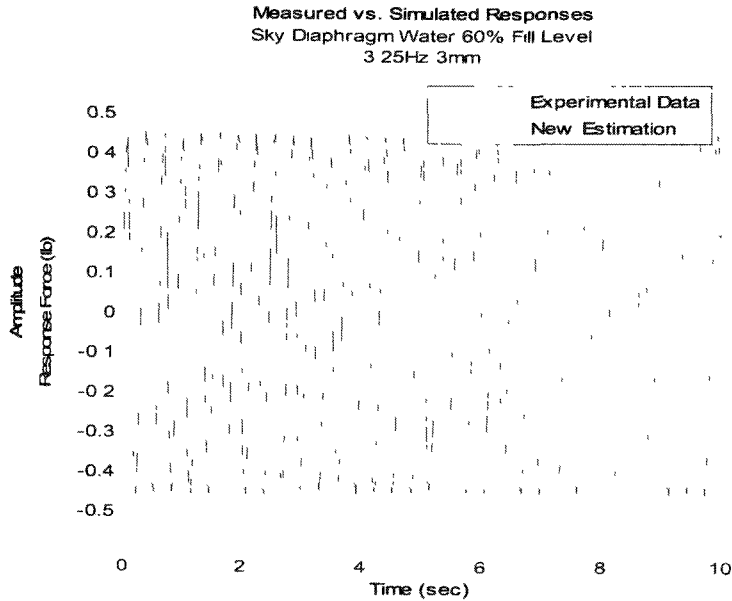


Figure 6-24. Sky diaphragm testing

### 6.4.2.1 Water

The following Parameter Estimation analyses are the results obtained after comparing the empirical data with the model simulation. In this case, the Sky diaphragm was evaluated against the simulated data. Figure 6-25 illustrates both of the experimental data and the simulation data plotted for comparison. When comparing the results for Spike and Sky in the case of water, the response force is slightly higher for the thinner (Sky) diaphragm. A comparison among the diaphragm and the response force difference is illustrated in Appendix C, the plots have all three diaphragms response force results for one of the tests performed.





**Figure 6-25. Plot for Sky diaphragm filled with water**

Although the empirical and the simulated data appeared to be close, the parameter values for the slosh mass are not what were expected. This was opposite to what occurred for the Spike diaphragm as the slosh mass estimated was acceptable, but the plot was not as close as the Sky comparison plot.

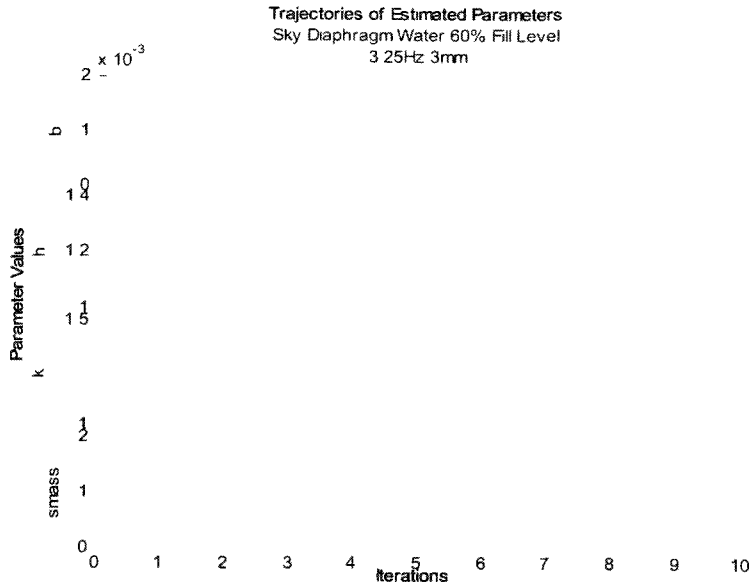


**Figure 6-26. Parameters trajectory for Sky filled with water**

### 6.4.2.2 Glycerine

For the glycerine testing, the behavior of the model simulation is different than the water testing for the Sky diaphragm as the response force is higher. Both Figure 6-27 and Figure 6-28 illustrate the results of the process for glycerine in the Sky diaphragm tank.

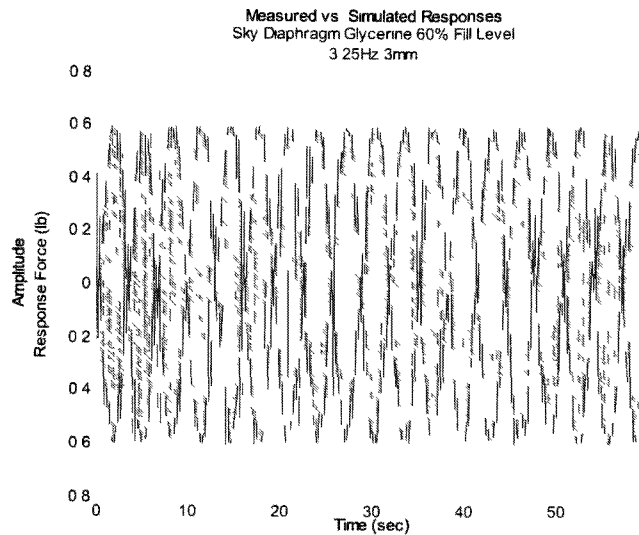


Figure 6-27. Plot for Sky diaphragm filled with glycerine

As experienced before, the glycerine values are higher than what was expected, similar to the stiffness parameter value.

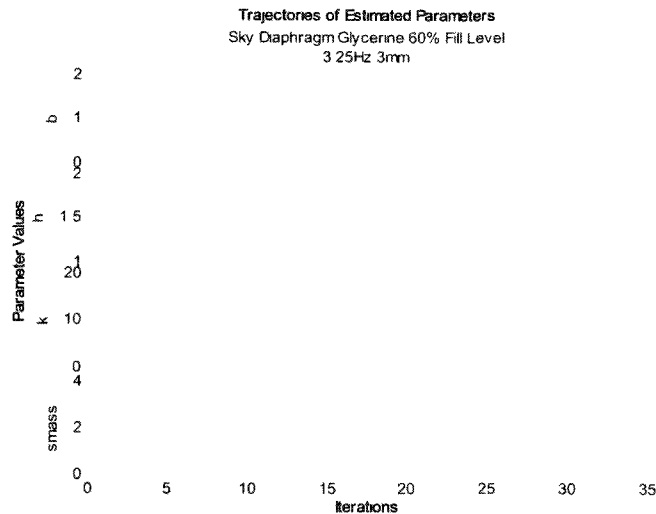


Figure 6-28. Parameters trajectory for Sky filled with glycerine

### 6.4.2.3 Corn Syrup

For the corn syrup testing, the behavior of the model simulation is very similar when compared with the Spike corn syrup results. The response force amplitude as shown in Figure 6-29 is roughly the same magnitude as with the Spike diaphragm.

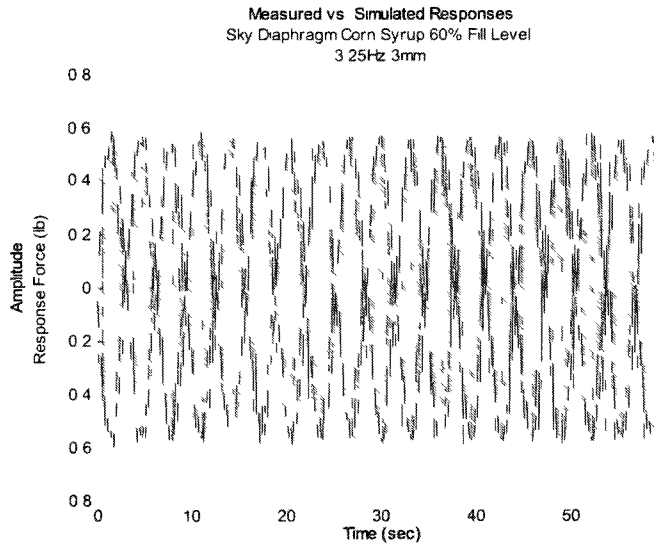


Figure 6-29. Plot for Sky diaphragm filled with corn syrup

Both diaphragms (Spike and Sky) yielded similar parameter values for corn syrup testing.

The progress of the parameter estimations are shown in Figure 6-30.

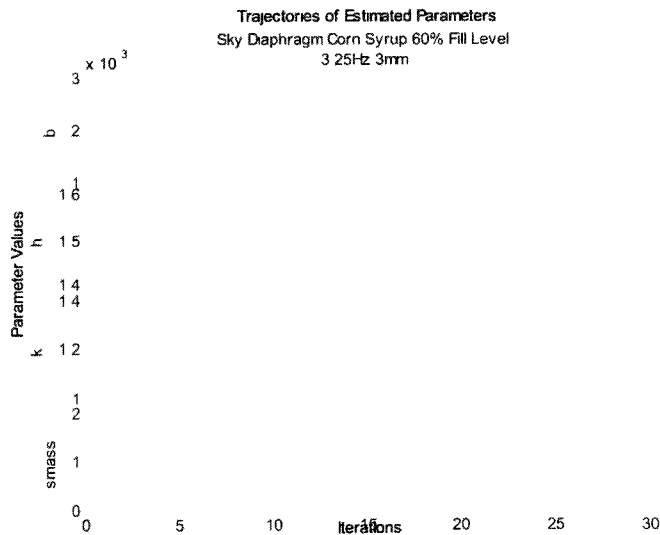


Figure 6-30. Parameters trajectory for Sky filled with corn syrup

### 6.4.3 Yellow Diaphragm

The last diaphragm to be tested was the Yellow diaphragm (Figure 6-31). The preliminary tests mentioned before were performed for all three liquids at each respective fill level. Consequently, the constant frequency runs were executed and the data was recorded and prepared for the analysis and simulation process.

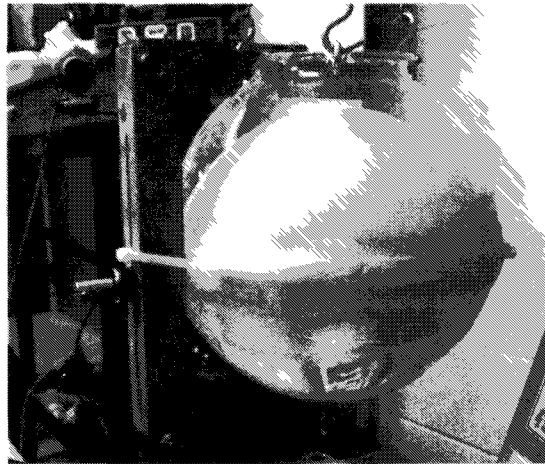


Figure 6-31. Yellow diaphragm testing

The Yellow diaphragm is the thickest of the three diaphragms. As a result, it was difficult to completely fill the tank for the 80% fill level. Therefore, this fill level was cancelled from the experiment matrix. This was also considered for the Spike tank as well, but the Sky diaphragm was tested under the 80% fill level conditions as the volume needed was completely filled in the tank.

#### 6.4.3.1 Water

The testing for the Yellow diaphragm began with the water testing. When comparing the response force with the other diaphragms, the amplitude is approximately the same magnitude. Figure 6-32 illustrates the comparison between the empirical data

and the simulated data after the parameter identification process was completed using Parameter Estimation Toolbox.

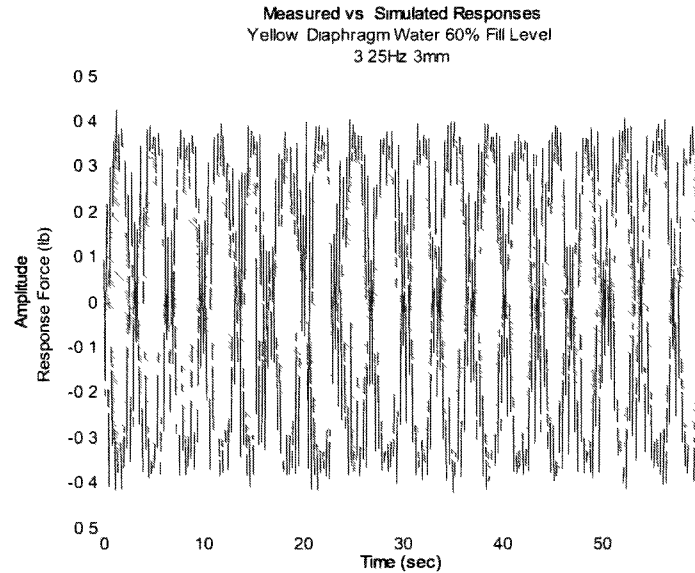


**Figure 6-32. Plot for Yellow diaphragm filled with water**

The parameter estimation values are then evaluated and compared with other diaphragms under same conditions. The damping value increased as expected due to the fact that Yellow is the thickest of the diaphragms as shown in Figure 6-33.

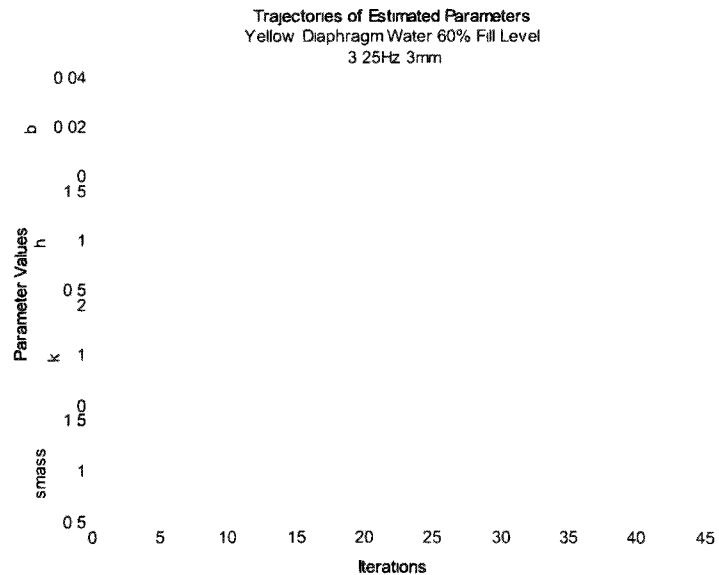


**Figure 6-33. Parameters trajectory for Yellow filled with water**

### 6.4.3.2 Glycerine

The estimation procedure was repeated with the other liquids. For glycerine, the response force is lower than with the Sky diaphragm as expected due to the thickness of the diaphragm (Figure 6-34).

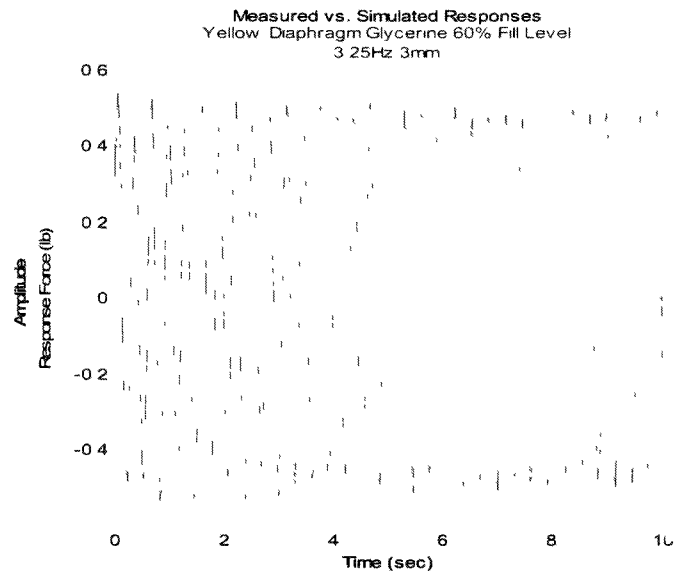


Figure 6-34. Plot for Yellow diaphragm filled with glycerine

When comparing the overall results for glycerine, some of the parameters did not behave as expected which was consistent with the other glycerine tests (Figure 6-35).

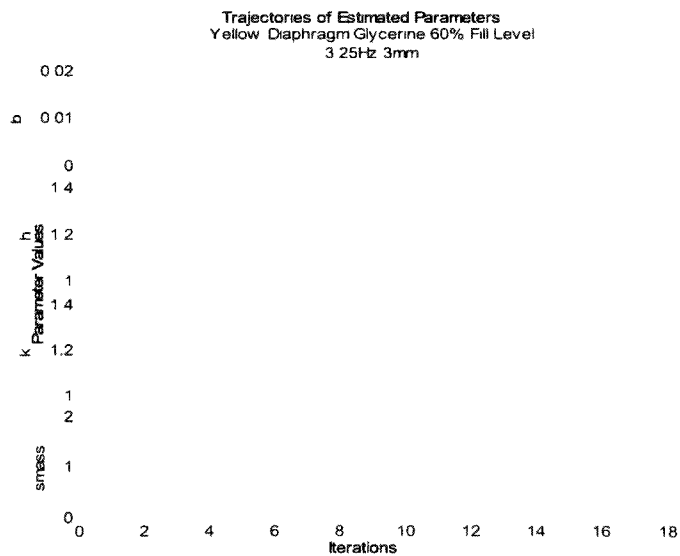


Figure 6-35. Parameters trajectory for Yellow filled with glycerine

### 6.4.3.3 Corn Syrup

Lastly, the corn syrup test was carried out and it was noted that the response force decreased when compared with the other diaphragms (Figure 6-36).

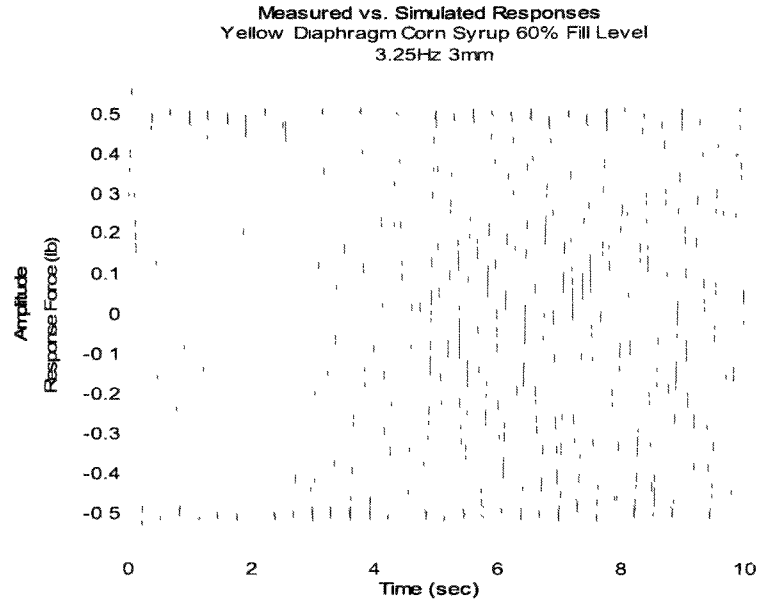


Figure 6-36. Plot for Yellow diaphragm filled with corn syrup

Overall, the results for corn syrup were consistent with the expectations for the damping parameter as it increased when compared to the other diaphragms (Figure 6-37).

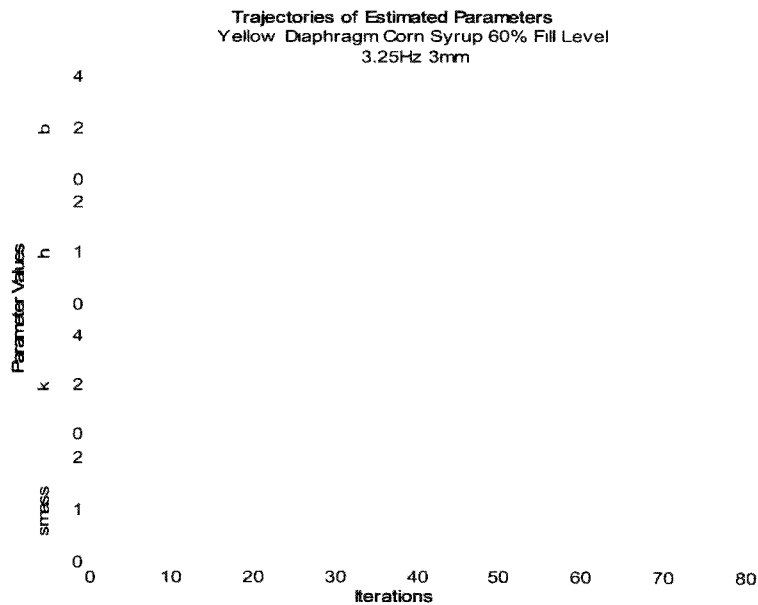


Figure 6-37. Parameters trajectory for Yellow filled with corn syrup

## 7 DIAPHRAGM DATA VERSUS SLOSH CODE

The SLOSH code is a very useful tool for estimating the mechanical pendulum parameter values. The code was designed for free surface slosh conditions. With the diaphragm testing data, it was desired to modify or develop a way to take into consideration the effects of the diaphragms while utilizing the SLOSH code for parameters estimation.

First, the experimental data of the diaphragms was compared with the data for free surface conditions. In this case, the water at 60% fill level was selected for comparison. The SLOSH code input parameters are the liquid density, viscosity and gravity values. Using the SLOSH code, the program was run using the corresponding tank characteristics and keeping the water density value constant. The other two parameters, viscosity and gravity, were adjusted in order to match the actual frequency and damping characteristics of the diaphragm tanks tested. Several code runs were carried out to obtain the desired output values. The results are listed in Table 7-1.

**Table 7-1. SLOSH codes parameters inputs and outputs**

<b>Tank</b>	<b>Fill Level</b>	<b>Gravity</b>	<b>Viscosity</b>	<b>Frequency</b>	<b>% Damping</b>
Water Free	0.6	9.8	0.000001	2.09	0.7318
Water Sky	0.6	55	0.00799	4.9563	13.52
Water Spike	0.6	41	0.0085	4.2792	14.57
Water Free	0.7	9.8	0.000001	2.28	0.9099
Water Sky	0.7	44.5	0.0023	4.8747	11.17
Water Spike	0.7	121	0.004	8.0382	11.38

The results were plotted in order to find a relation. The following graphs illustrate the relation found when the parameter values for the diaphragm tanks were compared (Figure 7-1 and Figure 7-2). Based on the fill level, one can determine the gravity input value for a diaphragm tank with characteristics similar to both the Sky and Spike



diaphragm characteristics. This relation can also be applied to the viscosity inputs based on the fill level of the diaphragm tank.

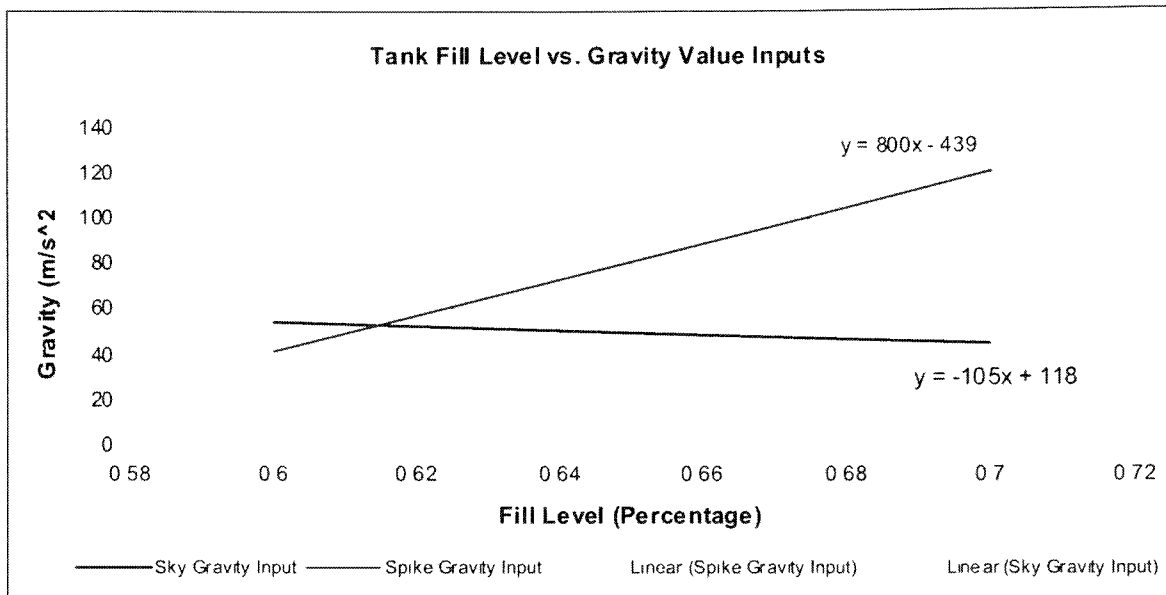


Figure 7-1. Gravity value inputs based on tank fill level

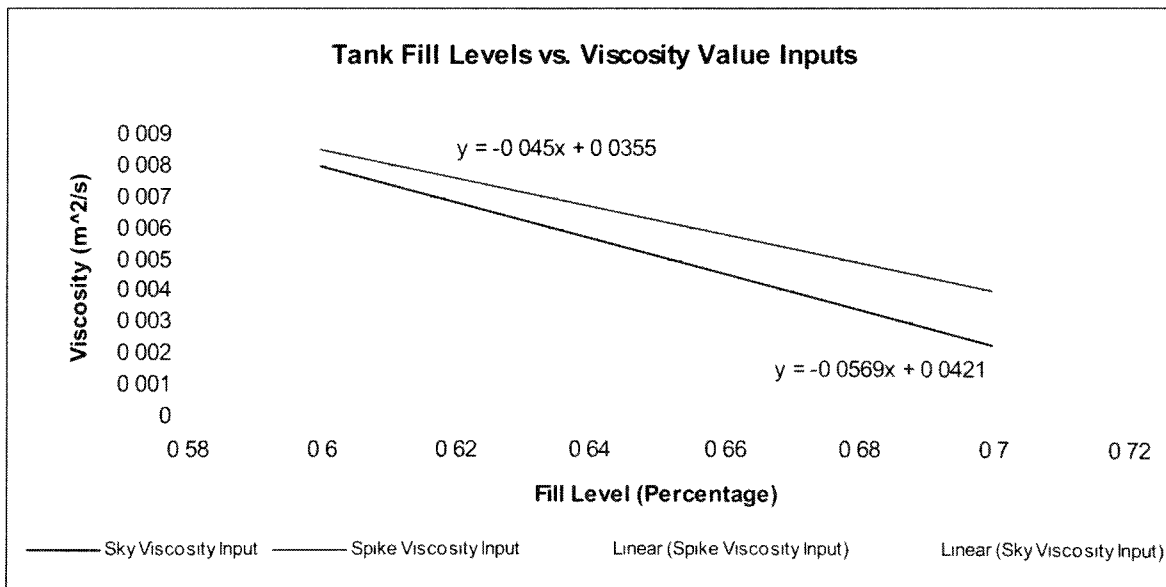


Figure 7-2. Viscosity inputs based on tank fill level

Two general equations were determined with the previous results for both gravity and viscosity parameter inputs. In order to verify the accuracy and effectiveness of these equations, data from previous research and experiments were analyzed and recalculated.

In this case, the data obtained from SwRI testing was selected for verification. SwRI conducted diaphragm testing where tanks were under similar conditions, as explained in their report.<sup>14</sup> Although, the testing was executed for different liquids, for this verification the water parameters are the ones used in this verification procedure. The SLOSH code was ran using the tank shape for the SwRI tests and the fill level used. The next step is to enter the parameter inputs needed in the code which are the liquid properties: liquid density, liquid viscosity, and gravity value. First, the liquid density was the water density value. For the viscosity and the gravity input values, the new equations generated were used to determine these values (Figure 7-3 and Figure 7-4 respectively). The equation used for the gravity input was  $y = 285x - 123$  and for viscosity input was  $y = -0.0509x + 0.0388$ .

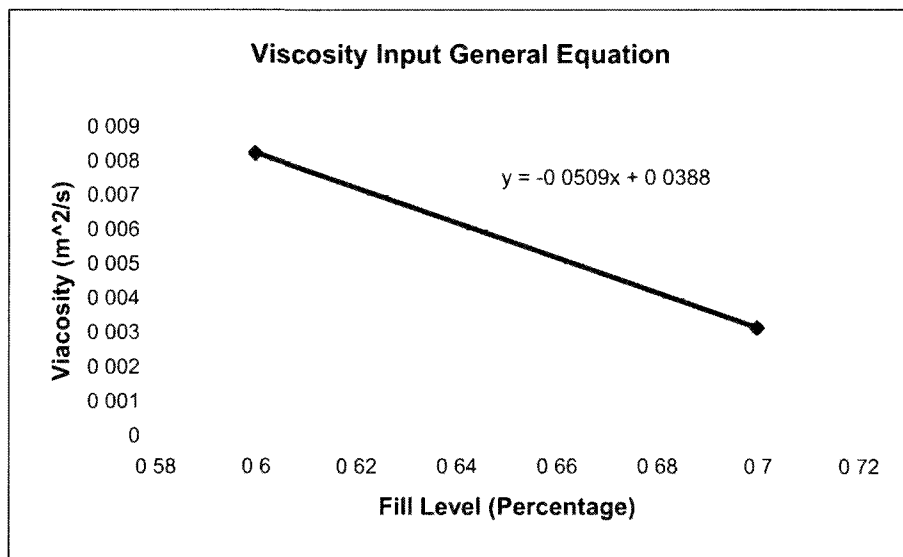


Figure 7-3. General equation for viscosity input

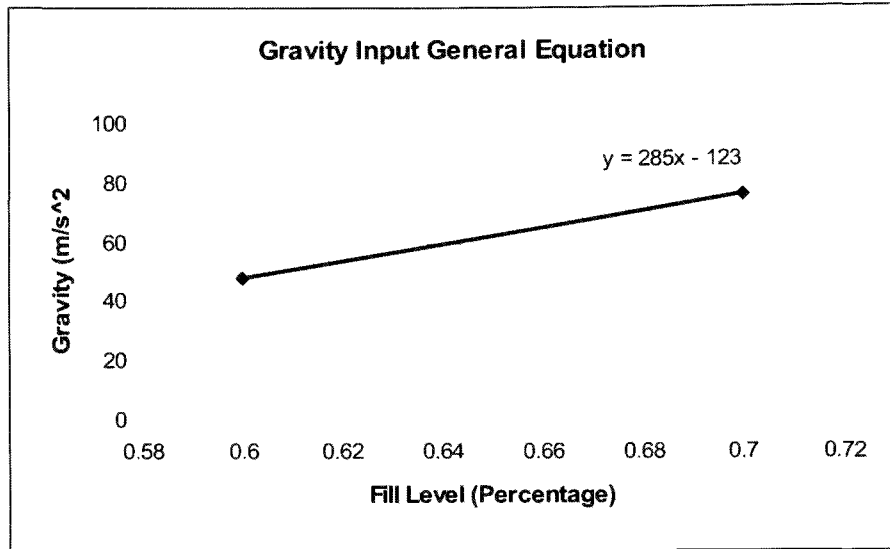


Figure 7-4. General equation for gravity input

The equations were solved with the corresponding fill level value, which is in this case was 61%, and the correct parameter values were entered in the code. Figure 7-5 illustrates the SLOSH code after the parameter inputs were ran and the frequency was determined.

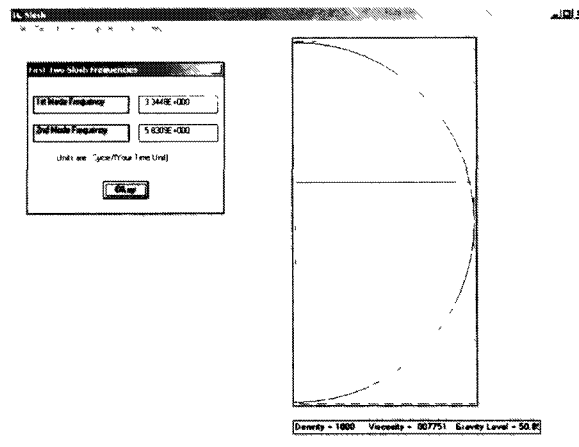


Figure 7-5. SLOSH code screen illustrating frequency output

The frequency value was obtained from the SLOSH code and it was compared with the frequency value given in the SwRI report. Table 7-2 lists the comparison of the actual values and the obtained values using the new equations.

Table 7-2. SwRI results vs. modified SLOSH code results

	<b>SwRI Report Data</b>	<b>SLOSH Code Results</b>	<b>Error Percent</b>
Frequency (Hz)	3.5	3.3448	4.43

## 8 DISCUSSION AND RECOMMENDATIONS

Several tests were performed in order to collect and determine the necessary information and characteristics for the modeling and simulation of the experimental set up. The preliminary tests were the sweep, damping, and the force vs. position test. Each of these tests aid in the determination of parameter values for the diaphragm tanks that were not possible to estimate with the application of the SLOSH code. The sweep test allows for the visualization of the frequency range where the resonance occurs for the tank tested. The force vs. position plots are used to determine when resonance takes place. The relation between both of these tests was useful to determine where the resonance occurs for the diaphragm tanks. The damping test aids in the calculation of the natural frequency for these diaphragm tanks. After modeling and simulating the experimental set-up, the results were compared with the empirical and calculated data. The results were satisfactory after evaluating all the components involved as well as the Parameter Estimation results. These results can be proven when used as inputs for the SLOSH code and the results which are compared to the empirical data. The general equations for the SLOSH code parameter inputs account for the presence of a diaphragm in the tank and promise a way to estimate the necessary parameters for the diaphragm tanks.

For future testing, the application of a new data acquisition system including a new force transducer could be of great help to facilitate the data recording as well as allowing for greater accuracy during testing.

## 9 CONCLUSIONS

Liquid sloshing in moving containers remains a great concern to aerospace applications involving spacecraft and launch vehicles alike. For many years, the analysis of the dynamic effects on spacecraft has become more complex due to the development of these structures in addition to the advances in stability and control systems. The need to develop more complex dynamic models as well to provide analysis techniques to determine the parameters involved are currently the foundation of studies and experiments. By extending the parameter estimation techniques previously developed to include the presence of a diaphragm, a greater number of real life missions can be analyzed. This research project and the on-going research will allow for earlier and easier identification of potential vehicle performance problems through improved simulation techniques.

## **10 FUTURE WORK**

To continue the progress of the research, a modern approach using a CFD model to determine parameters for a simplified mechanical analog slosh model will be developed. The future study will focus on the use of computational fluid dynamics techniques to help model the liquid propellant slosh. When utilizing the CFD approach to determine parameters for a simple mechanical analog slosh model, as previously used in this research, an increase in accuracy, time, and resource savings are possible. The future research will first model a spherical tank and consequently verify the previously obtained empirical data with the CFD results.

## REFERENCES

- [1] Abramson, H.N., “*The Dynamic Behavior of Liquids in Moving Containers: With Applications to Space Vehicle Technology*” NASA SP-106 Southwest Research Institute, 1966.
- [2] Vreeburg, Jan P.B., *Spacecraft Maneuvers and Slosh Control*, IEEE Control Systems Magazine, 0272-1708, June 2005.
- [3] Chatman, Y.R., Gangadharan, S.N., Marsell, B., Schlee, K., Sudermann, J., Ristow, J., Walker, C., and Hubert, C., *Modeling, Simulation and Parameter Estimation of Lateral Spacecraft Fuel Slosh*, 12<sup>th</sup> World Multi-Conference on Systemics, Cybernetics and Informatics, Orlando, FL June 29<sup>th</sup> – July 2<sup>nd</sup>, 2008.
- [4] Hubert, C., *Behavior of Spinning Space Vehicles with Onboard Liquids*, Hubert Astronautics, 2003, Carl@HubertAstro.com.
- [5] Abramson, H.N., *The Dynamic Behavior of Liquids in Moving Containers*, Applied Mechanics Review, Vol. 16, No. 7, July 1963.
- [6] Abramson, H.N., *The Dynamic Behavior of Liquids in Moving Containers*, NASA SP-106, 1966.
- [7] Quadrelli, Marco B., *Modeling and Analysis for Nutation Time Constant Determination of On-Axis Diaphragm Tanks on Spinners: Application to the Deep Space One Spacecraft*, Copyright AIAA 2003, AAS Paper 03-155
- [8] Chatman, Y.R., Schlee, K., Gangadharan, S.N., Ristow, J., Sudermann, J., Walker, C., and Hubert, C., *Modeling and Parameter Estimation of Spacecraft Fuel Slosh with Diaphragms Using Pendulum Analogs*, 30th Annual AAS Guidance and Control Conference, In Proceedings, Paper # AAS-07-004, American Astronautical Society, Rocky Mountain Section, Breckenridge, Colorado, February 3-7, 2007.
- [9] Green, S., Burkey, R., Dodge, F., and Walter, D., *Lateral Slosh Test for STEREO Propellant Tank*, Final Report SwRI Project#18.12441.01.008 2006.
- [10] Schlee, K., *Modeling and Parameter Estimation of Spacecraft Fuel Slosh Using Pendulum Analogs*, MS Thesis, Embry-Riddle Aeronautical University, Daytona Beach, Florida, July 2006.

- [11] Dodge, F.T., *Fuel Slosh in Asymmetrical Tank Software*.
- [12] Hubert, C., *Introduction to the Dynamics and Control of Spinning Space Vehicles*, Hubert Astronautics, 2001.
- [13] Ballinger, I.A., Lay, W.D., and Tam, W.H., *Review and History of PSI Elastomeric Diaphragm Tanks*, AIAA/ASME/SAE/ASEE Joint Propulsion Conference and Exhibit, San Diego, CA. July, 1995.
- [14] Green, S., Burkey, R., Viana, F., Sudermann, J., *Fuel Sloshing Characteristics in Spacecraft Propellant Tanks with Diaphragms*, 43<sup>rd</sup> AIAA/ASME/SAE/ASEE Joint Propulsion Conference & Exhibit, Cincinnati, OH. July 2007.
- [15] Unruh J.F., et al. *Digital data Analysis Techniques for Extraction of Slosh Model Parameters* American Institute of Astronautics 22 (1985): 171-77.
- [16] Schlee, K., *Modeling and Parameter Estimation of Spacecraft Fuel Slosh Using Pendulum Analogs*, MS Thesis, Embry-Riddle Aeronautical University, Daytona Beach, Florida, July 2006.
- [17] Stofan, Andrew, Sumner, Irving, *Experimental Investigation of the Slosh-Damping Effectiveness of Positive-Expulsion Bags and Diaphragms in Spherical Tanks*, Lewis Research Center, NASA Technical Note D-1712, June 1963.
- [18] Ibrahim, R. *Liquid Sloshing Dynamics: Theory and Applications*. Wayne State University, Michigan. Cambridge Publishing. ISBN-13: 9780521838856
- [19] Kana, D.D., and Dodge, F.T., *Dynamics of Sloshing in Upright and Inverted Bladdered Tanks*, ASME Journal Fluids Engineering, 109, pp. 58-63.



# APPENDIX

## A. Experiment Matrix

### Free Surface Slosh

Liquid Viscosity Variation

Liquid	Glycerine		
Frequency	1 757	1 855	1 953
Fill Level	60%	60%	60%
	70%	70%	70%
	80%	80%	80%

Liquid	Corn Syrup		
Frequency	1 757	1 855	1 953
Fill Level	60%	60%	60%
	70%	70%	70%
	80%	80%	80%

The Free Surface Slosh experiments with viscosity variation utilized the same model and simulation as for water as previously completed

### Lateral Slosh

#### Free Surface Slosh

Liquid Viscosity Variation

Liquid	Water							
Frequency	1 757	1 855	1 953	2 150	2 250	2 500	2 750	
Fill Level	60%	60%	60%	60%	60%	60%	60%	
	70%	70%	70%	70%	70%	70%	70%	
	80%	80%	80%	80%	80%	80%	80%	

Liquid	Glycerine								
Frequency	1 757	1 855	1 953	2 150	2 250	2 375	2 500	2 650	2 750
Fill Level	60%	60%	60%	60%	60%	60%	60%	60%	60%
	70%	70%	70%	70%	70%	70%	70%	70%	70%
	80%	80%	80%	80%	80%	80%	80%	80%	80%

Liquid	Corn Syrup											
Frequency	1 757	1 855	1 953	2 150	2 250	2 375	2 500	2 650	2 750	2 850	2 950	3 000
Fill Level	60%	60%	60%	60%	60%	60%	60%	60%	60%	60%	60%	60%
	70%	70%	70%	70%	70%	70%	70%	70%	70%	70%	70%	70%
	80%	80%	80%	80%	80%	80%	80%	80%	80%	80%	80%	80%

Liquid	Corn Syrup					
Frequency	2 500	2 650	2 750	2 850	2 950	3 000
Fill Level	60%	60%	60%	60%	60%	60%
	70%	70%	70%	70%	70%	70%
	80%	80%	80%	80%	80%	80%

\*Displacement: 4mm

The Free Surface Slosh experiments with viscosity variation utilized the same SimMechanics model using new linear actuator assembly

### Spike Diaphragm

Liquid	Water														
Frequency	1 757	1 855	1 953	2 150	2 250	3 250	3 500	3 650	3 750	3 850	3 950	4 000	4 250	4 500	4 750
Fill Level	60%	60%	60%	60%	60%	60%	60%	60%	60%	60%	60%	60%	60%	60%	60%
	70%	70%	70%	70%	70%	70%	70%	70%	70%	70%	70%	70%	70%	70%	70%

Liquid	Glycerine														
Frequency	1 757	1 855	1 953	2 150	2 250	3 250	3 500	3 650	3 750	3 850	3 950	4 000	4 250	4 500	4 750
Fill Level	60%	60%	60%	60%	60%	60%	60%	60%	60%	60%	60%	60%	60%	60%	60%
	70%	70%	70%	70%	70%	70%	70%	70%	70%	70%	70%	70%	70%	70%	70%

Liquid	Corn Syrup														
Frequency	1 757	1 855	1 953	2 150	2 250	3 250	3 500	3 650	3 750	3 850	3 950	4 000	4 250	4 500	4 750
Fill Level	60%	60%	60%	60%	60%	60%	60%	60%	60%	60%	60%	60%	60%	60%	60%
	70%	70%	70%	70%	70%	70%	70%	70%	70%	70%	70%	70%	70%	70%	70%

### Sky Diaphragm

Liquid	Water														
Frequency	1 757	1 855	1 953	2 150	2 250	3 250	3 500	3 650	3 750	3 850	3 950	4 000	4 250	4 500	4 750
Fill Level	60%	60%	60%	60%	60%	60%	60%	60%	60%	60%	60%	60%	60%	60%	60%
	70%	70%	70%	70%	70%	70%	70%	70%	70%	70%	70%	70%	70%	70%	70%
	80%	80%	80%	80%	80%	80%	80%	80%	80%	80%	80%	80%	80%	80%	80%

Liquid	Glycerine														
Frequency	1 757	1 855	1 953	2 150	2 250	3 250	3 500	3 650	3 750	3 850	3 950	4 000	4 250	4 500	4 750
Fill Level	60%	60%	60%	60%	60%	60%	60%	60%	60%	60%	60%	60%	60%	60%	60%
	70%	70%	70%	70%	70%	70%	70%	70%	70%	70%	70%	70%	70%	70%	70%
	80%	80%	80%	80%	80%	80%	80%	80%	80%	80%	80%	80%	80%	80%	80%

Liquid	Corn Syrup														
Frequency	1 757	1 855	1 953	2 150	2 250	3 250	3 500	3 650	3 750	3 850	3 950	4 000	4 250	4 500	4 750
Fill Level	60%	60%	60%	60%	60%	60%	60%	60%	60%	60%	60%	60%	60%	60%	60%
	70%	70%	70%	70%	70%	70%	70%	70%	70%	70%	70%	70%	70%	70%	70%
	80%	80%	80%	80%	80%	80%	80%	80%	80%	80%	80%	80%	80%	80%	80%

### Yellow Diaphragm

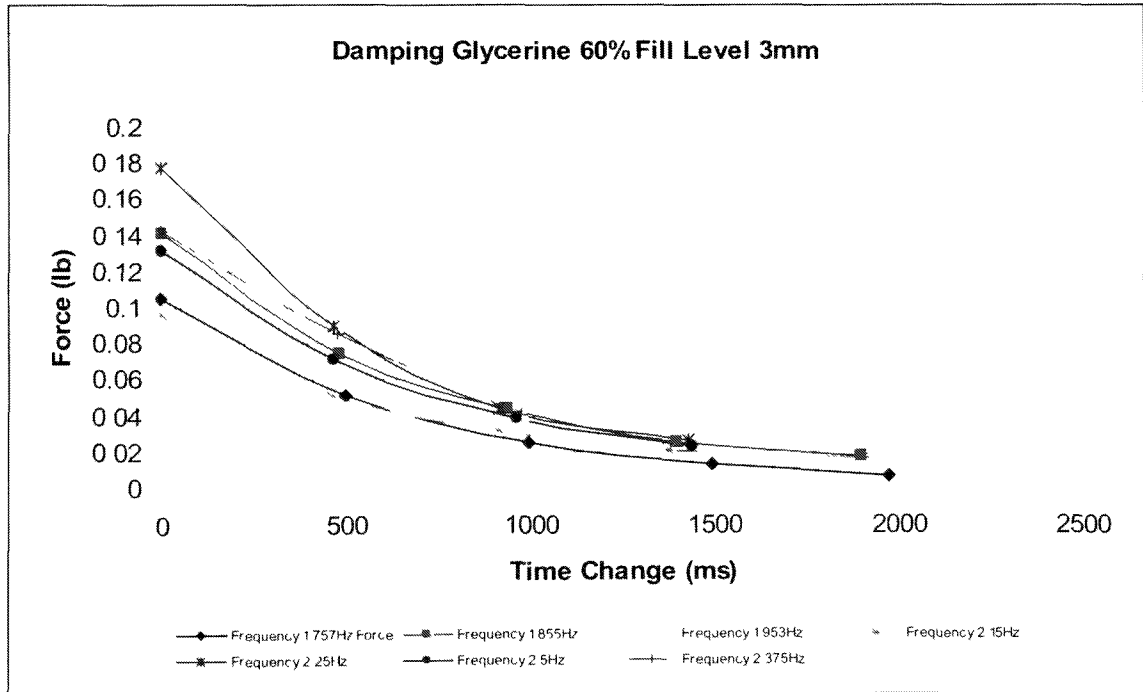
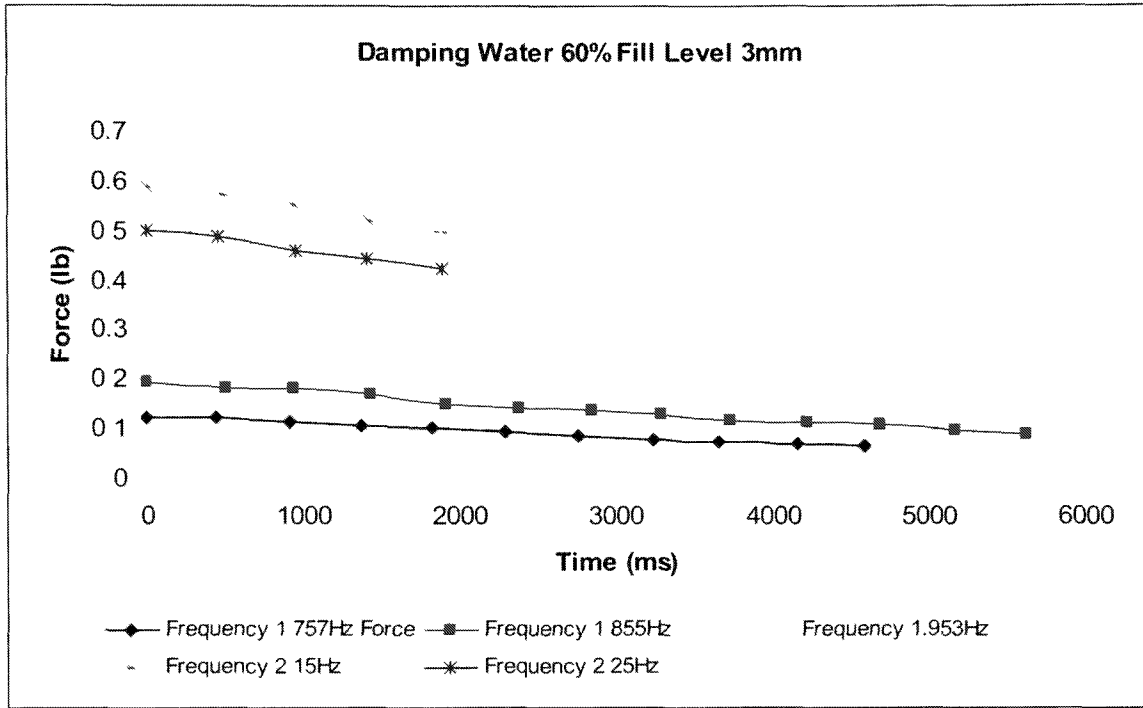
Liquid	Water														
Frequency	1 757	1 855	1 953	2 150	2 250	3 250	3 500	3 650	3 750	3 850	3 950	4 000	4 250	4 500	4 750
Fill Level	60%	60%	60%	60%	60%	60%	60%	60%	60%	60%	60%	60%	60%	60%	60%
	70%	70%	70%	70%	70%	70%	70%	70%	70%	70%	70%	70%	70%	70%	70%

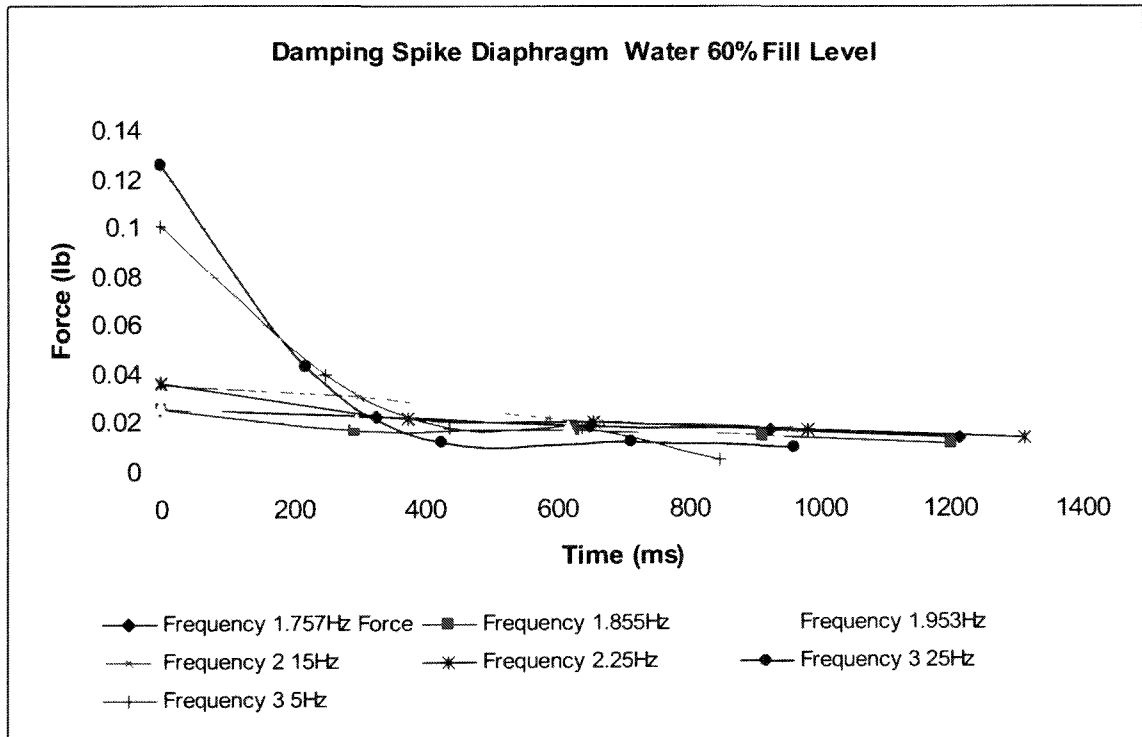
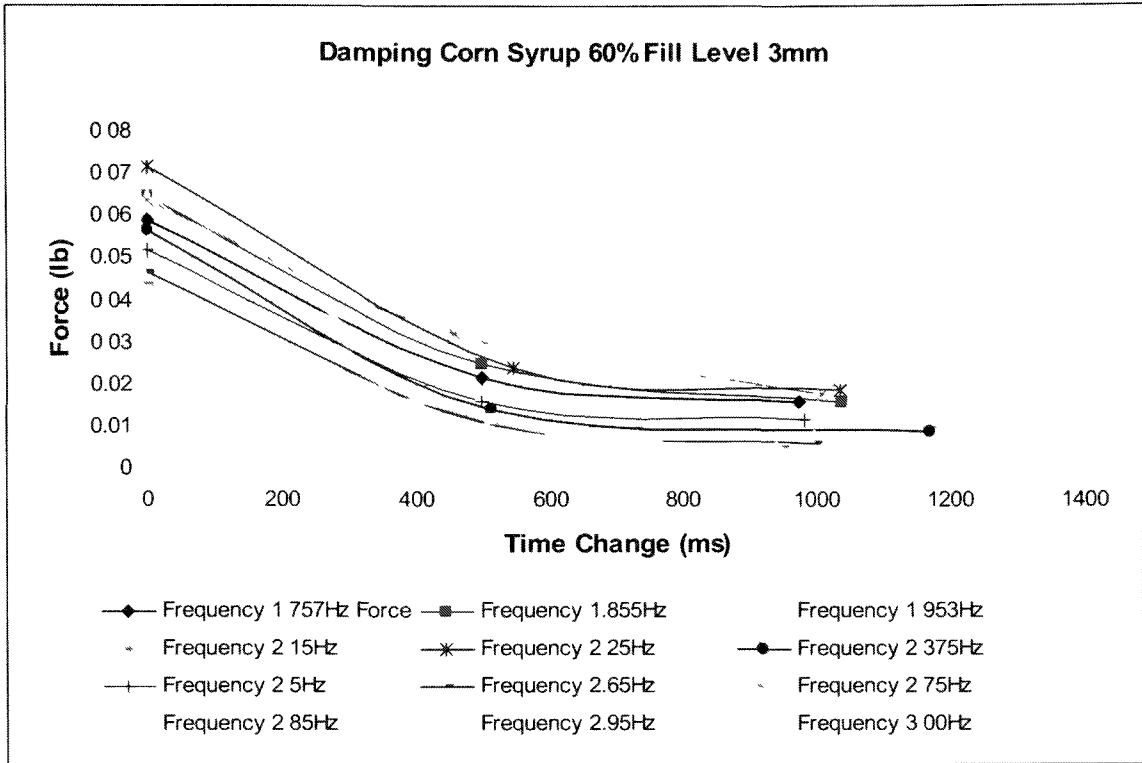
Liquid	Glycerine														
Frequency	1 757	1 855	1 953	2 150	2 250	3 250	3 500	3 650	3 750	3 850	3 950	4 000	4 250	4 500	4 750
Fill Level	60%	60%	60%	60%	60%	60%	60%	60%	60%	60%	60%	60%	60%	60%	60%
	70%	70%	70%	70%	70%	70%	70%	70%	70%	70%	70%	70%	70%	70%	70%

Liquid	Corn Syrup														
Frequency	1 757	1 855	1 953	2 150	2 250	3 250	3 500	3 650	3 750	3 850	3 950	4 000	4 250	4 500	4 750
Fill Level	60%	60%	60%	60%	60%	60%	60%	60%	60%	60%	60%	60%	60%	60%	60%
	70%	70%	70%	70%	70%	70%	70%	70%	70%	70%	70%	70%	70%	70%	70%

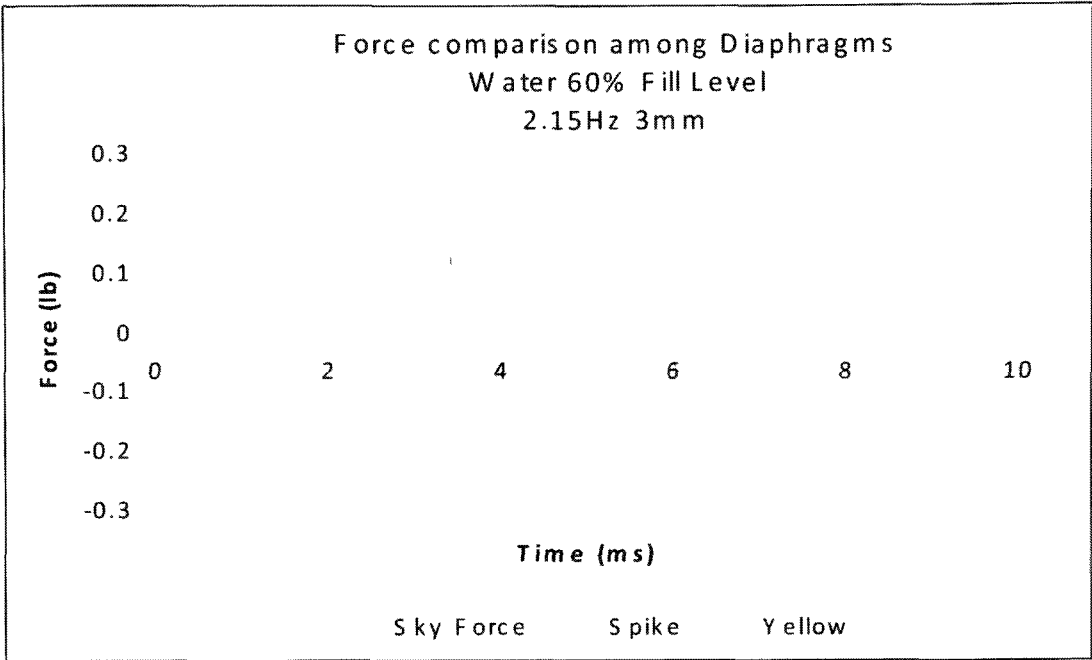
The Diaphragm Integration experiments will include a new model and simulation integrating the PMD

## B. Damping Characteristics





**C. Force Comparison among Diaphragms**



**CD. Experimental Database (attached Compact Disk)**